

# Advances in Polymer/Inorganic Nanocomposite Fabrics for Lightweight and High-Strength Armor and Ballistic-Proof Materials

Mohamed S. Selim<sup>a,b</sup>, Sherif A. El-Safty<sup>a,\*</sup>, Mohamed A. Shenashen<sup>a,b</sup>, Ahmed Elmarakbi<sup>c</sup>

<sup>a</sup> National Institute for Materials Science (NIMS), 1-2-1 Sengen, Tsukubashi, Ibaraki-ken 305-0047, Japan.

<sup>b</sup> Petroleum Application Department, Egyptian Petroleum Research Institute (EPRI), Nasr City 11727, Cairo (Egypt).

<sup>c</sup> Faculty of Engineering and Environment, Northumbria University, Newcastle upon Tyne, NE1 8ST, UK.

E-mail: [sherif.elsafty@nims.go.jp](mailto:sherif.elsafty@nims.go.jp)

[https://samurai.nims.go.jp/profiles/sherif\\_elsafty](https://samurai.nims.go.jp/profiles/sherif_elsafty)

## ABSTRACT

With increasing international and civilian conflicts, developing advanced body armor materials has become an emerging field in academia and industry. Continuous development of firearms entails improvements in ballistic-proof materials. Nanotechnology, by means of, incorporating nanomaterials, is considered a highly effective technique to achieve this goal, owing to high strength-to-weight ratios and excellent energy absorption capability of nano materials. Innovative, topographical polymer/inorganic nanocomposite fabric materials with high impact resistance, superlightweight, smart, high stiffness and elevated strength are of industrial interest for various ballistic and anti-impact applications. We consider recent designs of advanced ballistic-proof nanostructured materials by harnessing the outstanding structural surfaces and interfaces. Absorption and dispersion of a bullet's impact energy by a network of fiber materials in the armor result in bullet mushrooming. Robustness at speedy projectiles, adequate solidity, and super lightweight are the major requirements for an ideal bulletproof armor material. Different armor nanoengineered composites are used for protection against ballistics, and their protective mechanisms have been studied. Meanwhile, ballistic-related performances of various nanomaterials developed using single or hybrid techniques are collected and compared. Ballistic-proof nanocomposite clothing, such as armors and vests, can protect bodies or properties from destruction by bullets and steel weapon fragments. Advanced armors can be fabricated with the aid of reinforced ceramics or hybrid polymeric graphene nanocomposites and these materials can be used for additional protection. Hard NPs-intercalated, liquid carrier, hydrophobic self-cleaning, slippage, thicker reinforced armor fabrics are preferred. The yarns and coils show great promise for high performance, lightweight, and flexible energy harvesting materials. This review discusses uses of lightweight materials such as metal matrix composites, polymer composites, ceramic matrix composites, fiber composites in defence sectors. The findings indicate that introducing micro- and nano-fillers coating on armor fabrics is a

promising method for high ballistic impact resistance and impact energy absorption of the hybrid composite laminates. Such comprehensive review would motivate the futuristic bullet-proof armor materials with enhanced efficiency for the development of a protective environment.

**Keywords:** Superlightweight, Ballistic-proof, impact energy, bullet mushrooming, armor material, nanoengineered composites.

**Abbreviations:** NP, Nanoparticle; UHMWPE, ultra-high molecular weight polyethylene; MWCNTs, multi-wall carbon nanotubes; GNP, graphene nanoplatelet; FRP, Fiber reinforced plastics; WMR, weight merit rating; FRC, fiber reinforced composite; HEL; Hugoniot elastic limit; STF, Shear thickening fluid; PDMS, polydimethylsiloxane; g-C<sub>3</sub>N<sub>4</sub>, Graphenic carbon nitride; MLG, multilayer graphene; CSR, Core shell rubber; MMT, Montmorillonite; HA, hydroxyl A; VGCF, vapor-grown carbon nano-fibers; SWCNT, single-wall carbon nanotube; GO, graphene oxide; rGO, reduced graphene oxide; PA, PES, polyester resin; polyacrylate; o-SWCNT, oxidized SWCNT; m-SiO<sub>2</sub>, modified-silica NPs, PVB, poly(vinyl butyral); PI, polyimide; PP, polypropylene; Al, Aluminum; FML, fiber-metal laminates; CFRCs, carbon nanotube fibers reinforced composites; WMR, Weight merit rating; Al<sub>2</sub>O<sub>3</sub>, aluminum oxide; NIJ, National Institute of Justice; IF, inorganic fullerene-like; PET, polyethylene terephthalate; PA6, polyamide 6; FGO; functionalized GO.

## Contents:

1. Introduction .....	3
2. Basic features of ballistic forces .....	6
2.1. Ballistic types .....	6
2.2. Ballistic alleviation .....	6
2.3. Selecting bullet-proof fiber .....	7
2.3.1. Nylon .....	7
2.3.2. Low velocity impact behavior of aramides and UHMWPE Composites .....	8
2.3.2.1. Polyaramide fabrics .....	8
2.3.2.2. UHMWPE for ballistic-proof armor .....	9
2.3.3. Ceramic materials .....	11
2.4. Design of protective clothing .....	12
2.5. Bulletproof armor composites .....	12
3. Historical protective fashion clothes .....	13
4. Testing the ballistic-proof materials.....	15
4.1. Antiballistic armor standards .....	15
4.2. Failure mechanism of fabric fibers.....	16
4.2.1. Failure mechanism of metallic armor .....	17
4.2.2. Failure mechanism of ceramic and fibrous armor .....	17
4.2.3. Microscopic damage analysis .....	18
5. Antiballistic factors of woven fabrics .....	19
6. Nanomaterial-building blocks for armors .....	21
7. Recent body armor nanocomposite designs.....	22

7.1. NP-surface area for composite armor .....	23
7.2. Nanocomposites for high energy absorption .....	24
7.3. Key-effective NP-based filler stiffness.....	25
7.3.1. Key-geometric architectures of NP-based fillers .....	25
7.3.2. Volume fraction and interparticle distance of NP-based fillers .....	25
7.3.3. Sizable effects of NP-based fillers .....	25
7.3.4. Key- morphological architectures of NP-based fillers .....	26
7.3.5. Different types of nanofillers and matrices for formation nanocomposites .....	27
8. Superlightweight nanoengineered armors .....	27
8.1. Aluminum-based nanofillers .....	28
8.2. Inorganic fullerene-like (IF) fillers .....	28
8.3. CNTs-based bulletproof armors.....	29
8.4. CNT-based armor designs.....	31
8.5. Protective nanographite composites.....	31
8.5.1. Hybrid polymeric graphene nanocomposites .....	32
8.5.2. Widespread manufacturing of exfoliated graphene materials.....	34
8.5.3. Integrated, super-scalable modeling for graphene functional applications .....	35
8.5.4. Design of graphene-based nanocomposite structures.....	36
9. Multifunctional polymer/filler nanocomposite .....	37
10. Advanced armor nanomaterials materials .....	42
11. Nanomaterials merits for armor-designs .....	45
12. Conclusion and future outlook and directions .....	46
References .....	50

## 1. Introduction

Anisotropic nanocomposite materials represent an advanced filler terminology to design protective clothes [1]. Ballistic-proof materials aim to protect bodies or properties from bullet impacts and steel weapon fragments [2]. Armors protect personnel from ballistic impacts since time immemorial (Fig. 1) [3,4]. Continuous developments in new weapons prompted researchers to determine for protective solutions, so this is the time to write about this topic. Various materials, including aluminum, steel, leather, and silk, are utilized for armor design [5,6]. Failure mechanism of ballistic-proof armors against bullets is based on absorption and dispersion of the transmitted impact energy result in bullet's deformation and mushrooming. In the past, hard rigid materials for body protection from ballistic shootings can resist ballast penetration and distribute the load of impact (Fig. 1) [7]. Early materials used in body armors include leather, metal chain, and metal plate. Nylon (polyamide) possesses high toughness features and low cost, thereby making it an ideal ballistic-proof material [8]. Replacement of metallic armor systems with a nylon (polyamide) fabric composite can be related with the Korean War [9]. Recently, the progress in material science and synthetic

textiles enabled the design of new bulletproof materials based on load spreading over a large area and dissipating the impact energy. Polymeric fibers with high-performance antiballistic performance, high strength, and stiffness were applied. Because of their stress transfer ability and glass were extensively applied in the composite armor systems. However, these systems are unsuitable for resisting high-impacts from missiles; where high stabbing resistance and energy absorption are required [10].

### Fig. 1

Polyaramids, especially Kevlar, are well-known fibers used for protective armors because of their high strength (~3600 MPa), high modulus (~112,400 MPa), and good tenacity [11]. Aramid (Kevlar), a synthetic fiber, was developed in 1965 by two research scientists, Stephanie Kwolek and Herbert Blades [12]. Polyaramide materials possess excellent stiffness and normalized strength compared with those of nylon. This is caused by their strong hydrogen bonding, compact and closes molecular structure of polymeric chains, and monoclinic crystalline form with a dense building block. These factors enable their absorption of the shock waves produced by low and high-velocity projectiles [13]. Unfortunately, these materials are costly, and they require a complex technology [6]. Kevlar nanocomposites are new trend today to improve the antiballistic performance and reduce the cost [14]. As a robust thermoplastic material, ultra-high molecular weight polyethylene (UHMWPE) was also introduced as a new trend for ballistic-proof technologies because of its inexpensiveness and considerably long polymer chains [15]. Their fibers display excellent strength, low moisture absorption, and less dense fabric materials, among almost of all body armor fibers [5,15].

Given their high density, increased compressive strength, high elastic modulus, and outstanding hardness, ceramics are used for ballistic-proof purposes. These characteristics cause fast erosion of the bullet sharp points, result in low-mass blunt cylinder, and reduce the bullet impact energy. Unfortunately, ceramic's brittleness and lack of flexural strength are the major problems when applying ceramic as a single material in bulletproof armor. The high performance of advanced ballistic-proof composites when subjected to a missiles's impact can be achieved through effective techniques including consequence layer-by-layer buildings, a non-Newtonian or shear-thickening fluid (STF), embedding by nanostructured fabrics such as graphene, CNTs, SiC, and Al<sub>2</sub>O<sub>3</sub>, and yarn pull-out method [12,15] (Table 1).

Functionalized layers of fabrics with enhanced stress transfer and mechanical strength were introduced by layer-by-layer technique. However, their poor interfacial adhesion may limit their wide applications (Fig. 1). The STF technique was employed for aramid fiber functionalization to improve the absorption of the impacted energy as compared to the untreated fabrics. This is accompanied by fabric deformability to sustain the impacts of the high shock; where the fiber rupture is a limiting factor under critical shock. Also, yarn pull-out technique can produce highly protective aramid fibrous clothes with high energy dissipation governed by interyarn friction. The feature of interyarn friction improves the fabric mechanical strength by enhancing the yarns' alignment. However, this ballistic proof performance is increased until the threshold value. After this value, energy dissipation is reduced to yield surface failure during combat operations. As a

fascinating technique, functionalization by nanomaterials is the most popular antiballistic method as the nanomaterial's high aspect ratio, dispersibility, and surface area provide improved fabric performance. Also, this technique facilitates the reduction of fiber buckling under stress and produce matrix-reinforced fabric nanocomposites with improved interfacial adhesion. Inorganic nanofiller dispersion in these materials can remarkably improve the functionality toward mechanical and antiballistic performances. Controlling nanofillers type, size, morphology, and distribution concentration along the polymeric resins are key factors to develop nanocomposite with outstanding ballistic-proof features including, high strength, and stress-transfer capability associated with the absorption of the shock energy [16].

Considering the large amount spent on armor production and the benefits of human life protection, proper utilization of tailored nanostructure reinforces armors. Advances in light weight, low cost designs of body armors for personnel, vehicle, and structural applications are a field of high interest for armor manufacturers and users. Functionalization of armor fibers by using nanostructured materials is inevitable to provide high-performance antiballistic armor materials with reducing the fiber buckling under load for the protective application. Different nanomaterials including CNTs, SiO<sub>2</sub>, graphene-related materials, Al<sub>2</sub>O<sub>3</sub>, SiC, and inorganic fullerenes (IFs) included MoS<sub>2</sub> and WS<sub>2</sub> nanostructures were used to enhance the ballistic-proof applications. Nanomaterial reinforcement improves mechanical strength, tensile strength and modulus, and energy absorption ability. Controlling the nanomaterials' size, morphology and distribution in the polymeric matrix can improve the ballistic-proof feature and energy-absorption of the fabric nanocomposites to yield ultra-high and robust protective material.

In this review, we report in-depth research developments of nanomaterials, fabric nanocomposites, and nanofiller reinforcement design and process for next-generation of remarkably high mechanical and bulletproof armors. Several building blocks of fabrics using novel surface modifiers, polymeric resin matrices, controlled design of nanostructured multisystems, and highly sophisticated nanocomposites have also been investigated. The industrial-scale controls of superlightweight and high-strength ballistic-proof armors with simplicity and economic characters have also been widely explored. Lightweight materials are critical in defence applications because they allow components to be lighter without sacrificing strength. In this context, we discuss the vital accomplishments in advanced antiballistic armor materials. We also shed light on the balancing between high antiballistic performance of armor fabrics and their common-used conformity and requisitions in terms of ultra-lightweight, flexibility, cheap, comfortability and exposure surfaces. Accordingly, this review is designated to introduce a panorama of the up-to-date advances related to the architectural designs of bullet-proof armor materials and polymeric nanocomposite structures. Recent evidences were supplied for confirming our proof-of-concept, in which dominated that the nanostructured bulletproof clothing would be a manufacturing the future and a well-established platform to create cost-effective and long-term protection. This review summarizes and concludes much active sceneries for the futuristic trends in the development of a protective environment.

## 2. Basic features of ballistic forces

### 2.1. Ballistic types

Projectile's motion before launching from the weapon muzzle is termed as internal ballistics while external ballistics represent its flight in the air after launching from the muzzle and before infecting the object. Terminal ballistics express the projectile's path when reaches the object [17]. Internal ballistics is based on projectile's dimensions and muzzle speed. On reverse to rifle, hand guns shoot a low-velocity bullet, and handgun chambers can handle less. The weapon's speed and fineness are also affected by the muzzle length (Fig. 2) [18].

An ideal handgun has a 4–6-inch barrel while a rifle possesses a barrel with 22 inches. When the projectile leaves the muzzle without gunpowder push, a gradual loss in velocity takes place. Exiting muzzle velocity is controlled with powder's type and amount. A large amount of powder can be handled by the cartridge in a rifle bullet. The reliability and extreme possibility of wounding represent the main target at various projectiles' speed. Collapsing the projectiles' speed in the external ballistics is due to the following clues [18]:

- ❖ Losing of strong pushing up from the propellant device;
- ❖ Definite amount of drag on the bullet may create by the air; and
- ❖ A degree of yaw, which can be defined as the deflection amount observed on the object's upright direction, reduces velocity.

Tumbling of a projectile has a key function in wounding after penetrating the tissue [19]. Minimum weight, maximum mobility, and antiballistic performance are the main requirements for bulletproof armor materials [20,21]. Arms and legs are not covered in normal welfare because their wounding may not result in doom, while the indispensable organ should be wrapped. In hazardous jobs, heavyweight garments are used to cover the whole body. Energy absorption and its distribution characteristics are essential factors in the design of ballistic-proof materials. These characteristics include the kinetic and cumulative strain energies of the pyramid and the fabric as well as the friction energy lost as heat [22,23]. Armor analysis is selective because no armor material model can be used for all projectiles, so studying the mechanisms and dynamic designs of bulletproof materials remains challenging. Given the evolution of ballistic-proof nanocomposite fabrics for market requirements and the growing demand in the creation of superlightweight and high-strength armors based on novel fabrication of nanoscale structured materials would produce significant merits to remarkable ballistic-proof equipment devices.

**Fig. 2**

### 2.2. Ballistic alleviation

Alleviating the ballistic shocks is essential to buildings, transportations, and events that may be subjected to the explosion and provide a safe condition for life as well as improve the shock opposition of the important installations. Kevlar and Twaron have many advantages include their fivefold strength than that of steel,

opposition, thermal and chemical stability, and extreme shock resistance. They are widely used in preventive equipment and clothes. However, they also exhibit the following disadvantages exist: costly and poorly compressive features can only be cut by fraying, fuzz tendency, and invisible-damage after impact. These materials were used for archery bows, but they often fail after limited usage. Also, aramids can only be strengthened using definite terminators.

Ballistic materials may include laminates, fibers, particles, fabrics, and powder. To manufacture functional fibers for use in ballistic-proof vests, we need to understand some of the basic working principles of ammunitions. The topics related most closely to bulletproof fibers are projectile velocity and penetration theory. The projectile's kinetic energy is the key factor to measure the impact resistance of protective clothes. Projectile's In-bore dynamics and flight distance enable different speeds with different physical impacts on solid targets. The effective and foremost developments in ballistic-proof equipment strategies are crucial. The control penetration of fabricated materials would lead the accurate analyses of ballistic superlightweight impact and inexpensive manufacture of ballistic-proof vests or armors.

### **2.3. Selecting bulletproof fiber**

Robust fibers of bulletproof armor are necessary to capture and distort the projectile in a mushroom style to spread its activities in the bulletproof armor. Such fiber causes energy absorption from the projectile and stops its motion. To develop lightweight and robust fiber-based bullet-proof materials, fiber materials with high and balanced specific modulus and specific strength are preferred. Selecting bulletproof fibers is based on breakthrough opposition, impacted energy measure and projectile's strength, shock speed and mushrooming. To date, fabrication of diverse and multidisciplinary fibers is based primarily on controlling the robustness, reasonable superlightweight fabrics, and cost capability. The following fibers are appreciated material component scales that can be used in bulletproof fibers:

#### *2.3.1. Nylon*

Nylon is a thermoplastic synthetic polyamine with excellent mechanical strength and resistance to wear and organic chemicals. In the past, nylon fibers were the most widely used materials for antiballistic applications. In the early 1930s, Carothers at DuPont invented nylon fibers with 0.6–0.7 N/Tex strength. The American army was the first to produce protective steel coats contain polyamine fibers during the Second World War [4,24]. Such polyamine fiber was nylon 66. During the Korean War, hard armor made of a 12-layer nylon fabric was utilized by foot soldiers for protection against low-velocity shell fragments. The nylon fiber possesses high crystallinity, high tensile strength, and reduced elongation. Nylon 66 is extensively used for antiballistic applications because of its outstanding strength, and it also usually absorbs energy two times higher than that of p-aramids [24]. But the weak physical characteristics and modulus losing are undesirable features of nylon. Furthermore, nylon undergoes creeping under high strain rate and melting and fusion at the interlacement points, whereas aramids overcome these defects (Fig. 3a). However, nylon has a quarter speed of the transverse wave than para-aramid [8,25]. Thus, the strain in polyaramide



fabrics is spread over large distance with low elongation. The nylon creeping under high strain rates constrains its perfect usages as bulletproof fibers; however, the ballistics usually operated with melting and fusion when the interlacement point was noted. Thus, the simple-to-utilize fibers and effective fabric formats for manufacturing of high-ballistic protections remain challenge.

### *2.3.2. Low velocity impact behavior of aramides and UHMWPE Composites*

Aramid and UHMWPE fibers are the most often used reinforcement materials in various matrices when creating composites for ballistic applications. The composite materials utilized in this kind of application are exposed to a tremendous amount of energy, particularly those that are used as explosive armoring materials [26,27]. Recently, aramid-fibre reinforced composites are another type of composite that exhibit great performance, especially in terms of impact resistance UHMWPE fibre-reinforced composites have been widely used in applications due to their outstanding properties. The high impact resistance of these composites is one of the many advantages of UHMWPE fibre-reinforced composites. Karahan and Yildirim [28] reported that the most popular method to produce composites for ballistic application is to use aramid and UHMWPE fibres as reinforcement materials in different matrices. Because aramid fibers have a high heat resistance, they can be hybridized into UHMWPE fiber-reinforced composites as a supplementary reinforcing fiber to offset UHMWPE's aforementioned drawbacks. It was approved that mass optimization could be achieved without the loss of the high-level impact energy by preparing a hybrid composite with UHMWPE and aramid fibers [28].

#### *2.3.2.1. Polyaramide fabrics*

Kevlar, the most widely known polyaramide, was invented in 1972 as a high-ballistic protection [8,25]. Due to its excellent energy absorption, specific modulus and strength, and thermal stability, Kevlar can be used as alternative fibers of nylon. The high mechanical characteristics of polyaramide resulted from the remarkable regular internal structure of Kevlar. Kevlar monomeric units consist of amide groups separated by *para*-phenylene groups. Their configuration commonly shows long straight chains with regular hydrogen bonding to form a considerably strong lattice that is similar to crystals (Fig. 3a). Kevlar is much stronger than steel and only half as dense. The high modulus is caused by high crystallinity and oriented structure, which reduce creeps and increase wave propagation rate to  $77 \times 10^2 \text{ ms}^{-1}$  (nearly three times higher than that of nylon) and fast longitudinal mushrooming response. Kevlar creeping rate is homogenous and the creep strain amount enhanced linearly with log (time) for breaking. These Kevlar-based fiber properties are also supported by high tenacity (18–26 gpd, two times that of nylon) and moderate elongation (1.5%–4.4%), which provide the high absorption tendency of the impacted ballistic energy. The Large fraction of breaking load of Kevlar fibers cause longer lifetimes of these fibers than nylon. For long term and economical costs, Kevlar provides service life of > 100 years, and nylon gives 3–4 years [6,29,30]. P-aramid antiballistic protection was assessed by V50, the velocity at half of shock was broken through and the other half partly permeated [31]. Kevlar clothing with low weight/m<sup>2</sup> and soft ballistics is more prominent than hard ballistics



[32] (Fig. 3b). On the other hand, hard ballistic material is more efficient at weights greater than  $10 \text{ kg/m}^2$  because of the rigidity difference between soft and hard ballistics. Although Kevlar-based composite fibers are lightweight antiballistic materials, they suffer from their high costs.

**Fig. 3**

Ari et al. [33] examined the usability of several composite plates in level III and level IV body armors, along with the ballistic resistance, protection level, and production parameters of each plate. Wet and dry ballistics tests showed that the Level III plates had been punctured; these tests were conducted at a pressure of 90 Bar. The experiment's results showed that level III requirements did not offer enough security. After undergoing wet and dry ballistic tests, it was discovered that although the level III plates produced at 140 Bar pressure did not have any perforations, there were delaminations between the layers and deeper trauma than expected. As a result, it has been observed that this material will not provide the necessary protection. It has been discovered that Level IV wet aramid cloth loses its strength and ballistic capabilities. Delamination only occurs following the initial shot at Level IV, and there is no hole in the K-Flex reinforced ceramics.

$V50$  ballistic limit is a statistical test originally developed by the US military to evaluate hard armor. The ballistic performance of a target material is often determined by the ballistic limit velocity  $V50$ , of projectile. It is defined as “the velocity at which 50% of projectiles perforate the target [34]. Ballistic limit is an important parameter for designing a composite structure and understanding its dynamic damage behavior in order to effectively utilize it as a protective structure. It is a widely recognized criterion for assessing the efficiency of armors. Prosser [35] measured  $V50$  of fabric laminates by varying the number of layers and revealed that a linear relationship exists between the square of  $V50$  and the number of layers, as long as the energy absorption mechanisms remain the same. It was observed that ballistic limit velocity,  $V50$ , can be increased for the composites by adding E-glass layers to T300 carbon layers compared with only carbon composites for the same laminate thickness [36]. Higher ballistic limit velocity is achieved by placing E-glass layers on the exterior and carbon layers within, as opposed to carbon layers on the exterior and E-glass layers inside. The reinforced laminates made of woven and bi-axial fabric showed minor delamination and only localized damages. Nevertheless, there were significant damage regions in unidirectional laminates, primarily from bulging and delamination.

#### *2.3.2.2. UHMWPE for ballistic-proof armor*

UHMWPEs are nontoxic, thermoplastic polyethylene with remarkably long chains aligned in the same direction and molecular mass in the range of 3.5–7.5 million atomic mass unit. The tough nature and the highest impact strength of these materials are caused by the long chain structure. As a result, the impacted load can be transferred easily to the matrix backbone based on reinforcing the intermolecular bonding between chains. UHMWPEs possess high mechanical properties, excellent damage tolerance, and fatigue resistance; they also lose no significant amount of tensile strength when they fail in shear or compression [37]. According to the highest percentages of energy absorbed, these materials exhibit extraordinary strength and stiffness [38]. Similar to high-density polyethylene, they are stable against different pH solutions and

common solvents. Under high temperature, modulus can increase gradually with increasing deformation rate. Given the good structure, the tensile strength can increase to approximately 40% by ballistic impact with increasing mushrooming rate [39]. UHMWPEs also possess lower density (nearly 0.97) than that of Kevlar (1.45) and increased velocity of longitudinal stress wave, which is similar to that of diamond [40]. These characteristics made UHMWPE the most extensively used ballistic-proof materials.

Only at the smallest projectile diameter, aramid is more prominent than UHMWPE because of its elevated friction coefficient. However, the elevated hardness, erosion opposition and chemical stability of UHMWPE enable its wide scale of applications than para-aramid [41,42]. UHMWPE-based composites are applied in ultra-strong based materials such as bullet-proof body armor [43,43].

Although UHMWPEs exhibit superior antiballistic characteristics, they suffer from creep and low-temperature resistance and adhesion characteristics, which limit their applications [41,43] (Fig. 4). Modeling and dispersion of the anisotropic nanoparticles (NPs) is an effective method to enhance polyolefin effectiveness [44]. Many carbonaceous based nanomaterials were used for various mechanical purposes [45,46]. UHMWPE hybridized with electrostatically sprayed graphene nanoplatelet (GNP) provide a developed nanocomposite coating with enhanced tensile strength and toughness even at 0.1 wt.% of GNP [47]. As a consequence of necessitates moving, future efforts should focus on the design of novel bulletproof nanocomposite armors for economic savings, high performance, and prolonged longevity with high dissipation ability for the shock energy.

**Fig. 4**

A Split Hopkinson Pressure Bar apparatus was used to determine the compressive behavior of Aramid and UHMWPE composite panels reinforced with various fiber architectures at four high strain rates. Compression characteristics of Aramid and UHMWPE composites with different fiber topologies in the out-of-plane direction were tested at room temperature [48]. Hybrid samples showed better performance in the energy absorption compared with other samples. At various compression rates, the energy absorption and stress-strain behaviors of these composite samples were ascertained and compared with each other. Sandwich composites with a compressible core material increased energy absorption for the protective boot soles [49]. The honeycomb core sandwich composite material filled with glass microspheres was an innovative candidate for the production of blast protective armor, as well as mine boots, due to its high energy absorption capability. The protection efficacy of the innovative sandwich composite structure with a high energy absorption capacity has been proven. The protection efficiency of monolithic and sandwich composite materials was compared and used in the boot sole [50]. Aluminum honeycomb core sandwich composite material filled with glass microspheres was also employed. This was an innovative candidate for production of blast protective armor, as well as mine boots, owing to its high energy absorption capability.

The impact properties of composite samples of Para-aramid (PA) fabric made with thermoset resins (phenolic, vinylester), thermoplastic (Polyvinyl butyral) resin and their blends were tested [51]. Impact energy absorption of thermoplastic/Para-aramid composites is significantly higher than thermoset/ Para-

aramid composites. To delay the fabric deformation and strengthen its structure, Chitrangad [52] suggested hybrid fabrics that have weft yarns. he evaluated the ballistic performance of hybrid fabrics woven with different types of warp and weft yarns and obtained an increase of up to 7% in ballistic performance. In new-generation ballistic fabrics today, the warp and weft yarns with the same number and density are preferred. This fabric construction produces same crimps in both warp and weft directions and therefore the same amount of deformation occurs in both the warp and weft directions. This fabric property increases the energy absorption capacity of fabric.

With an increase in the number of fabric plies, panels' ability to absorb energy rises and the amount of energy communicated to their backs falls [53]. The quantity of energy absorbed by panels rose and the energy sent to the rear side dramatically decreased, especially after 24-ply. A ~59.8% reduction in the transmitted energy and 4.4% increases in the absorbed energy occurred when the fabric ply number increased from 20 to 32. The performance of ballistic protection panels formed with 100% woven and 100% unidirectional nonwoven para-aramid fabrics was studied at different fabric ply numbers [54]. Ballistic performance of the test samples was determined by measuring trauma depth and trauma diameter. The energy absorbed by fabric layers and the energy transmitted to the back of fabric layers were calculated from trauma depth and trauma diameter values. It was shown that the unidirectional fabric panels absorbed around 12.5–16.5% more energy than woven fabric panels for the unit panel weight. The ballistic performance of hybrid panels formed by combining woven and unidirectional para-aramid fabrics was investigated [55]. More energy per unit weight in hybrid panels was absorbed as compared to 100% Twaron woven fabric panels, and no significant difference was realized as compared to 100% K-Flex UD fabric panels. Best ballistic performance is shown by 70% K-Flex non-woven fabric–30% Twaron woven fabric hybrid type.

### 2.3.3. Ceramic materials

These ceramic composite materials are promising for armor design for protection against high-power ammunition due to high density values as metals, high compressive strength, excellent hardness, increased elastic modulus, and high compression strength [56]. Given the high dynamic stress of ceramics, the projectile sharp points are eroded rapidly which decrease the energy impacted [57] to a high extent and enhance the antiballistic performance of ceramics. Many ceramic materials are used to develop fabric tools in bullet-ballistic armors to a vastly greater degree. These ceramics materials include oxides such as  $\text{Al}_2\text{O}_3$ , while carbides and nitrides are employed as non-oxide ceramic materials [58].  $\text{Al}_2\text{O}_3$  is the most commonly used ceramic materials with many advantages, such as low cost, ease of preparation, and excellent resistance against ballistic impacts.

The mechanistic dexterity of ballistic protection of developed ceramic tools is as follows:

- ❖ Destroying the projectile tip by the hard ceramics;
- ❖ Generation of shock waves in the tile and orthogonal propagation of waves of the shear and compression stresses along the thickness; and

- ❖ Reflection of the waves in both directions after reaching the tile edge which causes rupture and material breakage [59].

The ceramic's impact opposition is affected by the mechanical properties of a surface such as hardness and toughness. Nevertheless, ceramics suffer from inherent brittleness and lack of flexural strength, which may also be a key to reduce their ability to be applied alone as single or origin component for antiballistic materials [60,61]. This problem-solving abilities and properties are attributed to that the single ceramic material can transmit a part of the shock wave through impact energy dissipating; consequently, windrows bend the tile [62].

## **2.4. Design of protective clothing**

With high exceptions, friction resistance is a vital step in ballistic protection which depends on production technique. Many ballistic-proof fibers are highly drawn with smooth surfaces that increase their effectiveness [63]. Thus, chemical and mechanical roughening of the smooth surface of fibers is essential to obtain prominent surface. Controlling the fiber coating is essential to provide enhanced features [64]. UHMWPE-based fibers with elevated friction coefficient and be hybridized with nanomaterials that exhibit elevated strength and modulus and decreased friction resistance to develop antiballistic composites [43,65] (Fig. 4). Combining of thin high-friction elements to thick high-performance components also enhances the antiballistic performance. With extensive investigations on structural features of functional hybrid nanocomposites, new armor-based materials can be developed with improved physic-mechanical and antiballistic features.

## **2.5. Bulletproof armor composites**

Different projectile types require the development of numerous and specialized preventive clothes. Given their viscoelastic, characteristic, and antiballistic performance, polymeric nanocomposites play a significant technological role as advanced materials or devices. The armor industry is challenged with the utilization of reinforced composites. Researchers have developed and evaluated many composite materials to be used as antiballistic solutions. Such nanocomposites are controlled via organic-inorganic hybridization of polymer-NPs performance [66]. Ceramics exhibit high resistance to UV degradation compared with that of polymers [67].

Changing the size of the molecular building in the nanoscale particle-unit-blocks can significantly influence the performance of ballistic resistance. Bulletproof composites can achieve good factors, such as the high antiballistic protection, inexpensiveness, low weight, and high comfortability [67]. Obtaining the synergetic effects of nanoscale filler materials may ameliorate the anticorrosion features of the armor composite surfaces as follows:

- (1) The enhanced surface area coverage of NP-based filler structures, conformational modeling along pronounced atomic-scale arrangement, and the improved matrix-NP surface interfacial bond strength along nanocomposites can provide flexible design structure.

- (2) Cost-effectiveness and long-term durability are among the advantages of adding nanofillers in the polymeric composites.
- (3) Remarkable stability, high compatibility, and surface activity of molecular building in the nanoscale particle-unit-blocks may provide evidence as practical and inexpensive bulletproof composites.

Among these nanofillers, graphene-related materials, CNTs, ZnO, SiO<sub>2</sub>, Al<sub>2</sub>O<sub>3</sub> and many other geometric nanomaterial structures can be facilely prepared from cheap and natural abundant sources. Nanomaterial-based fillers significantly provide feasible applicability and develop advanced structures in terms of multi-directional movements, and suitable channel/pocket accommodation along bulletproof composites [68] (Fig. 5).

These nanofiller materials can resist the shock waves from low and high projectile impact with high energy absorption tendency and antiballistic protection. Ballistic protective clothing is preferred to be made of hydrophobic materials [69]. The performance of normal bulletproof clothes is reduced by approximately 40% after wetting, which is not the case in non-wettable clothes. Water-used mediators facilitate the penetration of the projectile in the wettable clothes [70]. Fiber-reinforced plastic composites were successfully tailored with remarkable antiballistic performance [71].

The polymeric nanocomposites involved isoprene rubber layer put inside two layers of bisphenol-functionalized epoxy resin [72]. Polyurethane composites with high strength are useful in ballistic-proof layers, especially for sails, according to the reported article by Allied Signals [73,72]. A network of thermoplastic polyurethane resins (obtained from aliphatic diisocyanate and polyol) can be applied to fabricate high-strength fiber composites. Modeling ballistic-proof armor composites can protect the whole-body target. High-strength ballistic-proof nanocomposites may be supported with additional strength in the front of target that is more susceptible to shootings. A ballistic-proof dress was USA patented, and it accommodates wearers of various sizes with an inner layer from the front and back made from bi-component composite materials to draw perspiration [4,73].

**Fig. 5**

### **3. Historical protective fashion clothes**

Materials originally play a key role in manufacture protective clothing for human body from day-to-day hazard or environmental harm aspects along a wide-range of eras. Materials manufacturing from natural animal skins are used to make protective clothing for early peoples. With the civilization development, shield-protective materials based on wooden and metals are traditionally used. Diverse metals are widely applied as physically protective body armors in the middle ages [6,74]. No actual prototypes are available in archaeological findings about the history of armor fabrication, but such information is present in the ancient records. The major sources of information about ancient protective clothing's are collected from drawings and currencies of different ages. Thus, a timeline of armor development overtime [6,74,75] is outlined in **Table 2**. Early written testimonies on armor fabrication were provided by Sumerian soldiers in 2500 B.C.; these soldiers used copper helmets and body leather as body armor. A bronze armor was primarily

introduced in 1500 B.C. [75]. In 1100 B.C., Egyptians and Acadians used linen, bronze, and boiled leather breast plate wood to fabricate armors [76]. An armor system developed of iron, bronze, wood and wool was introduced by the Assyrians (600 B.C.) [77]. Then, leather and iron are used by Persians. Large bronze plates are used by Greeks, and the Romans in 500 B.C. largely exploited iron for protection against contemporary weapons and arms [78-80]. Celtic people used chainmail body armor in the 4th century B.C. Coat of scale armor (jazerant) is used in the Charlemagne's era; quilted iron, bronze, and leather armors are used by Norman [77,81,82]. In the Charlemagne age and later, Jazerant armor, steel armors, and saxons were used during combat operations. In the 14th century, armor materials that can cover different instruments and body organs were used. Channeled Mg-based armor was used [83]. Metal breastplate and helmet are used during the English civil war (1642–1651), while thick armors were used in the 17th century to resist fire [84]. In 1905, silk vests as armor are used in the Japanese–Russian war. During World War 1, machine gun, rifle fire, and shrapnel produce appalling casualties. Hence, metal helmet, heavy metal breastplate, and armored waistcoat were used. In the Second World War and Korean War, steel laminates contain fiberglass and polyamine materials were used [6,74,84]. Ceramic body armor using aluminum oxide ( $\text{Al}_2\text{O}_3$ ) was first introduced in 1960. In 1965, an American chemist patented Kevlar which was widely produced for antiballistic clothes in 1975. Significant developments on spider silk bulletproof body armor were introduced in 1999. During the Iraq war (2003), the US army used the Interceptor Body Armor system which is made from layered Kevlar, to provide protection against shell fragments for the most organs and Kevlar helmet protects the head [83,84]. Of particular interest is that bulletproof nanostructured armor developments were generated at recently with high performance standards [85,86]. Various nanostructured designs were reported for designing ballistic-proof armors (Fig. 6 A, B). Ceramic armors were developed by using ceramic materials such as  $\text{Al}_2\text{O}_3$  and  $\text{SiC}$  nanomaterials for ballistic protection. Ceramic Fiber metal laminate (FML) was developed and applied as antiballistic skin material in 2004 [87]. Also, bullet proof armors were developed extensively in 2005 based on IF-materials such as IF- $\text{WS}_2$  and IF- $\text{MoS}_2$  with high strength and ballistic protection [88]. Fiber composites based on CNTs with high energy absorption and carbon nanotube fibers reinforced composites (CFRCs) were developed recently for high-performance antiballistic protection. Graphene-related materials such as graphite sheets and nanoribbons were incorporated in nanocomposite laminates for antiballistic applications [89]. Hybrid nanomaterials such as graphene anchored with  $\text{SiO}_2$  and  $\text{Al}_2\text{O}_3$  were employed to provide nanocomposites with (i) ultra-high robustness, (ii) ultimate strength of potential maps, (iii) high surface area coverage, (iv) multidirectional interfacial tension, and (v) enhanced energy absorption capacity.

Nanomaterial hierarchy exponentially allows the creation and exploration of a wide array of materials and designs, including all the conceivable ballistic nanomaterial used in various applications. Further developments in nano-object designs are not only powerful forms for primary body armor function materials of different projectiles but also offer challenging in manufacture of effective protection aspects, flexible and comfortable usages (i.e., light and physiological functions), and particular suiting to social attitudes.



Nowadays, body armor structures and designs provide extensive antiballistic performance. Nevertheless, the ceramic materials with ultrahigh ballistic protection represent a proximity solution in super lightweight and cost-effective armor designs [90]. The developed nano-composites based on strengthening nanofibers were wisely applied as antiballistic materials for humans, motor vehicles, and aircraft structures.

**Fig. 6**

#### **4. Testing the ballistic-proof materials**

When evaluating the performance of ballistic proof materials, ballistic protection and weight efficiency should be considered (Fig. 6C). Ballistic protection represents the protection degree against an impacted projectile or a series of projectiles [91]. Reducing the mobility of the armor fibers is necessary for mechanical robustness and absorbing the load stress. Such mobility restricting can be achieved by incorporation of hard NP-based fillers (Such as SiO<sub>2</sub>) more than soft particles (ex. Polymethylmethacrylate) and by using a liquid carrier with distributed NPs. Weight merit rating (WMR) is used to investigate weight efficiency of an armor compared with that of the standard [92]. WMR equals the standard material density divided by a developed material density. Cotton duck fabrics and MIL-A-12560 steel are standard materials to study antiballistic armor properties [93].

##### **4.1. Antiballistic armors standards**

Testing in dry and wet states of the antiballistic armor material is essential because the wet state shows different behavior from that of the dry state. A high performance is commonly observed for hydrophobic and superhydrophobic coatings because water can support projectile penetration by acting as a lubricant surface. Suitable firearms and bullet type should be selected. Shooting is performed at a suitable velocity at 3 inches away from the edge of the armor and almost 2 inches away from former shots. Two shots are fired at a 30° of incidence and four at a 0°, where one shot should fall on a seam. This shooting technique forms a wide triangle of bullet holes. Many standards and specifications are utilized, as indicated in Table 3, where each standard applies different method to evaluate the performance of the antiballistic armor materials. Based on the final applications, the analysis test standards of bullet-proof armour differ from country to another per of requested protection environment. The high specificity and spatial sets of test standards are those applied in USA (established by the National Institute of Justice (NIJ)) and European Union (EU). For instance, the body armor effectiveness is determined according to test standards which vary in different countries based on the final application; where the USA and European standard are the most widely used. National Institute of Justice (NIJ) standard is the most widely used standard for ballistic tests [18] as illustrated in the schematic representation of the ballistic test apparatus (Fig. 2B). NIJ standard explains two threat levels and two subparts; which range from the very low mass projectile and speed (Level 1) to high mass projectiles and speed (Level IV). The target was held by steel frame to provide a clamped condition for all the edges and a rectangular container was put behind the target to express the human body as described by the NIJ



standard. Alkhatib et al. [94] introduced hybrid composite plates for ballistic protection, which were investigated experimentally and numerically to reduce the weight of currently used body armor inserts and satisfy the requirements of the NIJ ballistic protection standards. Risby et al. [95] reported the potential use of coconut shell powder-epoxy composite panel bonded with Twaron CT716 fabric as a hard armour material and the characteristics of its fracture imprints from a specific threat level when subjected to ballistic tests (NIJ Standard 0108.01). The developed coconut shell powder-epoxy composite/Twaron test panel was found to withstand impact equivalent to NIJ Level IIIA using 9 mm FMJ ammunition but perforated at NIJ Level III of 7.62 mm FMJ bullet impacts.

#### 4.2. Failure mechanism of fabric fibers

After impacting the fibrous material with a bullet from a high energy projectile, penetration mechanism take place producing pental forming (dishing), the arrangement of ductile hole and fragmentation. Material properties, projectile's shape, impact speed, target support position, and target dimensions. Distortion of a projectile as a transformation of its energy by the action of the main idea of ballistic protective armors made from fibrous materials [93]. Thus, tensile strength and deformation mode are essential parameters for an armor material [96]. Failure mechanism is observed after impacting a fibrous material with a bullet that exhibits longitudinal waves with a negligible velocity [97] (Fig. 7). When the armor surface is stroked by a projectile, a large strain is produced at the periphery, which results in periphery fracture after reaching a critical value. As the projectile penetrates the armor surface, tensile stress is produced at the target surface. At this regard, the result in adiabatic plugging can be considered, if the projectile geometry and armor features enable energy absorption and heat dissipation. The sound velocity (C) of a substance [6,98] is represented in Equation 1:

$$C = \text{Initial modulus/density } (\rho) \quad (1)$$

A material's failure mechanism is a complicated approach between the projectile and fabric surface which dissipate the energy and minimize the impact damage [99]. For instance, polymer matrix incorporated fabrics enables a fast energy transmission between layers by friction contact [100]. Therefore, polymeric matrix bonding restricts the yarn movement in the armor structure, thereby improving the antiballistic behavior [101]. The impedance (I) and sound velocity (C) also can be expressed based on the mechanical impedance (i) as in Equation 2.

$$C = i/\rho \quad (2)$$

Equations (3 and 4) can express the reflection or transmittance of elastic waves:

$$P_t = [2 I_t / (I_t + I_o) \times P_o] \quad (3)$$

$$P_r = [(I_t - I_o) / (I_t + I_o)] \times P_o \quad (4)$$

where  $P_t$ ,  $P_o$ , and  $P_r$  represent the stress amplitude of transmitted, incident, and reflected waves, respectively, and  $I_t$  and  $I_o$  represent the impedance of transmitted and incident materials, respectively.

The abovementioned equations (1-4) clearly illustrated the elasticity of the impacted waves of a projectile. Thus, the absorption of the impact energy is increased by wave transference to the polymer matrix; this causes matrix cracks in a parallel way to fibers and squandering of the shock energy [102]. Given their wide applications, excellent antiballistic and energy absorption characteristics, water repellent armor nanocomposite surfaces have gained worldwide concern.

**Fig. 7**

#### 4.2.1. Failure mechanism of metallic armor

Arrangement in a ductile hole, cruising and pettalling formations are the most widely reported mechanisms for the antiballistic performance of metallic armor. Projectile's dimensions and shock speed are important in studying the antiballistic performance of material properties [103]. Released and compressive waves are produced when a bullet hit the external surface metallic armor layer. The damage takes place in the impacted place when the impact strain reaches the critical rate. Projectile's penetration produces tensile stress at the impacted surface, adiabatic blocking if the plastic deformation is more than the thermally dissipated value. If the speedy projectile penetrated the objected surface, the penetration may affect its physical characteristics. For thin and thick laminates, the momentum and energy balances, respectively, are widely used. The appreciated modeling facilitated the data correlations for metallic armors have been reported [104]. According to the following equations (Equations 5–7):

$$mV_{12} = Cd\beta \alpha; \quad (5)$$

$$mV_{12}/d^3 = C(t \sec \theta)\alpha/d; \text{ and} \quad (6)$$

$$V_s - V_R = Ct\alpha\beta V_s; \quad (7)$$

where  $m$ ,  $d$ ,  $t$ , and  $\theta$  are the projectile mass and size, the thickness of the armor and the obliquity;  $A$ ,  $\beta$ ,  $\gamma$ , and  $C$  are empirical most remarkable parameters;  $V_s$ ,  $V_R$ , and  $V_L$  represents striking, residual and limits velocities, respectively.

#### 4.2.2. Failure mechanism of ceramic and fibrous armors

Considering their remarkable antiballistic advantages, ceramic armors have attracted considerable attention. The failure mechanism of ceramic armor is discussed based on the bullet's type and velocity; nature of the ceramics; armor configuration; armor thickness; and angle of impact [105]. V50 is used to evaluate the combat responses and the depth of projectile penetration. The failure mechanism is significantly controlled by (i) the structural response period, and (ii) the bullet's erosion. However, the non-backed ceramic is perforated via plugging after the impact reached the elastic border. In addition, the erosion increases the micro-crack formation and form a comminuted area that enhances the bullet's erosion and spread the focused shock on a larger ceramic distance [106].

Extensive research studies are focused on the failure mechanism intents of high-performance fibers. The tensile strength of Zylon, a Japanese fiber, is identical to p-aramids and doublet to Kevlar. Although Zylon provides ultra-lightweight and comfortable vests, it suffered from weak thermal, chemical and humidity resistance. Such limitations reduced restricted their applications in various fields [107-109]. The ballistic

fibers' failure mechanism can be categorized into failures of an individual fiber, individual-ply and multiplied-ply fabrics, and reinforced nanocomposites. A fiber spun type, friction resistance, fabric bonding and bullet properties can control the failure mechanism and antiballistic characteristics of fiber materials. Hitting an individual fiber with a bullet produces both; longitudinal wave with the same sound speed and transverse waves with lower speed [110].

Fibers flow toward the impacted area as a result of spreading the tensile waves away from the projectile zone. The speeds are altered as a result of spreading the velocity of the strain waves [111]. At the contact area of a projectile and armor material, the velocity of the projectile deflects and the perpendicular fiber is removed. Wave spreading induced by friction resistance causes disordering and bending of the perpendicular fibers, according to the determined surface parameters and energies in [Equations \(8 and 9\)](#) [112].

$$\Delta E_{pk} = E_{ys} + S_{yk} + E_f; \quad (8)$$

$$\Delta E_{pk} = (1/2)m(v_i^2 - v_r^2); \quad (9)$$

Where,  $\Delta E_{pk}$ ,  $E_{ys}$ ,  $E_{yk}$ ,  $E_f$  represent the missing kinetic energy, surface's energy of strain, kinetic energy of the surface, as well as the wasted fractional energy. Also, the projectile' mass, initial speed and remaining speed are expressed by  $m$ ,  $v_i$ , and  $v_r$ ; respectively.

#### 4.2.3. Microscopic damage analysis

Microscopic analysis of the damaged specimens can help in better understanding the mechanical response of composites. Filho et al. [113] recorded the microscopic evidence of the failure mechanism of epoxy matrix composites reinforced with piassava fiber against high energy ammunition after the ballistic impact. The main mechanism involves dissipation of energy and composite fragmentation, which is a characteristic of the brittle epoxy matrix. Observations using scanning electron microscopy identified fracture processes associated with piassava microfibril rupture and fiber pullout, in addition to brittle rupture of the epoxy matrix. According to Chouhan et al. [114], microscopic damage investigations demonstrated how the polyurethane matrix could support the retention of UHMWPE fibers under dynamic stress conditions, even after moisture ingestion. Shear and tensile fractures were visible in the fiber failure of the neat fabric, according to microscopic images of failure fracture for the test samples at similar velocities.

Wang et al. [115] investigated the microscopic damage mechanism of B<sub>4</sub>C/2024Al of functionally gradient materials following the ballistic test using SEM pictures of various sites around bullet holes. They reported that the fractured ceramic particles and micro-vacancies caused microscopic damage to the hard and brittle top layer. The fracture of reinforcement particles can take away part of the projectile energy. The degree of microvoid damage and fragmentation is significantly less than that in the top layer in the transition area. The fracture extent of B<sub>4</sub>C tends to decrease remarkably along the penetration direction, which illustrates the difference in energy dissipation and perforation mechanisms at different locations in the B<sub>4</sub>C/2024Al functionally graded materials. Cracks on the surface are also caused by fast solidification and porous

structures. Most of the energy is lost by erosion of the projectile material, and the projectile is exposed to intense abrasion and breakage at the top and transition zones [116]. The extrinsic mechanisms include crack deflection, crack blunting and uncracked-ligament bridging, occurring mainly in the metal-rich region. Because of the difference in ductility between the alloy and ceramic layers, the uncracked ligament bridge of the ductile alloy layers appears in the wake of the crack tip to prevent crack growth, along with zig-zag crack deflection paths [117]. The breakdown of ligament alloy lamellae during significant inelastic deformation is caused by the nucleation and coalescence of micro-voids [118]. Improved resistance to crack propagation is caused by local shielding of the driving force for crack growth, which is primarily caused by the processes of crack arresting and re-nucleation. A number of microcracks are created perpendicular to the loading direction as the ceramic layers are ruptured after a specific amount of strain has been applied. The microscopic damage analyses revealed that this composite had noticeable fracture bridging and convoluted, therefore prolonged crack paths as well as crack bridging, which improves the damage resistance of composite materials [119]. The large instantaneous stresses resulting from the high-speed impact are sufficient to induce dislocations in the composite structure and supply the required energy for the development of dislocations [120]. The presence of sub-grains within the matrix is confirmed by the enlarged micro structure, indicating that the dislocations within the matrix are extensively obliterated [121]. Jackson et al. [122] proposed that the presence of hard particles causes inhomogeneous plastic deformation of materials at high strain rates. Al and its composites are susceptible to developing dislocation microbands through cross-slip of high dislocation energies.

Chaves et al. [123] studied the antiballistic mechanism of epoxy matrix composites reinforced with 10, 20, and 30 vol.% of babassu fibers. The fracture modes of the composites were uncovered by scanning electron microscopy investigations, highlighting brittle fractures in the epoxy matrix, as well as other mechanisms such as fiber breakage and delamination in the fiber composites. According to Li et al. [124], the inclusion of a polyurea coating changed the failure mechanism and resulted in bond breakage in some fibers because of viscosity effects. It was noted that the mechanism of fiber failure shifted toward tensile fracture, which is typified by fiber bifurcation and necking. Microscopic images of failure fracture for some typical test samples at similar velocity showed that fiber failure of neat fabric exhibited shear and tensile fractures.

## 5. Antiballistic factors of woven fabrics

The mechanism of ballistic protective materials is based on two principles as follows [54,125];

- (1) Absorption of impact energy before it completely penetrates the protective material, and;
- (2) Redistribution of impact energy across the surface of the materials.

Accurate assessments of stretching, compressing, and destroying specificities are the direct and vital methods that allow the protective materials to absorb the energy. The fundamental principle of building blocks of body armor is based on fast changing the projectile's kinetic energy to strain energy [126]. Ballistic body armor provides protection via three techniques:

- (i) The kinetic energy of a ballistic projectile is decelerated, stopped and dissipated by the armor material.
- (ii) The armor completely bounces the projectile.
- (iii) A possible combination of the above two techniques.

The generated longitudinal waves (that move in fabric plane) and the transverse waves (that move perpendicular to the fabric planes) are the main factors that can control the antiballistic mechanism. When the tensile waves propagate far from the shocked area, the backed surface moves in the direction of the impacted point and deflected. Energy absorption is the ability of the fabric to control the waves' propagation velocity during a bullet shock. The ballistic structure is influenced with the propagation of the shock waves at high velocity [127]. Fabric's tensile strength, structure, and thickness can control the impact energy dissipating. The missile is deformed and mushroomed as a result of dissipating the missile's energy after collision to the armor surface. Energy absorbed by every layer can be spread across the surface of the armor to approximately 900 m/s speed, until the bullet is stopped.

Hard body armors, such as metals and reinforced plastics, provide antiballistic performance via bullet's bouncing and dissipating the produced energy. The tensile waves express the hitting the armor surface by a ballistic projectile. This result in fracture of the armor surface which results in mechanical failure and cause a perforation. At a certain tensile stress value, multiple fractures can occur. The material changes to plastic when it reaches the extent of elasticity as the applied load increases. The steps are as follows:

- (i) The armor fiber is deformed into a cone-like form by shocking with a missile.
- (ii) The size of the cone of deformation in terms of diameter, height and width enhances progressively with shocking time.
- (iii) The utilized armor fabrics should ensure the complete dissipating of the impacted energy to prevent injuries to the body.

The variation in the size of the cone after shocking was studied under applying of cloth ballistic panels [127]. The speed of the transverse waves was initially enhanced, and then it becomes stable at the rest of the ballistic process. As the cone heights are related to the projectile velocity reduction during the ballistic impact, they are reduced. The armor absorbs and disperses the kinetic energy of a penetrating object.

Woven fabric's architecture is controlled via determining the number and cross-sectional of wrapped yarns. These parameters influence fabric's cover factor, fabric's weight, and the level of energy absorption [128,129]. Different architectures of woven fabrics including plain and basket weaves can be utilized in soft body armors [86,90,128] (Figs. 6B and 8).

The three fabric materials have 50×100 mm in-plane dimensions and composed of the same aramid fabrics. These fabrics vary with changing the yarn's numbers and frequencies; which can affect fabrics' energy absorption. Other methods for soft body armors' woven fabric includes fabrics impregnated with STF, bi-modulus fabric weaves, and electro-rheological fabrics.

**Fig. 8**

## 6. Nanomaterial-building blocks for armors

With the progress in the weapon penetration capability, new armors that protect people against projectiles should be developed. Future body armor should be able to mitigate advanced threats caused by different ammunitions. A critical issue in modeling advanced armor applications is the development of lightweight, ultra-strong, and remarkably tough materials. Other future requirements for designing advanced body armor include minimized bulk, enhanced thermo-physiological comfort, and tactical mobility. Moreover, integration of nanoscale and functional materials represents advanced properties of multirole safeguard included low cost, lightweight and sustainable materials [130]. At the end of the armor's life cycle, recycling and/or easy disposal of bulletproof armor with no hazards in the environment is also essential.

Composite nanomaterials have been focused as a modern trend in ballistic armor because they provide lightweight body armor with enhanced protection from high-velocity projectiles. Super lightweight, robust, ballistic-proof, anti-firing, high energy absorption properties can be introduced by innovation smart nanomaterials. From the military point of view, nanotechnology offers the unlimited advantages for protective surfaces. Nanotechnology allows the creation and exploration of new antiballistic materials [128,131] (Fig. 9).

Recently, body armor is one of the most important applications of nanomaterial-based filler and nanocomposites. The modern generation of ballistic armor system is effective against different ballistic projectiles. Current antiballistic armor materials based on ceramics suffer from high-cost, brittleness and heavy weight, thus developing new armor nanocomposite surfaces is in a continuous progress [132].

Distribution of nanomaterials as fillers in the polymeric matrix provides high synergetic effects on the final composite structure and provides advanced antiballistic fiber materials. These materials exhibit high UV-resistance, resistance to pH solutions and humidity as well as enhanced ballistic-protection and energy absorption. Nanofillers are extensively preferred than microfillers because of the enhanced surface-area to volume ratio in the nanocomposite matrix.

Reinforcing the polymeric matrix with nanofillers afford outstanding high aspect ratio, lightweight, and preferred distribution effects. These nanofillers include graphene-related materials, CNTs, SiO<sub>2</sub>, ZnO, SiC, and Al<sub>2</sub>O<sub>3</sub> and inorganic fullerene-like (IF) materials including WS<sub>2</sub> and MoS<sub>2</sub>. The produced polymer/inorganic hybrid nanocomposite are affected by nanofiller type, size, morphology, production method, and distribution ratio. Nanofillers can also produce multifunctional composites with robustness, high durability, and load-sharing features of the produced fibers, leading to the thermal resistivity, hydrophobicity, and antiballistic performance. Well-distribution of nanofiller in the polymer matrix can improve the nanocomposite's interfacial interactions and bonding strength. Multifunctional composite armor materials can be fabricated by using hybrid nanomaterial fillers for advanced protective applications. Hybrid NPs such as CNTs functionalized with Al<sub>2</sub>O<sub>3</sub> and SiO<sub>2</sub> NPs as well as graphene materials hybridized with one-dimensional NPs (including nanorods, nanowires, and nanotubes) can develop nanostructured multifunctional armor as futuristic protective nanocomposite materials. The charming features of these

materials such as ultra-high robustness, ultimate strength, high surface area, and interfacial tension provide material robustness with enhanced energy absorption. In addition, many nanoreinforced armor systems that can provide notable weight/protection relationships were strongly introduced. These systems offer a potential market for novel ballistic materials with a desirable miniaturization that enables wide applications and comfortable properties.

**Fig. 9**

## **7. Recent body armor nanocomposite designs**

Modeling innovative and ballistic protective nanomaterials for body armor structure is a challenge today. Antiballistic body armor composites have become a better bulletproof layer than the traditional steel body armor because of the weight reduction and improvement in ballistic resistance [133]. Tailored design of newly developed antiballistic nanocomposites has received considerable attention because of reduced weight, cost effectiveness, and high-efficacy body armor. Many military applications included marine bodies, aircraft structures, and lightweight armors are based recently on the design of fiber-reinforced composite (FRC) materials [134]. FRCs offer good mechanical characteristics, design flexibility, ease of fabrication, excellent anticorrosion, and wear and impact resistance [135]. Body armor composites are essential to protect the wearer against many attacks, and they can stop various kinds of threats, such as bullets, weapons, knives, or a combination of different attacks [136]. Body armors can be divided into soft and hard [137]. The first can be utilized in regular bullet and stab-proof vests; the second type is rigid, reinforced armor used in high-risk states by police tactical units and combat soldiers. Scientific interest is directed toward enhancing the shielding capacity of armor structure against projectile impacts. The design of hybrid nanocomposite laminate configurations can provide modern protective shields with lighter and leaner characteristics and higher antiballistic potential than those of commercial armor plates prepared from monolithic materials. Micronano binary structure involved in hybrid nanocomposite materials is technologically structured to allow the superposition of their characteristics to achieve high impact resistance and antiballistic performance [138].

In this aspect, developing of consequence layer-by-layer buildings combines the characteristics of robust structures combined with controlled NPs structure to achieve improved protection capability and distinct surface-strengthening effect [139]. Polymeric resin incorporation also increases the mechanical characteristics, strength, stiffness, impact energy dissipation, and thermal characteristics [140]. A small amount of nanofiller percentages can provide a high degree of strength, toughness, thermal stability and hydrophobicity [141]. An aramid/CNT functionalized nanocomposite fiber with high strength (383 MPa) and stiffness were fabricated vacuum-assisted layer by layer technique. This is caused by the hydrogen bonding and  $\pi$ - $\pi$  correlation and enhanced the mechanical features [142]. A STF was impregnated with Kevlar to improve the antiballistic performance of Kevlar. This STF is composed of polyethylene glycol and colloidal silica. When STF is impacted by a projectile, it behaves as a solid-like surface; then returns back to its fluid



state after finishing the impacted load [143]. Enhancing the performance against ballistic impacts is also caused by the colloidal silica (450 nm) particles that create a sealing coat and form hydro-clusters that improve the hydrodynamic stress in the suspension [144,145]. This impregnation can also provide higher elasticity, lighter weight and higher antiballistic performance than the un-impregnated Kevlar material [146]. Thus, the impregnated STF can increase the friction between the yarns during projectile impact with 50% increased energy absorption capacity and approximately 80% decrease in the Kevlar layers in composite laminate [147]. STF provides yarn flexibility, high opposing to missiles' penetration, and decreased back face deformation after shocking.

For enhancing the antiballistic performance, yarn pull-out technique is also used extensively using inter-yarn friction. This friction force between the individual yarns provides improved fiber alignment which controls the fabric's energy dissipation value. After this value composite failure takes place which limits its applications. The forces of pull-out of less dense material exhibit reduced values as compared to highly-dense analogs. This technique concentrates on fabric dimensions and the directional crimp ratios which affect the crimp extension of the yarn. Aramide-based yarn pull-out fibers with the interface of ZnO nanowire were developed by Hwang et al [148]. The results indicated that this technique enhanced the friction of the aramid/ZnO nanowire interyarn, which improve the energy absorption with higher peak load (11 times). As the most efficient technique, functionalization by nanomaterials is used to provide antiballistic clothes with high performance. Nanomaterials possess active surface area, enhanced aspect ratio, distribution ability at the molecular level, which increase the fiber efficiency for resisting high impact projectiles [149].

### 7.1. NP-surface area for composite armor

The remarkable antiballistic features added by the large surface area of NPs in composite armor technology have attracted considerable attention recently. The improved surface area distributes the ballistic impact forces and consequently prevents projectile penetration. This surface can also reduce the blunt trauma, which is the non-penetration injuries, to the internal organs. A single-ply material cannot afford construction of such ultrahigh ballistic protection, but functional hybrid nanocomposites can afford this purpose. Computational analysis of ceramic hard-faced with  $\text{Al}_2\text{O}_3$  impregnated nanocomposites was reported by Cristescu et al [150]. Results indicated relatively well antiballistic performance with dispersion of kinetic energy through the high-strength dissipation modes, including high shear accompanied with delamination behavior between the adjacent layers, which is the failure mode of composite material. When the backing plate thickness increases, the lamination degree decreases the interlaminar shear fracture energy; the length and the number of delamination are the major factors determining the absorbed energy. The hard shell can cause bullet mushrooming and deformation and retard its movement; the shock absorber distributes the projectile energy and enhances the fracture performance. Graphene nanomaterials, including graphene,

two-dimensional (2D) graphene oxide (GO) hierarchy, and reduced graphene oxide (rGO) structures are effective toward mechanical and antiballistic behavior (Fig. 10A). Graphene possesses the highest ballistic resistance per thickness; hence, it can result in a robust and protective surface [151-153]. Also, they exhibit ultrahigh mechanical stiffness, antibacterial properties, lightweight, large surface area, and ultrahigh thermal conductivity; as a result of their two-dimensional (2D) structure. Graphene has an ultimate tensile strength (nearly 130 GPa), which is greater than CNT. GO sheets are thicker than the pristine graphite sheets. Also, the carbon atoms of GO sheets are hybridized in  $sp^3$  type with the presence of covalently bound oxygen atoms. The high negative charges of GO surface obtained after dispersion in water is caused by the ionization of -COOH and -OH units. The sheet plane of GO contains ketone carbonyl, acid and ester units as edged groups. Such reactive groups are ready for surface modification reaction to yield functionalized graphene-based materials.

Fabrication of graphitic carbon nitride  $g-C_3N_4$  materials with high chemical, mechanical, and thermal stability, low cost, ease of preparation, visible light response is of interest to produce effective protective materials [154]. However,  $g-C_3N_4$  is universally known to be efficient photocatalyst, their superior mechanical characteristics have driven research toward their utilization for bull-proof nanocomposite armors. As a multi-layer NPs, GNPs consist of 10-30 graphene sheets and it has much retention to the single layer features. These materials are a cost-effective and facile way to produce graphene with a single layer. Therefore, the insertion of graphene sheets and platelets to a polyurethane matrix can reinforce the ballistic protective properties (Fig. 10B). This model introduces an essential three-layer bonded polymer to the oxygen bonded to the graphene. This model can provide high antiballistic properties, durability, low cost and lightweight armor fibers. Block copolymers can fuse together the mechanical and surface advantages of two polymers to introduce many unique properties. Other block copolymer based on polystyrene/polydimethylsiloxane (PDMS), which is widely utilized as polystyrene, can model the stiff crystalline regions of polyurethane; PDMS can also simulate the rubbery amorphous regions of polyurethane [155,156]. Such copolymer represented an advanced model for combining the robustness of polystyrene and the surface inertness of PDMS.

## 7.2. Nanocomposites for high energy absorption

Because metals possess high absorption energy to the projectile shocks, they are extensively used for antiballistic purposes. The ability to absorb the impact energy represents a main task in designing ballistic-proof surfaces [157]. Energy absorption of polymer composites is different from that of metals; metals exert no plastic deformation, and polymer composites show stress-strain relationships, and they can absorb the impacted energy. Toughness and internal damping are essential polymer properties that can control the vibration, fatigue, and fracture toughness. These properties can control the crack growth and fracture, which are major factors affecting the impacted energy [158]. The use of nanoscale reinforcement fibers or particles affords better antiballistic performance in the focused composites than that of microscaled composites. The

nanofiller nature, morphology, dispersion, dimension, and volume fraction of the resin are the main factors in the antiballistic properties. Also, the matrix-NPs' interfacial characteristics are essential to design protective nanocomposites [159]. Micro-nano binary structure can also considerably influence the impacted energy absorption. Glassy spheres and rubber particles are examples of micro-sized rigid and elastic particles, and rigid NPs are represented in several nanomaterials, such as silica, titania, and alumina NPs as well as CNTs [160].

### 7.3. Key-effective NP-based filler stiffness

Elastic NPs can increase the impact toughness of nanocomposites. Elastic modulus and hardness are improved by incorporation of rigid fillers. The impact energy of high-density polyethylene can be improved to approximately 200% by incorporation of 0.2 vol. % rigid  $\text{CaCO}_3$  (600 nm particle size) [161]. The stiffness, impact energy, and failure strain of epoxy resin are also improved with incorporation of  $\text{Al}_2\text{O}_3$  NPs (1 vol. %–2 vol. %) [116,161]. These excellent characteristics are achieved only by using nanofillers. By contrast, such improvements are not observed in conventional microparticles. An epoxy vinyl ester matrix was supported with a core-shell rubber (CSR) NPs to improve the toughness properties. Nanoclay is also used to improve the polyester resin (PES) characteristics in conventional glass FRC; results reflected that the interlaminar nanocomposites' fracture toughness is largely decreased compared with that of the unfilled resin [162]. The attachments between matrix and NPs-based fillers with different sizes, shapes, morphologies, geometries and features can control the ability of rigid particles for energy dissipation [163].

#### 7.3.1. Key-geometric architectures of NP-based fillers

$\text{SiO}_2$  and  $\text{Al}_2\text{O}_3$  NPs, nanofibers, nanotubes, and nanoclay represent extensively applied nanofillers. Impact toughness can be reduced with the dispersion of montmorillonite NPS, while the fracture toughness is enhanced by insertion of  $\text{Al}_2\text{O}_3$  nanowhiskers and glass fibers in polymer resin [43]. Polypropylene (PP) impact strength is also improved with the addition of 1 wt. % CNT [164]. High impact toughness and stiffness, which are main functions of the Young's modulus of CNTs, are observed for polymers reinforced with CNT [165].

#### 7.3.2. Volume fraction and interparticle distance of NP-based fillers

To increase the toughening of particle-modified semi-crystalline polymers, the interparticle distance is introduced. The interparticle distance belongs to both the NP concentration and average size [166], where controlling these parameters result in toughness. Enhancing the size of NP can enhance the fracture toughness. Also, nanoclay was used to improve the epoxy toughness owing to its high volume fraction [167].

#### 7.3.3. Sizable effects of NP-based fillers

Toughness and energy absorption are largely influenced with the distributed filler size ranging from micro- to nanoscale. The tensile characteristics of epoxy polymer enriched with titanium dioxide (32 nm) are higher than those of their analogs enriched with micro-sized  $\text{TiO}_2$  (24  $\mu\text{m}$ ). Silica nanofiller composites exhibit superior failure strain than that of silica micro-composites [168]. The compression strength of flexible polyurethane is improved compared with that of analog with micro-composites. The tensile strength also improves with particle diameter reduction, and it only reduces with reduced NP diameter only for poor dispersion [169]. Higher tensile modulus, elasticity, and robustness were reported for nanofilled polyurethane than microfilled analog. The fracture toughness of an epoxy/micro-silica composite is improved by incorporating  $\text{SiO}_2$  NPs. Fig. 11A indicates the rupture of an epoxy resin filled with micro-silica after and the incorporated with silica NPs [151,170].

Fig. 11B reflects the influences of NP-diameter on the strain and stress of vinyl ester composite enriched with spherical  $\text{Al}_2\text{O}_3$  particles [163]. With the reduction of particle size scale from micrometer to the nanometer, Young's modulus increased slightly. Also, the tensile strength reduced with decreasing the particle size at the nanometer scale because of the poor nanofiller distribution. Excellent-distribution of nanofillers in the polymeric matrix can improve the mechanical, antiballistic and durability of the armor materials. This is caused by the increased surface area of NPs, enhanced matrix-nanofiller interfacial tension and bonding strength. Also, energy absorption and tensile strength are increased while the fracture resistance is reduced by nanofiller distribution. Nanoengineered composites with energy absorption properties are important for the current field of study. Embedding process of nanofiller-type materials and formulation of nanocomposites can result in the following:

- ❖ Cause cost savings via addition of small quantities of inexpensive nanofillers;
- ❖ Reduce the weight and thickness of the tailored nanomaterial composites; and
- ❖ Increase the specific absorption energy, specific strength, and tensile modulus.

#### 7.3.4. Key- morphological architectures of NP-based fillers

NPs with smooth particle topology commonly possess minimum resistance to debonding and maximum energy absorption compared with that of coarse NPs. High-density polyethylene reinforcement with microsmooth hydroxyl A (HA) particle can increase the interfacial strength and absorbed impact energy. The surface roughness may represent an important factor for reinforcement because surfaces with smooth topology show disordered shapes, but particles with rough morphology are spherical. The angularities and edges of nanofillers enable failure under impact energy because of the localized stress concentrations [171]. Well-distributed nanofiller can remarkably increase the energy absorption capability [172,173]. Nanofiller distribution is enhanced by using several techniques, such as grafting silane molecules onto the surface of CNTs [174]; treating CNTs with a nonionic surfactant [175] also enhances CNT distribution in an epoxy matrix. Consequently, fracture toughness is directly improved compared with that of composites containing

untreated CNTs. Decreasing the impact strength of the carbon nanofibers is carried out by treating with oxygen plasma [176].

#### 7.3.5. Different types of nanofillers and matrices for formation nanocomposites

Different interfacial bondings and antiballistic performances are observed by applying various types of fillers and matrix pairs. The stress transfer energy of MWCNT matrix is essential for ballistic fibers [177]. Transferring the impacted load from the polymeric bonds to the CNT surface depend on the nanocomposite formation process which alters the stiffness features [178]. Enhanced surface strengthening and improved interphase region can be largely affected with NP modifications [168,179]. Different CNTs included single-wall CNTs (SWCNTs), double-wall CNTs (DWCNTs), and MWCNTs were mixed with epoxy resin to study nanocomposites' fracture toughness (Fig. 12) [180]. Utilizing the same preparation technique, the best effect was caused by dispersing double-wall carbon nanotube in the epoxy polymer. Polyacrylate (PA), polyimide (PI) and PP resins were supported with SiO<sub>2</sub> NPs to form developed nanocomposites with lower energy impact than virgin PA. The effect of lowering the impact was in the following order PA/SiO<sub>2</sub> > PP/SiO<sub>2</sub> > PI/SiO<sub>2</sub> > PPA [181]. Additionally, absorption of the shocked energy can be significantly changed with nanofiller insertion compared with that of unfilled matrix [182,183] because of the changed interfacial bonding. The plastic deformation of high-density polyethylene is greatly influenced by incorporation of nano-CaCO<sub>3</sub> [184]. A failure mechanism is observed for WS<sub>2</sub>-glass/epoxy nanoclay [185]. By using different nanoclay concentrations, the lowest impact speed was observed at 5 wt.%.

Improving toughness and antiballistic performance of PP/clay nanocomposites is affected with the strong bonding and nucleating influence of clay loading by large integral space and decreasing spherulite size. Weak interfacial interaction between PE and clay can also reduce toughness [186,187]. Thus, any change in the geometry of material or dispersion of nanofiller in the same resin can directly influence the failure mechanism and energy absorption of the armor surface [187-189].

**Fig. 12**

### 8. Superlightweight nanodesigned armors

The overall scales to develop new antiballistic materials are increased after the worst terrorist incidents in beginning of 21<sup>st</sup> century. High impact resistance, super lightweight, smart, high stiffness and elevated strength are among the most important requirements in the modern armors [190,191]. Given values that the specific properties of nanocomposites are higher than those of conventional materials, such as steel. These super lightweight nanocomposite materials are promising nowadays for engineering of antiballistic armors.

The antiballistic nanostructured armors are subjected to different loadings and impact conditions during their surface life. Designing antiballistic nanocomposite armor is based on the impact resistance properties and energy dissipating techniques [192]. The shock velocity (low or high) is an essential parameter in controlling impact events. High velocity impact is accompanied with shorter contact time of the impactor than that of

the low velocity impact [193]. Hence, the response from the structured armor is controlled by the composite behavior and feature in the adjacent impacted zone. Fiber type, volume fraction, resin-matrix property, NP-based filler' size, shape geometry, and morphology and projectile's energy are the main factors that can control high velocity impacts [194,195]. Punching, fiber breaking and delamination are the three segmental stages that can control the penetration process. These stages are the focal for modeling antiballistic materials with considerable failure mechanism. The strain energy of the nanocomposites was also added in Gu's model [196] to simulate delamination and damage from high velocity impact [197]. According to these modeling studies, the delaminated area increases with increasing impact velocity, until penetration of the ballistic limit. Then, the delaminated area decreases with the velocity increase. Another study considered the nanocomposites' compressive strain and propagation of stress wave through the thickness [198]. Considering the resistance against damage of the polymer and NPs is necessary to develop antiballistic composites.

### 8.1. Aluminum-based nanofillers

Given their cost effectiveness, ease of process ability, and excellent antiballistic performance, aluminum (Al) ceramic material represents a unique NP in developing nanocomposites [199,200]. Al ceramics can dissipate impacted energy accompanied with bend prevention of the tile [201,202]. Aluminum materials and nanocomposites are also introduced as suitable alternatives for steel armor [13,203]. Al is one of the most commonly used metal alloys with weight reduction as its major importance. Nanoengineered Al-based armor materials display outstanding ballistic protective characteristics [204]. The antiballistic impact of nanostructured aluminum composites is carried out through the following:

- ❖ Enhanced mechanical characteristics with remarkably high antiballistic performance;
- ❖ Reinforcement of nanocrystalline core structure;
- ❖ Strengthening effect through particle size length-scale reinforcement; and
- ❖ Enhanced ductility via incorporating a certain volume fraction of particles.

High ductility with superior specific strengths under high deformation rates are the major properties of aluminum-based materials. Fiber-metal laminates (FML) was investigated as antiballistic skin by Villanueva and Cantwell [85]. Results revealed that applying aluminum foams associated with FML causes good performance of approximately 120 J. A new solution is developed through well dispersion of NPs in the FML and epoxy systems and formation of nanocomposites [205]. Nanofillers of  $\text{Al}_2\text{O}_3$  are also incorporated in epoxy resin-reinforced Kevlar fabrics to develop newly structured bulletproof nanocomposite armor [206,207]. Different thicknesses of nanocomposite plates are used for comparable studies and to indicate the degree of energy absorption of each plate in the antiballistic tests. The highest energy absorption with 400 m/s impact velocity is achieved via a stacking sequence of 30 layers of laminates [208].

### 8.2. Inorganic fullerene-like (IF) fillers

In 1985, a soccer-ball shaped Buckminster fullerene was discovered by Harry Kroto, which accomplished a developed branch of chemistry [209]. IF materials are closed cage NPs and the IF nanostructures are represented by  $\text{MX}_2$  such as  $\text{WS}_2$ ,  $\text{MoS}_2$ ,  $\text{NbSe}_2$ ,  $\text{TiSe}_2$ , and  $\text{WTe}_2$  which generally result in nonhollow nanostructures [210]. IF materials are applied in various fields, such as chemistry, physics, material science, and biology. Extensive research is focused on IF; this material presents many important properties, including considerably high mechanical performance and the ability to transform to diamond under pressure [211,212]. These IF-based filler materials exhibit high resistance against flammability and it is chemically stable. These IF-based fillers of elastic matrices produced flexible-outstanding composites for ballistic armors. The IF-incorporated composites also showed an excellent capability as shock absorbing materials of missile energy after impacting [213]. Furthermore, IF-incorporated polymer composites also possess various advantages, such as toughness, processability, and ease of application with remarkable geometrical characteristics. These ultrahigh-strength fullerene-like materials were successfully prepared by Tenne et.al. in 1992. Although they exhibit a similar closed-cage configuration to carbon, a typical polyhedral lattice with a spherical and stretched structure was reported [214,215].

A film of  $\text{WS}_2$  was prepared on a quartz substrate via annealing in hydrogen sulfide at  $1000\text{ }^\circ\text{C}$ , while a 3D  $\text{MoS}_2$  with concentric structures and 20 nm of molybdenum layer thickness was annealed in hydrogen sulfide and  $\text{N}_2/\text{H}_2$  mixture at  $1050\text{ }^\circ\text{C}$  after oxidized at  $550\text{ }^\circ\text{C}$ . Such materials resemble the graphite structure in forming layers over each other that can establish ultra-strong interfacial bonding [215]. Also,  $\text{MoS}_2$  films are attached via van der Waals bonds with highly anisotropic layers that control their chemical and physical characteristics [216]. In  $\text{MoS}_2$  structure, the S atoms are commonly inert; Mo shows fourfold bonds, and S displays twofold bonds in the nano-regime structures, leading to instability in the planar structure. Stable non-tubular or spherical structures can be attained by folding these sheets. These IF types exhibit excellent functional properties, such as the outstanding lubricant behavior with a reduced friction coefficient and depressed wear rate, particularly under high loads, over covalent platelet crystal analogues. Additionally, insertion of such IFs in porous resins results in reduced friction and enhanced wear-resistant performance.

Nearly 1000,000 Kg of  $\text{WS}_2$  was ordered in 2005 and it continuously increases. As antiballistic material, IF materials resist 25 GPa impacts or more without any structural degradation. Consequently, these nanostructured materials are applied in antiballistic armors. These achievements are inevitable result of their mechanical properties obtained by their excellent structural and crystalline features. IF- $\text{WS}_2$  can largely resist the increased hydrostatic pressures; nonetheless, at low pressures, they are totally exfoliated by compressive uniaxial Hertzian contact [217,218].

### 8.3. CNTs-based bulletproof armors

The Lightweight properties and robustness of CNTs enable their antiballistic performance. According to the Swedish Defense Research Agency, the ballistic proof requirements for energy absorption materials [219,220]:



- ❖ NT-reinforced polymeric nanocomposite fibers with increased strength;
- ❖ Shock and acoustic absorption of porous nanocomposites;
- ❖ Reduced flammability;
- ❖ Ability to be used as microwave absorber in aerospace application; and
- ❖ High resistance against impact/damage of CFRP.

CNT structures are analogues to those of fullerenes, but they are characterized by their cylindrical shape, not spheres, with shape [221,222]. CNTs possess many advantages, such as ultrahigh tensile strength, high modulus, and low density, which support their applications in various fields [223,224]. CNTs require lower energy for breaking the bonds (600 J/g) than para-aramid and a spider's web thread which require 27–33 and 150 J/g, respectively [225,226]. Fig. 13A was developed to explain the ballistic resistance capacity of CNT materials by discussing the bullet impact mechanism. The mechanism discusses how energy, force, and velocity differ with changing the time at ballistic striking. The bullet speed is reduced because of the energy by impacting the CNTs which reflected that CNTs absorb the energy until the energy reaches zero. When the CNTs release their energies, the bullet is bound back. The outstanding features of CNTs enabled their potential as nanofillers to reinforce the fabric polymer resins used in lightweight bullet-proof armor manufacturing. Consequently, CNTs show evidence as a reinforcing phase for resistant materials against ballistic penetration or high-speed impact.

Also, CNTs exhibit the best elastic modulus among different materials because of their structure order makes them the strongest fibers [227]. These characteristics have directed extensive research on CNTs toward lightweight and low-density armor nanocomposites. A major challenge is that the small diameter of CNTs allows their applications only as nanofillers; therefore, fabrication of fibers with billions of CNTs can provide the mechanical characteristics of a single nanotube with high elasticity and low Young modulus [228,229]. The main features of CNT-based armors were mentioned in Table 4.

CNTs dispersion may enhance the nanocomposite robustness and also can improve the aluminum and nickel alloys' strength parameters [230]. CNT-based fibers possess high tensile strength, large aspect ratio, tensile strain energy, and bridging with local deboning [231]. They also exhibit higher interfacial shear strength when incorporated in a polymer matrix than that of the other fillers. This high shear strength is a result of the formation of supramolecular bonding that covers the nanofillers with thicker interface layer than those of conventional composites [232,233]. MWCNTs (0.5 wt. %) are dispersed in epoxy resin to enhance the antiballistic impact of CFRP. Results indicated that the fracture resistance, energy absorption capability, and antiballistic behavior of the CFRPs are remarkably improved with incorporation of well-dispersed MWCNT fillers [217,232]. Addition of CNTs and nanosized CSR particles to Kevlar fiber-reinforced epoxy also improves the impact energy absorption capacity. Sing et al. [234] reported the effect of bucky paper interleaves and dispersed MWCNT network on static and dynamic mechanical properties of Kevlar-epoxy composites (Fig. 13 B-D).

**Fig. 13**

#### 8.4. CNT-based protective armor designs

CNT forests were prepared over iron-coated silicon wafer using acetylene-based chemical vapor deposition at 700 °C [233]. A major property of CNT forest is that when CNTs at the forest's edge are pulled a way, the CNTs can attach to one another to form a continuous strand. CNTs assembling in this technique to form twisted form result in sheets suitable for yarn production. Typical, scanning electron microscopic (SEM) images of CNT drawable forests and its potential assembly in geometric yarns were shown in Fig. 13e-I. The CNT drawable forests provide fiber toughness and high electrical conductivity. This CNT forest drawability assembling diminishes the need for its distribution in fluid and provides well-distributed nanocomposite. A comparison between conventional cotton and CNT-based yarns reflected the high effectiveness of CNT forest yarns. Although, the cotton fiber exhibited ribbon-like structure with a dimension of 10 mm and friction of about 100 fibers, but the CNT yarn showed much fine size and morphology, leading to form fibers with high mechanical strength. Compared with conventional carbon yarns, the CNT-based yarns exhibit high toughness and mechanical strength, leading to outstanding antiballistic properties. A closer look to microscopic images of CNT-based yarns in Fig. 13e-I indicated that the CNT is streaming off the forest and also showed the close-up of the CNTs adjacent to the forest wall alignment. Such CNT-based yarn fillers are superior to form high robustness, elastic modulus and lightweight armors compared with Kevlar analogue [232,234].

As a force-driven modulation of CNT composites, developments of CNT sheets and nanowebs are promising for multifunctional ballistic protective armor. Another technique was reported to completely deform CNT sheets in a reversible way with a stable conductive property. Developed spinners were used to spin forests based on CNTs; which was reliable for the world fabric production. This method is also promising for CNT yarns in antiballistic performance.

#### 8.5. Protective nanographite composites

Modeling novel nanocomposite-based armor materials is at the research interest in the recent days. This part presents the recent route to control design of graphene nanostructure with its intrinsic organization, structural configurations, and geometrical assemblies for next generation of multi-functional nanocomposite matrices, leading to hierarchical model and large-scale manufacture of protective ballistic armor.

Graphite sheets are added to fiber glass/epoxy laminates. The resultant nanocomposites offer real space of evidence of an improvement in antiballistic performance in terms of high-velocity impact resistance and failure mechanism [235]. The dominant loads of graphite sheets can also improve the delamination for the front and back surfaces of the bullet proof armor nanocomposites. Vacuum filtration and van der Waals forces usually produce closely-packed graphite sheets which suffer from improper distributions nanofillers in polymeric composites [236]. Exfoliation and good compatibility yield graphene which can be achieved via mechanical treatment or anchoring sheets with definite NPs. The exfoliated graphene sheets exhibit high impact resistance, lightweight, durability, high mechanical features such as stiffness and strength. Thus,

exfoliated graphene materials exhibit higher antiballistic features than the unexfoliated analogous. Fig. 10 (A-a) is a schematic illustration of the closely backed graphite sheets and Fig. 10 (A-b) is the SEM image of the graphite sheets before the volume expansion or exfoliation. After thermal shock the closely backed material shape is damaged as indicated in the SEM micrograph in Fig. 10 (A-c). Exfoliated graphene oxide with nanoparticle distribution can be carried out by mechanical or chemical routes. High mechanical properties were caused by graphene anchored with SiO<sub>2</sub> nanocomposites in the nitrile rubber and a schematic illustration and SEM of graphene/inorganic silicate layer sheets are represented in Fig. 10 (A-d and A-e). The Young's modulus of the epoxy composite was increased with 54% and the tensile strength was decreased with 36% by incorporation of 10 wt.% of layered SiO<sub>2</sub> silicate [236].

A newly developed composite for ballistic protection is based on oxidative unzipping of MWCNTs into functionalized graphene nanoribbons; this stacked band nanocomposites is also suitably distributed in Kevlar composites. Structurally-shaped graphene nanoribbons are functionalized to prevent agglomerations and clustering by Interiorly uniform particle–particle interaction. One of biggest prospects for renovation of powerful built-in nanocomposites is the well distribution and multifunctionality, which can successfully increase the mechanical properties. Furthermore, a super-scalable model of nanocomposites fabricated by using magnesium-titanium (MgTi) alloy-incorporated graphene-based nano-geometric structures offered a diverse range of spatial yield of fabric materials with toughness, tensile strength, and failure strain characteristics [237].

#### 8.5.1. Hybrid polymeric graphene nanocomposites

Owing to their extraordinary mechanical properties, graphene composites are extensively used in different fields [238,239]. As primary structural materials, the graphene-based nano-geometric structures were incorporated in various metals, metal oxides, polymers, organic-inorganic hybrids, and alloys would allow for the uniqueness of all module configurations to utilize their spatial properties (Fig. 10, 11). Excellent physical, chemical and mechanical features as well as elegant stiff and tough, and thermally-conductive characteristics are the main merits of graphene composites [240,241]. However, graphenic composites are still suffering from the lack of modeling constitutes for building blocks of ballistic protection [242-246]. For example, polymeric graphene nanocomposites are affected by the used resin features, the sort of graphene, distribution percentage and interfacial bondings of polymer-graphene interactions [246]. In specific, thermosetting polymers are affected greatly by the distribution of graphene-based nano-geometric structures; where the electrical conductivity, hardness, and stiffness are improved. The high mechanical properties and lightweight of the formed graphene composites enable their utilization especially in military fields [247]. The mechanical reinforcement of an epoxy matrix was greatly improved by 30-120-fold ranges with incorporation of graphene fillers compared with other-epoxy composite fabricated by addition of silica, alumina, and titania nanomaterials. The functionality of it rich spatial distribution of small amount of graphene nanofiller affords on-site matrix's robustness by more than 50% of toughness of other silica,

alumina, and titania nanofillers. [248] The CNTs filler-incorporated epoxy matrices may offer 48% increase in a fracture toughness of, but the resultant epoxy composites showed fourfold higher weight-fraction than that of equivalent amount of graphene filler-reinforced polymer epoxy-matric composites.

Graphenic carbon nitride ( $g\text{-C}_3\text{N}_4$ ) attracted great interest in materials science arena and attracted extensive interdisciplinary hotspots for designing robust and high mechanical materials.  $g\text{-C}_3\text{N}_4$  were employed to enhance the mechanical features of epoxy vinyl ester; where the tensile strength was increased up to 49.49% [249].  $g\text{-C}_3\text{N}_4$  nanosheets are hydrophobic, low solubility and aggregation features in different solvents, which are due to the strong  $\pi\text{-}\pi$  stacking of the  $sp^2$  hybridization. The  $S_{\text{BET}}$  of pristine  $g\text{-C}_3\text{N}_4$  is ca.  $8\text{ m}^2/\text{g}$  because of its densely stacked layers. Such a small  $S_{\text{BET}}$  greatly obstruct the wide applications of  $g\text{-C}_3\text{N}_4$ .  $g\text{-C}_3\text{N}_4$  could be fully exfoliated into monolayer with  $S_{\text{BET}}$  of  $2500\text{ m}^2/\text{g}$ . Many techniques included liquid phase, strong acid/base chemical and thermal oxidation etching exfoliations have been developed to controlled fabrication of  $g\text{-C}_3\text{N}_4$  nanosheets, or single atomic layers. The antibacterial and mechanical features of  $g\text{-C}_3\text{N}_4$  are enhanced by decorating with aminated  $\text{Ag}_3\text{PO}_4$ . A membrane of polyethersulfone membrane filled with a nanocomposite of  $g\text{-C}_3\text{N}_4/\text{Ag}_3\text{PO}_4$  was developed to introduce mechanical and antibacterial applications through the nonsolvent induced phase inversion [250] (Fig. 14A). Also, an antibacterial nanocomposite of  $\text{GO}/g\text{-C}_3\text{N}_4$  hybrids was designed with photocatalytic properties via sonochemical technique at ambient temperature (Fig. 14B). The nanocomposite approved antibacterial efficiency against *Escherichia coli* and also stable photocatalytic features after using for four times and applied for water purification [251]. Large-scale manufacturing technologies of graphene-reinforced resin composites are still required a major challenge included graphene cost, methodological standardization of graphene-incorporated matrix, and super-large modulation of graphene dispersion routes, respectively. To develop high-performance, low capital and smart antiballistic clothes, multifunctional solutions and challenges in terms of materials, composites, fabrication process and product features or properties should be controlled as follows:

- Producing multifunctional graphene composites in large quantities.
- Developing of applicable exfoliation methods that overcome the mechanical-controlled strategy.
- Difficulty to create new functionalization methods.
- Characteristic analyses of fabricated graphene materials.
- Overcoming the problem-based reduction of flexibility of graphene composites.
- Further studying of the mechanical influence of distributed graphene materials into polymer nanocomposites.
- Limitation to find out suitable model objects and software simulation programs to structurally - controlled designs of graphene nanocomposites at wide-ranges of truckloads of graphene materials.
- Providing non-prescribed geometric and structural features of composites fabricated by polymer-incorporated variable graphene materials.

Up-to-date, fabrication method of antiballistic graphene composites that provide multi-functionalities in terms of elevated strength, predictability, flexibility, super lightweight and the high adsorption energy remains challenge. In addition, the overall quality scales of a broad-range accessibility of novel graphene-based nanocomposites in vehicle body manufactures or architectures did not yet consider as potential in industry. As mentioned above, several critical points should be covered within the development of graphene-nanocomposite materials. Although, significant attention has been created to evaluate the CO<sub>2</sub> in life-cycle assessment of the developed materials, however, no reliable information is now available on how to evaluate the advantages and disadvantages of the ultimate design and manufacture process of the ballistic protection.

**Fig. 14**

#### *8.5.2. Widespread manufacturing of exfoliated graphene materials*

The extraordinary electronic, thermomechanical, and physical characteristics of graphene materials in various fields have prompted research toward engineering innovative structures for various application fields. Controlling the properties of their graphene nanocomposites is necessary for achieving the maximum benefit of their potentials with long-term durability. Also, for enhancing their rich spatial mechanical, physical and surface features, the polymer-nanofiller interfacial interaction and prescriptive effect of graphene materials in terms of structurally-shaped geometry, usage loads, formidable diffusion and dense interaction along matrices should be studied extensively.

Chemical and mechanical exfoliation, chemical vapor deposition, and epitaxial growth on SiC surface are mainly the fabrication routes to produce graphene-based nano-geometric materials. It is essential to merge the excellent graphene features of electrical, physico-chemical and mechanical characteristics in structurally-stable and mechanically-exfoliated graphene-based composites. The primary keys for exfoliated graphene composite fabrication are the cost-savings and large-scale production and purification, and prospectively-dense structure without defects, which may open widespread applications.

Developing exfoliated graphene nanomaterials on a large scale and cost-savings can be carried out by microwave and gases-based exfoliations. Also, the mechanical process can produce nanoflakes and nanosheet structures via ultrasonication process. A great concern was awarded to control the design of graphene nanosheets with enhanced number of sheets and their reinforced nanocomposites. Graphene flakes were reported to strengthen a polymeric resin, while graphene trilayers suffer from interlayer spacing which may reduce the polymeric chains in the composite which reduce the strengthening ability [252]. Many layers of graphene exhibit elevated fractional volume than a single layer. Therefore, it is necessary to balance loading on the number of layers of graphene and reinforcing ability.

GO was reduced to graphene via chemical or thermal methods for nanocomposite applications, however, these methods can produce large defects. This may decrease the product's quality and limit their applications.

Graphene functionalization is enviable to improve the features of graphene composites. Excellent graphene oxide should possess suitable percentage of oxygen to facilitate introducing functional units that chemically-activated the surfaces [253]. These actively-functionalized surfaces enabled to create formidable covalent and non-covalent reactions on graphene layers and along their edges, undulations, ridges and anticlines [253]. In turn, reactions of pristine graphene can only be radical reactions or interaction on the C-C linkages [254]. The developing a rich diversity of graphene-based composites with potential occupant surface patterns may lead to complex ballistic protection applications.

#### *8.5.3. Integrated, super-scalable modeling for graphene functional applications*

New concepts of control modeling and entire shape orientation of graphene-based nano-geometric composites will lead to unlimited applications and structural design developments [255] (Fig. 15). Worldwide concerns are given to graphene-based polymer composites and fiber-based polymer composites for designing the antiballistic and protective material surfaces. Unlocking control of the deformation, fracture and failure of graphene-based nano-geometric composites is still at basic research level for armor applications [256,257] (Fig. 15C).

An outstanding process and integration along methodologies used for design modeling can offer high performance structural material applications. For instance, studying the changes in the modulus of elasticity as a function of temperature is necessary. Thus, elastic modulus of these graphene nanocomposites was studied at a definite thermal condition [258].

In terms of developed nanocomposites, the molecular model was used to determine the atomic interactions and resin-nanofiller bonding [259], and continuum model was applied to study the mixture function [260]. However, the multiscale approach was focused on studying both of the previous models. Wang et al. [260] and Awasthi et al. also established their models that are based on stimulating the dynamics of molecular approach. These studies included transporting the load between polymer and graphene nanofillers. Continuum model was applied for exploring the standards of nanocomposite elasticity, when graphene materials were dispersed in a random distribution [261,262]. Also, the multiscale approach was utilized for investigating the standards of elasticity of nanocomposites [263] and for explaining the nanocomposite's bucking property [264].

Together, modeling aims to develop and apply methods, algorithms, and tools to support the graphene-based polymer composite simulation. This procedure is depicted in Fig. 15; where electronics, automatic, microstructures and microscale materials are modeled based on the length scale control. This modeling for woven fabric can combine both macroscale and mesoscale models. Graphene-based multi-scale models are efficient antiballistic fiber materials. The multiscale can provide much information about fabric response, damage, and failure after impacting by a projectile's bullet [265]. Towards impact blast purposes, studying the elasto-plastic performance and mechanical properties is essential for designing nonlinearity materials based polymeric matrix nanocomposites [266]. In general, constructive super-scalable models are demanded

to provide information about graphene composite structures, crashworthiness simulation and the undergoing deformation.

**Fig. 15**

#### *8.5.4. Design of graphene-based nanocomposite structures*

In-situ, solution casting, melting, electrospinning methods have been developed for establishing robust graphene materials into graphene-polymer nanocomposite structures [267,268]. Graphene distribution and interfacial bondings with the matrix should be discussed extensively. Modified graphene surface is an important process to develop supreme characteristics. This surface modification process can be carried out via (i) covalent interaction as result of surface esterification and amidation, and (ii) non-covalent binding through hydrogen bondings and interfacial interactions. Graphene modification can determine the types of bondings between the polymeric resin and graphene-based fillers in a nanocomposite material. Thermoplastic polymer materials can be recycled much easier than thermosets. These thermoplastic materials undergo faster curing, yield lighter films and more robust materials than thermosets [269].

Developing graphene multilayers, producing GO sheets by Hummers approach, chemical and mechanical exfoliations, functionalization of graphene materials are essential methods to produce controlled graphene structures. Excellent distribution of graphene nanofillers in the polymeric resin can enhance the nanocomposite features in terms of high modulus, low density, and giant in-plane speed of sound. The mechanical exfoliation of pyrolytic graphite may form MGL. Because of its layered building blocks based on 2-dimentional carbons, multilayer graphene (MLG) is outstanding anisotropic fillers (Fig. 15B). The MLG-polymer composites certainly provide spatial antiballistic features, high resistance to tensile deformation, significant surface area, and penetration energy compared with a single graphene sheet used (Fig. 15B,C) [270]. According to miniaturized ballistic tests, a 10-100 nm MLG-membrane thickness showed a high-strain rate tensile deformation to equivalent 30-300 nm thick of graphene layers at similarly specific area. Given to the demanded penetration energy for projectile penetration through MLG-membrane, the in-plane strain-rate tensile is thickness-dependent function. The specific penetration energy for MLG is 10 folds more than that commonly used microscopic steel fabric sheets at projectile distance target of 600 m/s (meters/second) (Fig. 16A). Furthermore, confined, 20- $\mu$ m-thick elasto-layers distributed along PDMS matrices may form a antiballistic nanocomposites with high-temperature, and sound-proof resistance, leading to powerful inhibition of shock waves exaggerated through air.

The impact of composites in terms of extensive damage area, and penetration hole forms after striking exposure face area is evidence in Fig. 16. Typically, a set of petals described the penetration hole shapes, as an exemplary breakthrough penetration puncture. Under the impacted projectile, a wide range of surface deterioration included fractures, folding, losing parts or ridges, and delamination of membrane, as illustrated (see arrow and its direction). As a result of membrane body damage, radical cracks may be initiated strongly at the impact ridges, edges and center, leading to asymmetric shapes in penetration holes, likely to



be petal-, circular-hole objects (Fig. 16 B-a to B-d). Using MLG nanofillers may reduce the penetration energy; diminish the crack directions and orientations and then the deleterious damage on strike face surface area.

In turn, the impact of crack orientation and direction is preferentially diminished the influence of the sixfold symmetry of graphene filler in composites that may cause in-plane isotropic feature. The preferential zigzag and armchair crack directions inhibited the in-plane isotropic effects along membrane matrices at cracks angle of  $30^\circ$  [271]. A correlation of membrane orientation can show distribution of angles between the neighboring cracks at small multiples of  $30^\circ$ , (Fig. 16 (B-c and B-f)). The significance of anisotropic structure, toughness, high-strength and –dynamic tensile stress, and in-plane speed of sound of  $\mu\text{m}$ -thick GLM membrane leads to produce and extraordinary powerful armors with delocalization in the penetration energy impacts. On the base of the projectile penetration objects, the microballistic materials may have specific adsorption energy, high-energy resolution, and high-strain-rate, leading to practical need for armors. Xu et al. [272] tested microstructural and mechanical the ballistic performances of the CNT- MLG films with graphene and polymer films (Fig. 17).

Fig. 16

Fig. 17

## 9. Multifunctional polymer/filler nanocomposites

Aluminum (Al) was proposed to replace armors made of steel [273]. As primary structure, the sandwiched FML was studied to be used as antiballistic surfaces to resist speedy projectile's [274]. High-performance armor was produced using Al foams and FML mixture. This Al-FML composite was developed to enhance the shielding capacity of the antiballistic armor surface with lighter-weight and more potent effect than that of commercial armor plates [275] (Fig. 18).

The developing technique is based on the fabrication of multilayer armor structures through using different materials such as fibers, alloy, natural components as well as nanoparticles to provide ultrastrong armor. In this aspect, epoxy polymers filled with  $\text{Al}_2\text{O}_3$  nanorods and reinforced with Kevlar 29 fabrics were developed for enhancing the antiballistic nanocomposite features [273]. Fig. 18A indicate the FML composite layer composition, the front- and back-view of the composite armor layer, cross section of the composite, the penetration depth and delamination by the impacting projectile. This modern development for FML is based on the dispersion of alumina NPs into epoxy laminate composite systems. Hybrid laminate-based nanocomposites prepared using different matrixes (Kevlar, epoxy and sheets of Al alloys) filled with SiC, Al, and colloidal silica nanopowders deposited on the surface of PEG-400 was assessed by Haro et al. [275] Fig. 18B,C showed the microscopic images of Kevlar fibers, which reinforced with nanopowders for developing laminate structures. The laminate orientation is composed of 20 fabric layers stuffed inside to sheets of Al alloys. The microscopic investigations confirmed that the introducing of three nanofillers

strengthens the surface structure with high energy absorption capability and high antiballistic protection. As ceramic materials, SiC structures were extensively applied in industrial fields owing to their cost-effectiveness, enhanced surface area, antibacterial features and high mechanical and chemical properties even in harsh conditions. Certainly, the addition of SiC nanoparticle can improve the hydrophobic characteristics of composites. The SiC powder supplied in [276, 277] Al 7075 material can provide an antiballistic armor. In 2017, Obradovic et al. [278] developed multiaxial Kolon fabrics that composed of polyurethane/p-aramid and reinforced with hybrid nanomaterials of oxidized SWCNT (o-SWCNT), modified-silica NPs (m-SiO<sub>2</sub>), and poly(vinyl butyral) (PVB)/ethanol solution, leading to the enhancement of dynamic mechanical and high antiballistic performance (Fig. 19A). High ballistic prevention characteristics are observed for the prepared Kolon/PVB/o-SWCNT/m-SiO<sub>2</sub> nanocomposite fabrics with 35% enhancement in absorbed energy and 50% enhancement in the storage modulus compared with those of unfilled Kolon/PVB material [277,278]. A composite of bismaleimide (BMI) matrix/pristine CNT film nanomaterials was modeled. The structural investigations and analyses indicated the antiballistic performance of the unfilled and filled surface. The reported data confirmed enhancing the strengthening effect for random and oriented composite films, reducing the tensile mode of the pristine CNTs with spatial spread loads.

**Fig. 18**

**Fig. 19**

Currently, modern antiballistic armor material is based on self-reinforced polymer composites called all-aramid composite by using surface dissolution technique. This technique is used for fusing fibers together [279]. Excellent strengthening and elevated reinforcement characteristics are obtained using this technique. The extraordinary structural and mechanical features of graphene/SWCNTs hybrid are promising for applying in bulletproof armor [297,280] (Fig. 19B). This method can provide exfoliated graphene material and yield a hybrid of graphene/SWCNTs composite with improved surface structure. The antiballistic armor layers were prepared by using these nanocomposite structures. A 2.5D hybrid woven fabric composites fabricated with well-oriented symmetric fibers were simulated and modeled to produce stiff and strengthened film against damage. Also, three-dimensional textile composites were oriented as force-driven modulation of high antiballistic performance in terms of tolerable and resistible body against damage with cost-capital manufacture [280] 3D idealized modulation and multi-scale analysis system of nanostructure unit crystal design modal are needed to control progressing of the damage and failure.

3D weave composite architectures and binder placement was studied by using six designed types of carbon fabric materials. These composites have similar fiber types using ordinary polymeric matrix, nanofillers, and molding methods. Elastic strength for the three-dimensional woven nanocomposites are higher than their analogies with 2D laminated composites. Figs. (20 & 21) discussed using conventional loom of weave to develop various sorts of 3D composites based on 3D woven materials; the resin transfer

modeling procedure was used for the manufacturing [281]. Testing the compressive, tensile and flexural modulus was carried out in the warp direction for all the designed fibers [282].

The weave architectural designs influence the weaving process and the ballistic protection. The tensile strength of the composites was determined through waviness of fiber load modeling. The highest compressive properties were shown for W-3, while W-2.1 showed the lowest compressive values of frizzy distortion in the fibers. Altering the sequence of binding can decrease the fiber delamination and affect the flexural features [283,284].

As a result, W3 angle interlock showed the best design and resistance against shock, but also exhibit low fiber delamination when expressed to bending or compression loads. SiCR based on three (aluminum/nickel, PTFE/aluminum/nickel and Copper/aluminum/nickel) composites with high performance were used for antiballistic protection [285]. Cu addition exhibited elevated impact resistance as the activation energy is increased with the addition of Cu while the impact capacity is reduced. A reverse behavior is observed after the PTFE addition, where PTFE participates in the nanocomposite interactions with improving the released energy with reducing the activation energy. Lighter (nearly one-third) Spectra® fiber composite-based armor than Kevlar composites reveal similar antiballistic properties.

**Fig. 20**

**Fig. 21**

Aramid nanofibers, that is, Kevlar, are isolated via an efficient, facile and cost-effective technique based on dissolution. High tensile modulus, toughness, strength was introduced by preparing epoxy/aramid nanofiber composite as well as CNT-based composites [286]. Kevlar polymer is modified with highly purified and functionalized CNTs via one-step method. The resultant product is influenced with the nature of the polymer and the CNT's volume fraction. A hybrid epoxy nanoclay system was developed by Yasmin et al. [287] based on using dispersed NPs of organically modified montmorillonite–Cloisite 30B with different concentrations. Modulus of elasticity was improved by changing Cloisite 30B concentrations from 1% to 10%. Ho et al. [288] also established other models of epoxy nano-clay systems with nanoclay addition (5 wt.%) the produced nanocomposites exhibited tough and stiff characteristics. This is the result of mixing properties and nanofiller dispersion.

Absorption of the shocking energy of Closite 30B was studied using epoxidized fiberglass/nanoclay hybrid at speedy projectile [289]. High shock opposition and energy absorption was increased by adding 5 wt.% nanoclay. Modification of Kevlar fibers with inorganic nanomaterials for ballistic protection display remarkably high antiballistic performance. Kevlar/STF based composite exhibit robust antiballistic properties. Modeling nanocomposite bullet-resistant body armor was carried out by using Solid work 2012 and Abaqus 6.10 software [290]. The modeling materials of composite body armor are based on Kevlar-29 fiber and PES with 20 layers (10 mm thick) of woven fabrics. Results showed no penetration through the

modeled composite body armor (1.5 kg weight) by a projectile of 7.62 mm × 39 mm bullet impact load at 10 and 50 m with a muzzle velocity of 720 m/s.

Many lightweight nanocomposites are also based on magnesium because of its more super lightweight than other metals such as Al, Ti and stainless steel [291]. Magnesium is also available in nature [292]. Low density, elevated electro-static shielding, easy to form a coating enabled its applications in various antiballistic fields in Second World War. Magnesium suffers from reduced modulus of elasticity, robustness and increased corrosion ability and ductile properties; however, these disadvantages can be overcome via reinforced nanocomposite-based magnesium alloy [293]. AZ31 which is Mg alloy resists dry oxidation and anticorrosion against salt water by adding NPs [294].

Modeled polymer/Mg hybrids exhibit enhanced strength and improved ductility, which is commonly associated with ceramic nano reinforcements [280,294] (Fig. 22A). A hybrid polyester composite reinforced with curaua mat and aramid fabric subjected to UV radiation in terms of dissipated energy from the impact of projectile in ballistic tests was evaluated by DaSilva et al. [295] (Fig. 22B).

The obtained finding presented that the toughness reduction of because of the mat fragility leading to the fiber macromolecular scission, but it gives a share in the ballistic impact energy dispersion via delamination process [296]. Ultrahigh strengthened kevlar WFK of PES was developed by using low-temperature hydrothermal technique grown with ZnO nanorods. The hybrid WKF/ZnO/PES composites were prepared via VARTM process with enhanced robustness and thermally stable features [297] (Fig. 22C-a). Growing ZnO nanorods on the kevlar WFK of PES prompted the antiballistic performance and also provide hydrophobic features. UHMWPE fabric-based armor possesses the advantages of the ultralightweight and high level of protection. By using a composite of propylene reinforced with woven glass fibers, the failure mechanism of an impacted projectile is discussed. After the projectile shock, a cross-section of a hole was depicted through projectile simulating (Fig. 22C-b). A hole enlargement toward the nanocomposite backside has happened, results in a failure mode. Local deformation and fiber fracture can absorb the energy of the nanocomposites. Fig. (22C-c) indicated the fabric fracture and fiber pullout at the back; the other failure mode showed localized bulging at the zero impact.

### Fig. 22

Shear thickening fluid (STF) treatment exerts remarkable effect on the high strain rate characteristics of UHMWPE composites for antiballistic armors [298]. STF is synthesized by using nanosilica spheres. Four Dyneema® UHMWPE composites targets were modeled to study the mechanisms of penetration resistant structures [283] (Fig. 23). The targeted fabric materials were as follow:

- (1) Aluminum plate as a blank material;
  - (2) The Dyneema® aluminum plate with a thickness of 6 mm;
  - (3) The plate with a part of Dyneema® deleted from the front side to allow shocking to the aluminum plate;
- and

(4) The plate with a part of Dyneema® deleted from the back side to allow shocking to the aluminum plate without double penetration of Dyneema® layers [299].

The antiballistic performance of such targeted fabric surfaces increases in the following order: (1) < (4) < (2) < (3), respectively. The model analyses confirmed that Dyneema® exhibited both beneficial and detrimental influences on the target's antiballistic properties and can be applied in designing a multi-material structure. These models concluded that:

- ❖ These various structures of aluminum plates can distribute the shock energy from the missile's on the surface of the plate.
- ❖ Bullet fragmentation is delayed through providing low Dyneema® impedance on the shocked face.
- ❖ At higher impact velocity, a decrease in the ballistic performance was concluded for the shocked surface of the material.

Also, it was reported that hybrid ceramic composites with show considerably high impact resistance [300]. Hybrid ceramic and fibrous composite layer materials were applied as antiballistic materials where the fibrous structure and the ceramic's shape and thickness ceramics can control the antiballistic properties. A ceramic-UHMWPE hybrid composite armor was developed on the basis of ceramics made of SiC and Al<sub>2</sub>O<sub>3</sub> (of various shapes and sizes) with Dyneema®HB26. The hybrid ceramic - multi-layered UHMWPE composite armour showed high antiballistic protection [301].

### Fig. 23

Recoil and knot (bend) tests were employed to determine the compression of SK76 fibers. In the recoil tests, compressive strength of direct kinks along normal knot tests is higher than that kinks associated with micrometric buckling along SK76 fibers [302]. Along with this, the aramid fibers formed by these micrometric buckling exhibited a double or triple compressive strength than conventional analogues (Fig. 24). Furthermore, the compressive strength of carbon-fiber polymer reinforced composites can be predictable according to the following features: (1) high compressive strength is produced by micro-buckling; (2) the width of the kink prevents fabric tensile fracture; (3) in these composites, shock broadening is limited and neglected so fast. Moreover, macroscopic fibers with only SWCNTs composites were produced via conventional wet spinning approach using fuming H<sub>2</sub>SO<sub>4</sub> [303]. Excellent robustness and strength were developed by the neat SWCNT fibers.

Orlovskaya et al. [304] developed three-layered and nine-layered B<sub>4</sub>C-SiC ceramics as ceramic laminates via rolling and hot pressing. A highly elevated surface state with considerable compressive residual stresses and low tensile residual stresses is obtained by controlling the thickness of the component layers. SiC/CNT layers showed a high response against dynamic load caused by speedy nanodiamond bullet as reported by Makeev and Srivastava [305] Results concluded that the ultrahigh dissipating of the impacted energy is the main function of the utilized CNTs. Glass-epoxy/nanoclay/graphene hybrids was studied by

Avila et al. [306] for antiballistic applications. The tailored fiber glass–epoxy/nanoclay/graphene nanosheet nanocomposite laminates exhibit ultrahigh velocity and impact resistance.

Nowadays, hierarchical graphene nano-geometric composites with overall control scales in orientations, configurations, and functionalities can be used as modulated-replica of conventional structure composites. One of significant values is the control fabrication of hierarchical graphene nanocomposites via a facile, eco-friendly and cost-effective melt mixing approach. Glass-fiber GPN-polypropylene reinforced hierarchy composites can enhance the mechanical performance with an elevated interfacial bonding for well-dispersed PP-GF composites [307]. Higher antiballistic features of PEN/CF/graphene multilayer nanocomposites were confirmed than that virgin PEN matrix and surfaces filled with a single nanomaterial [308].

**Fig. 24**

## **10. Advanced armor nanocomposite materials**

Future requirements for increased armor reactivity include improved nano-properties, such as reduced weight, high strength, increased durability, increased reactivity, and the ability to vary or adjust definite characteristics. These characteristics can allow a remarkable potential by reducing soldier equipment's weight and improving lethality and survivability. Several innovations are introduced for protective coatings, such as changing the molecular configuration of polymeric materials and stability against different environmental conditions.

Advances protective armors should possess excellent antiballistic properties, durability, super lightweight and eco-friendly armor. Modeling advanced nanomaterials that possess the distinct characteristics of nanoscale systems is promising. Nevertheless, ceramic armors display remarkably high resistance to UV degradation, and their brittleness and specific density limit their application. Ceramic-modified nanomaterials can effectively shield the material against UV and improve the antiballistic performance. Modified Kevlar 29 is also supported by NPs for enhanced properties. Armor design should overcome the humidity problems. Chemically functionalized organic/inorganic composite nanomaterials offer a possibility of presenting a chemical barrier to water molecules with stable physicochemical features, no detachments and high hydrophobicity.

STRATUM nanoPROTECTM, which is the initially synthesized nanoarmor [309], is a Kevlar fiber treated thermally to become ribbon-like fibers and woven for antiballistic protection. Recently, a candidate to achieve this multi-functionality is based on fibrous nanomaterials by their lightweight and structure absorbance of approximately 98 J/g. To obtain self-reinforcement at points of high stress, nanofibers were twisted to generate extra-high robustness. Coils and yarns with high stretching ability and twisted structures can be developed through electro-spinning method of polyvinylidene fluoride trifluoroethylene fibers through over-twisting [310] (Fig. 25). Coils and yarns are formed through over-twisting of ribbons [311] (Fig. 26).

These nanofibrous materials exhibit increase tough properties and friction resistance to ballistic penetration and are favorable lightweight and flexible materials for mechanical applications [310,312].

**Fig. 25**

**Fig. 26**

Polymer/inorganic nanocomposites based ballistic-proof composite structures made using automated techniques are mostly used by the armor and vests, automotive and aerospace, sports goods, and robotics industries. A solid nanocomposite armor namely; ApNano was produced recently by using WS<sub>2</sub> onion-like structures [298,313] (Fig. 27). The modeled IF based armor material showed extra-high ability to absorb the impacted energy. These facile and cost-effective nanocomposites based on WS<sub>2</sub> were produced with more flame-retardant and safer characteristics compared with organic fullerenes; this material is also chemically stable. Such armor exhibited high antiballistic performance when exposed to sharp projectile's impact (withstand pressures caused by 250000 kg/cm<sup>2</sup>) at a high speed (1500 m/s). The WS<sub>2</sub>-based armor exhibits higher protective strength than steel. The WS<sub>2</sub>-based IF materials have double antiballistic durability that of B<sub>4</sub>C and SiC. Nonetheless, WS<sub>2</sub> is relatively heavy and the investigations on the ApNano showed that TiS<sub>2</sub> can introduce a superlighter and more powerful solution for ballistic impacts.

**Fig. 27**

Many studies have been conducted on ballistic nanocomposites. Glass-epoxy nanocomposites were produced via the matrix system using nano clay. Elamination absorbed energy and tensile failure in simple yarns. The study focused on glass-epoxy composites that included nano clay and graphene. These nanoparticles enhanced high-velocity impact resistance but also increased delamination, particularly at the back of the laminate [314]. Ballistic performance measurements were used to evaluate graphene oxide's effect on aramid fabric. The graphene oxide coating significantly increased the energy absorption of the fibers as compared to uncoated fibers. The transverse mechanical characteristics of the fibers were enhanced by a coating of UHMWPE containing silica nanoparticles. After adding SiO<sub>2</sub> nanoparticles, the coefficient of friction increased. For ballistic impact performance, two epoxy matrices were studied: one reinforced with carbon multiwalled nanotubes of modification (COOH-MWCNTs) and the other scattered with silica nanoparticles. The number of COOH-MWCNTs in the composite system enhanced energy absorption. When silica nanoparticles were added to composites at a weight percentage of 1%, the ballistic limit velocity and energy absorbed were maximized, but dropped at higher concentrations.

The Multilayer Armour System was constructed using various typical synthetic materials, including Kevlar fibers (Dyneema) and aluminum, which are among the most exciting new materials [315]. The aerospace and automotive industries can benefit from 3D printing's ability to produce lightweight structures with a high strength-to-weight ratio. The aerospace and automotive industries can benefit from fiber/nano-reinforced composites 3D printing's ability to produce lightweight structures with a high strength-to-weight ratio. Nanocomposites exhibit increase in the delamination properties and electrical and thermal conductivities [315].



CFRCs' high stiffness and specific strength have made them prominent in the aerospace industry. One effective method for creating intricate composite structures was to use 3D printing to create CFRCs. In 2014, NASA completed the first-ever study on 3D printing in space, using Made onboard orbit to create more than 20 pure printed polylactic acid samples on board the International Space Station. Using continuous carbon fiber reinforced PLA composites, researchers from China's Academy of Space Technology and Xi'an Jiaotong University successfully completed the nation's first spacecraft 3D printing experiment in 2020. NASA's SpiderFab concept calls for the use of continuous carbon fiber reinforced polyetheretherketone composites by a space robot to construct a massive helical structure. Roll, pitch, and yaw may be controlled only by morphing control surfaces, as demonstrated by the morphing drone that the CMASLab at ETH Zurich built and tested using 3D printed CFRCs. In the aerospace sector, 3D-printed CFRCs have to withstand a variety of harsh circumstances, including powerful radiation, large temperature variations, and high vacuum [315,316].

The versatility of Carbon fiber reinforced plastics (CFRP) is a huge plus for the sporting goods industry. Ski boards, rackets, fishing rods, golf clubs, bows and arrows, bicycles, baseball bats, boats, ice hockey sticks, and rowing oars are among the items that are frequently crafted using it. The racket's composite structure allows for a tighter string with greater specific strength and modulus, allowing faster serves and reduced shock during rebuffs. In terms of bicycles, carbon fiber reinforced polymers ensure optimal shock absorption and maximum speed with minimal effort. A novel addition to the wheel of a terrain racing bicycle is called "NAWASStich," which combines CFRCs with CNT to increase the wheel's strength and resistance to impact damage in comparison to standard composites. This happened as a result of the inside rim's higher buckling resistance during the high compression phenomenon [317]. European automakers have studied the use of boot linens, seat backs, parcel shelves, front and rear door linens, door-trim panels, and truck linens among other interior vehicle applications. Applications outside car interiors, such the area between a passenger bus's fender and headlights, are ripe for the incorporation of natural fiber into plastics. Polyjet AM with multi-material manufacturing is promising because it improves mechanical qualities including strength, durability, stiffness, and resistance to heat. Particles and continuous as well as discontinuous fibers can be used as filler materials in 3D-printed multi-material constructions. As an alternative to intricate and costly composite constructions, these prefabricated structures have been thoroughly studied. The state of multi-material polyjet 3D printing is improving. Multi-material polyjet printers, which are capable of producing a wide range of industrial goods and prototypes, are among the recent innovations. The well-known production series polyjet 3D printers Stratasys J 735TM, Objet 1000 plusTM, and Stratasys 750TM can be achieved by FRCs. At different sizes, multi-material additive manufacturing that uses polyjet technology enhances the dimensional conformity between proposed designs and constructed buildings. Soft robotics, four-dimensional printing, and bio-inspired polymer composites have expanded design space and overcome production constraints [318].

## 11. Nanomaterials merits for armor-designs

The influences of nanostructured armors based on IF NPs and inorganic nanotubes on the morphological and structural characteristics of thermoplastic polymer nanocomposites are highlighted on the thermal, mechanical, and tribological characteristics. IF based Nanocomposites with thermoplastic property enhance the antiballistic performance with the incorporation of multi-scale nanomaterials. Incorporation of CNTs, nanoclays, and spherical NPs in multifunctional composite systems is an eco-friendly, cost-saving and efficient approach. This micro-nano binary surface enhances the durability, flame retardancy, resistance against different environmental conditions and stability against thermal degradation and solidity. Utilizing these nanocomposites for protective clothing offers super lightweight, eco-friendly and cost-saving strategies

Future trends should also offer the following properties:

- ❖ Extreme antiballistic properties with super lightweight characteristics.
- ❖ High fiber flexibility and durability.
- ❖ Smart nanoarmor materials with enhanced physicochemical properties and self-cleaning characteristics.
- ❖ Improved thermal control and switchable camouflage.

Ellis et al. [319] investigated Spectra™ hybrid graphite nanocomposites against ballistic impacts. A large increase in the energy absorption of the modified armor is observed. E-glass/Kevlar™-29 hybrid nanocomposites showed higher antiballistic performance when compared with E-glass based plastic fibers [320]. CFRP reinforced Kevlar™-29 materials exhibited high resistance against projectile's impact as was investigated by Hazell and Appleby-Thomas [321]. E-glass-epoxy and carbon-epoxy laminates were studied by Pandya et al. [322], and they observed high antiballistic performance when layered in the armor's interior than exterior. 3D based Epoxy/E-glass composites showed elevated resistance against speedy impacts than 2D analogous.

Modeling new armors requires some design considerations for the selection of composite materials are as follows:

- ❖ Glass, carbon, aramid, and UHMWPE are examples of fiber and matrix materials that can be used either as thermoplastic or thermoset (Fig. 28).
- ❖ The produced layers are present in prepreg or dry fabric form. The dry fabrics can be woven or nonwoven.
- ❖ The multilayer armor systems were tested via Ballistic back-face signature experiments, where the curaua nonwoven fabric epoxies composites were used as a second layer. This composite layer was compared against aramid (Kevlar™) fabric laminates and showed higher antiballistic properties with the ability to keep its integrity after the ballistic impact and is a better substitute for aramid in these armor systems [323].

- ❖ Absorbing energy in thin composites follows elongated failure mechanism and friction between the projectile and the armor surface. Ideal materials for antiballistic performance possess ultrahigh wave dissipating features.
- ❖ When the ballistic mass increases, the ballistic limit decreases. Higher interlaminar fracture toughness and higher damage tolerance are reported for 3D weaves than those of 2D weaves.
- ❖ Instantaneous delamination is encountered with brittle resin systems, whereas controlled delamination growth is observed for tough systems.
- ❖ Glass-epoxy laminates show higher antiballistic performance than that of carbon-epoxy because the V50 of carbon-epoxy laminates is lower than that of glass-epoxy, and the extent of damage is larger in fiberglass-epoxy than that in carbon-epoxy. Hybrid nanomaterials exhibit remarkably high penetration resistance, especially for 3D textile composites, which possess high resistance for thicker films.

Fiberglass/epoxy structures reinforced with nanoclay and nanosheets of graphene exhibited extraordinary opposition against speedy projectiles with energy transfer properties.

- Previously, halogenated hydrocarbon additives are used in fire-retardant fabrics conventionally for increasing surface's fire retardancy; however, their harmful environmental effects have drawn research toward isocyanate free-based nanocomposites.
- Kevlar fibers/epoxy resin/AA 5086 layers deposited with SiC/Al/silica nanofillers by using ethylene glycol 400 and sandwiched aluminum alloy sheets showed superb antiballistic performance against different projectiles.
- The chemical resistance ability represents a vital issue for future bulletproof armor.
- Self-cleaning fabrics are crucial to resist the reduction in antiballistic performance after wetting. Previously reported self-cleaning fabrics based on nano-TiO<sub>2</sub> photocatalyst oxidize dirt and other contaminations.
- The antimicrobial performance of protective clothing is essential and achieved by coating with Ag NPs.
- Superlight weight nanomaterials, such as MgO and Al<sub>2</sub>O<sub>3</sub>, and their modified hybrid composites represent new trend that provides maximum comfort and optimal protection to the wearer.
- Other important characteristics in bulletproof armor are resistance against UV and different environmental conditions.

**Fig. 28**

## **12. Conclusions, outlook, and directions**

The continuous progress in the munitions technologies has driven research to develop effective bulletproof armor materials. This review paper summarized nanotechnologies and other main approaches adopted in developing ballistic and anti-impact materials. It is the first to provide a critical review of what is

currently known about the energy absorption of engineered nanomaterials by focusing on potential antiballistic mechanisms. Accelerated progress based on functional hybrid fabric nanocomposite materials with large surface-area with modified physico-mechanical characteristics has enabled developing improved bulletproof armor materials. Excellent properties for bulletproof armor nanocomposite structures are necessary because of their features:

- i. Long-term durable features, cost-effectiveness, simplicity, and impact energy absorption layers;
- ii. Improvement in the mechanical properties with remarkable lightweight advantages;
- iii. Flexibility, comfortability, multi-functionality, and applicability to be used in different conditions; and
- iv. Desirable water-repellent surfaces with ultrahigh mechanical properties, rough surface, and functionalized nature.

A newly developed armor is made of external covering of polyamide fabric coated with PU; its internal lining (for wear comfortability polyester 3D) consists of sheets of thermoplastic foil-reinforced para-aramide fiber covered with watertight vapor-permeable material.

Lightweight nanostructured antiballistic armor is among the future challenges with high comfortability. The projectile impacts on mosaic armor involve destroying the projectile's tip by the rigid armor material and subsequent shock waves and tile generation [324]. Afterward, the mechanical properties especially the stress waves improved with increasing the armor thickness [325,326]. Textile structure optimization can also be adopted to enhance the mechanical strength and penetration resistance of fiber-reinforced composites. Stress waves can increase the overall stress, which results in rupture and material breakage [327]. Controlling the nanocomposite structures in terms of all module configurations has been introduced to control the energy absorption and ballistic protective behavior. The nanocomposites using STF, CNTs, and  $\text{Al}_2\text{O}_3$  impregnation nanofillers in the matrix are widely investigated to enhance the antiballistic performance. Extent of NP percentage into the hybrid layers is important to achieve excellent-distribution and reinforced antiballistic armor performance

Physical, mechanical, and surface characteristics should also be described on the basis of the changes in energy absorption, tensile modulus, compressive strength, flexibility, and water hydrophobicity. Many new nano-antiballistic armor materials are in continuous progress for high-energy impact resistance with multifunctionality. Nano-material design can produce functional nanocomposites for bulletproof armor. New techniques for fabricating superlightweight and robust nanostructured composites for protection against ballistic impacts were highlighted here. Parameters to control the features of nanocomposites such as nanofiller type, morphology, size and its extent of distribution in the matrix material and the successful designs with multifunctionality have been demonstrated.

The production of more stable and flame-retardant armor materials can be facilely achieved by IFs than organic fullerenes. They possess high dissipating performance for the impacted energy waves; thus, are employed extensively for protective armors [328]. Furthermore, supporting IF- $\text{WS}_2$  NPs with lubricants

especially (inorganic products) which may be available as powders increase the antiballistic performance of bulletproof nanocomposites [329]. The present work illustrated a spatial strategy that discusses the overall view of the futuristic direction of lightweight antiballistic armor nanocomposite materials. Functionalized graphene-based nano-geometric composite fibers can provide ultrathin, hydrophobic, durable as well as flame retardant armors. Failure mechanism of the impact-resistant nanocomposites and fabrics is a focal point for tailoring advanced armor architectures. Future directions for antiballistic armor composites directed scientists toward new innovations:

- ❖ Thermoplastic matrixes hybrids with IF-WS<sub>2</sub> and/or MoS<sub>2</sub> can establish new nanocomposites and integrate novel techniques for future directions [168,228,330] (Fig. 28). An ultra-strong antiballistic composite material is obtained by the corporation of WS<sub>2</sub> nanomaterials in UHMWPE matrix. Such composite can provide high energy absorption and heat dissipation, high strength and fracture resistance.
- ❖ Design of hybrid multifunctional GO/MoS<sub>2</sub> nanomaterials for ultrahigh strong and lightweight nanoarmors (Fig. 8, 18A and 22A). To achieve better distribution of graphene nanosheets as fillers in the polymeric resin, these sheets are exfoliated (chemically or mechanically) or functionalized through decoration with robust inorganic particles such as MoS<sub>2</sub> NPs. GO nanosheets anchored with MoS<sub>2</sub> represent promising materials for antiballistic applications.

\* Hard NP-intercalated armor can provide better antiballistic performance because of the fiber's improved friction, energy dissipation and transmit the extreme stress. In spite of extensive research, two major challenges still exist, which are (1) the uniform distribution of nanomaterials in polymer matrices and (2) poor fiber-matrix interfacial adhesion. Adding liquid carriers can entrain hard NPs in the armor capillary which results in more robustness, hydrophobic self-cleaning and antibacterial features.

\* Slippage of fabric layers over each other is important to dissipate energy, relax stress and improve friction and antiballistic characteristics. Crimped fibers are efficient to resist speedy projectiles.

\* Incorporation of nanorods (ID)-structured composite materials is favorable for mechanical and self-cleaning applications. Selim et al. [331] developed a hybrid composite material of PDMS/GO-alumina as a superhydrophobic rough surface with enhanced mechanical characteristics and surface robustness when incorporated in the polymeric matrix (Fig. 29). The densely backed polymer/hybrid nanocomposite can reinforce the lotus-like superhydrophobic and rough structure of the surface. This surface can trap air and increase the non-wetting ability of the surface. Such air trapping will amplify surface hydrophobicity since air is a superhydrophobic material (contact angle of 180°). Water cannot sneak into the surfaces' nano-grooves, because of the decreased surface free energy, and water drops slip directly on the surface. This structure may stabilize the model of Cassie-Baxter and the surface superhydrophobicity. This hybrid GO sheet/alumina nanorod composite can be applied for extreme ballistic protection and shock energy absorption as a result of their stiff nature. As a result, such nanofiller control represents a strategic goal for bulletproof clothes.

\* Multifunctional nanohybrid materials, such as ceramic nano-Al<sub>2</sub>O<sub>3</sub> incorporation of epoxy resin-reinforced Kevlar fabrics, to develop newly structured bulletproof nanocomposite armor.

\* Considering their high fracture toughness and tensile strength, electrostatic spraying of GNP (6–8 nm) on UHMWPE produces antiballistic armor composites.

\* Functionalization of suitably distributed graphene nanosheets incorporated on UHMWPE can also afford a novel material with improved stiffness, elongation at break, impact absorption resistance, and ultrathin thickness of only one carbon atom. Higher graphene antiballistic materials were obtained at thicker films.

Developing economic, lightweight, and high-performance armor composites is our long-term vision. Our policies established the requirements of lightweight antiballistic innovations and elucidate the applicability in war environments. On the basis of the research works that were examined, a number of recommendations are offered for work that will take place in the future.

- Advanced armour systems employ carefully arranged hierarchical multilayered structures to achieve properties, including an excellent combination of stiffness, strength, toughness, energy absorption, impact resistance and light weight, which need to be considered when designing high performance armor.
- It is anticipated that organic-inorganic polymer nanocomposite hybridization would produce new materials with a combination of the qualities of their ingredients, in accordance with the principles of mixtures.
- Controlling the morphology, size and functionalization of nanofillers support engineering mechanical and superhydrophobic micro/nano-scale surface. There have been reports that larger loading ratios cause nanoreinforcements to agglomerate, which restricts their application to lower concentrations, thus future studies should investigate methods to minimise agglomeration. To achieve better dispersion of nanoparticles, ultrasonication is carried out for the desired period in various media.
- Well-distributed nanofillers in armor composites at various concentrations can significantly improve the physicomachanical and antiballistic behavior.
- Fiber-reinforced polymer composites are fabricated with improved ballistic resistance for applications such as enhanced body armors, trauma plates, and stiff ballistic products.
- Nanomaterials, especially CNTs and graphene, are extensively studied as nanofillers in polymer and fiber-based polymer nanocomposites for improved mechanical properties, energy absorption capacity, and/or impact resistance.
- Incorporation of Al or magnesium nanofillers in armor composites can improve the hardness, tensile modulus, compressive stress, corrosion resistance, and fatigue and wear properties compared with those of conventional matrices.

- UHMWPE fiber reinforced composites, propylene reinforced with woven glass fibers, CNT-based yarns, and ceramic fabric-based armor have the merits of the ultralightweight and outstanding ballistic-proof features.
- Armor materials based on CNT forests exhibited unique durability as a result of establishing a web with a high gravimetric strength than steel surface; these webs are able for light emission. Also, SWCNT/graphene nanosheets hybrids exhibit extraordinary elasticity, super lightweight, and flame-retardant properties.

This review introduced futuristic trends for designing upcoming armors. The achievements summarized in this work are the most relevant examples of how nanochemical research can help protect human body and dissipate life hazards caused by newly developed weapons. The current work outcomes help in designing new materials and techniques for high-response bulletproof armor and promote the use of nanotechnology in life sciences.

### Fig. 29

#### Conflict of Interest

The authors declare that there is no compete of interest.

#### References

- [1] G. Mittal, K.Y. Rhee, V. Mišković-Stanković, D. Hui, Reinforcements in multi-scale polymer composites: Processing, properties, and applications, *Compos. Part B: Eng.* 138 (2018) 122-139.
- [2] P.Y. Chen, J. McKittrick, M.A. Meyers, Biological materials: functional adaptations and bioinspired designs, *Prog. Mater. Sci.* 57 (2012) 1492–1704.
- [3] E. Medvedovski, Ballistic performance of armour ceramics: Influence of design and structure, Part 1. *Ceramics Inter.* 36 (2010) 2103-2115.
- [4] P. Bajaj, Sriiram, Ballistic protective clothings: An overview, *Ind. J. fibre Tex. Res.* 22 (1007) 274-291.
- [5] S. Siengchin, A review on lightweight materials for defence applications: Present and future developments, *Defence Technol.* 24 (2023) 1-17.
- [6] R. Yadav, M. Naebe, X. Wanga, B. Kandasubramanian, Body armour materials: from steel to contemporary biomimetic systems, *RSC Adv.* 6 (2016) 115145–115174.
- [7] N.V. David, X-L. Gao, J.Q. Zheng, Ballistic resistant body armor: contemporary and prospective materials and related protection mechanisms, *Appl. Mech. Rev.* 62(5) (2009) 050802–0508020.
- [8] U.S. Tewari, J. Bijwe, Recent development in tribology of fibre reinforced composites with thermoplastic and thermosetting matrices. In: Friedrich K, editor. *Adv. Compos. Technol.* Amsterdam: Elsevier. 8 (1993) 159-207.
- [9] A. Wilson, Chapter 21 - Smart textiles for personal protection equipment (PPE), Editor(s): J. McCann, D. Bryson, In *The Textile Institute Book Series, Smart Clothes and Wearable Technology (Second Edition)*, Woodhead Publishing, 2023: 583-597.



- [10] (a) Ballistic Resistance of Body Armor NIJ Standard-0101.06.89; (b) P. Priyanka, A. Dixit, H.S. Mali, High-strength hybrid textile composites with Carbon, Kevlar, and E-Glass fibers for impact resistant structures, *Mech. Compos. Mater.* 53 (5) (2017) 685–704.
- [11] R.J. Morgan, C.O. Pruneda, W.J. Steele, The Relationship between the physical structure and the microscopic deformation and failure processes of poly (p-phenylene terephthalamide) fibers, *J. Polym. Sci.* 21 (1983) 1757.
- [12] S.H. Siyal, S.A. Jogi, S. Muhammadi, Z.A. Laghari, S.A. Khichi, K. Naseem, T.S. Algarni, A. Alothman, S. Hussain, M. SufyanJaved, Mechanical characteristics and adhesion of glass-Kevlar hybrid composites by applying different ratios of epoxy in lamination, *Coatings* 11 (2021) 94.
- [13] P.M. Gore, B. Kandasubramanian, Functionalized aramid fibers and composites for protective applications: A review, *Ind. Eng. Chem. Res.* 57 (2018) 16537–16563.
- [14] Y. Pan, M. Sang, J. Zhang, Y. Sun, S. Liu, Y. Hu, X. Gong, Flexible and lightweight Kevlar composites towards flame retardant and impact resistance with excellent thermal stability, *Chem. Engin. J.* 452 (4) (2023) 139565.
- [15] M. Chhowalla, D. Jena, H. Zhang, Two-dimensional semiconductors for transistors, *Nature Rev. Mater.* 1 (2016) 16052.
- [16] (a) D. Micheli, A. Vricella, R. Pastore, A. Delfini, A. Giusti, M. Albano, M. Marchetti, F. Moglie, F. Mariani Primiani, Ballistic and electromagnetic shielding behaviour of multifunctional Kevlar fiber reinforced epoxy composites modified by carbon nanotubes, *Carbon* 104 (2016) 141-156; (b) M.S. Selim, S.A. El-Safty, M.A. Shenashen, Superhydrophobic foul resistant and self-cleaning polymer coating, In: *Superhydrophobic Polymer Coatings*, (Eds: S.K. Samal, S. Mohanty, Nayak SK) Elsevier Scientific Publisher Company, New York, 2019, Ch. 8.
- [17] A.H. Shirdel-Havara, R.M. Saadabad, Ballistic-diffusive approximation for the thermal dynamics of metallic nanoparticles in nanocomposite materials, *J. Appl. Phys.* 117 (2015) 114304.
- [18] M.V. Zhikharev, S.B. Sapozhnikov, Two-scale modeling of high-velocity fragment GFRP penetration for assessment of ballistic limit, *Inter. J. Impact Engin.* 101 (2017) 4248.
- [19] P.K. Stefanopoulos, G.F. Hadjigeorgiou, K. Filippakis, D. Gyftokostas, Gunshot wounds: A review of ballistics related to penetrating trauma, *J. Acute Disease.* 3 (3) (2014) 178-185.
- [20] J. Gibson, J. McKee, G. Freihofer, S. Raghavan, J. Gou, Enhancement in ballistic performance of composite hard armor through carbon nanotubes, *Int. J. Smart Nano Mater.* 4(4) (2013) 212–228.
- [21] M.A. Abtew, F. Boussu, P. Bruniaux, C. Loghin, I. Cristian, Ballistic impact mechanisms – A review on textiles and fibre-reinforced composites impact responses, *Compos. Struct.* 223 (2019) 110966.
- [22] K. Mylvaganam, L.C. Zhang, Ballistic resistance capacity of carbon nanotubes, *Nanotechnol.* 18 (2007) 475701–475704.

- [23] A.F. Wilde, D.K. Roylance, J.P.M. Rogers, Photographic investigation of high-speed missile impact upon Nylon fabric part I: Energy absorption and cone radial velocity in fabric, *Text. Res. J.* 43(12) (1973) 753–761.
- [24] N.J. Wegner, F.J. Brady, Shear thickening in colloidal dispersions, *Phys. Today.* 62 (2009) 27–32.
- [25] D. Tanner, J.A. Fitzgerald, B.R. Phillips, The Kevlar story an advanced materials case study, *Angew. Chem., Int. Ed. Engl.* 28 (1989) 5.
- [26] S. Doddamani, S.M. Kulkarni, S. Joladarashi, M.T.S. Kumar, A.K. Gurjar, Analysis of light weight natural fiber composites against ballistic impact: A review, *Int. J. Lightweight Mater. Manuf.* 6(3) (2023) 450-468.
- [27] M. Karahan, N. Karahan, Effect of weaving structure and hybridization on the low-velocity impact behavior of woven carbon epoxy composites, *Fibres Text. East. Eur.* 22, 3(105) (2014) 19-25.
- [28] M. Karahan, K. Yildirim, Low velocity impact behaviour of aramid and UHMWPE composites, *Fibres Text. East. Eur.* 3(111) (2015) 97-105.
- [29] Y. Regassa, G. Likeleh, R. Uppala, Modeling and Simulation of bullet resistant composite body armor. *Inter. J. Res. Stud. Sci. Engin. Technol. [IJRSSET].* 1(3) (2014) 39-44.
- [30] J.W. Mead, K.E. Mead, I. Auerbach, R.H. Ericksen, Accelerated aging of Nylon 66 and Kevlar 29 in elevated temperature, Elevated humidity, smog, and ozone, *Ind. Eng. Chem. Prod. Res. Dev.* 27 (1982) 158–163.
- [31] (a) P. Schaaf, J-C. Voegel, B. Senger, From random sequential adsorption to ballistic deposition: a general view of irreversible deposition processes, *J. Phys. Chem. B.* 104 (10) (2000) 2204–2214; (b) D. Hua, Y. Zhanga, Z. Shena, Q. Cai, Investigation on the ballistic behavior of mosaic SiC/UHMWPE composite armor systems, *Ceram. Intern.* 43 (2017) 10368–10376.
- [32] D.P. Kalman, R.L. Merrill, N.J. Wagner, E.D. Wetzel, Effect of particle hardness on the penetration behavior of fabrics intercalated with dry particles and concentrated particle-fluid suspensions, *ACS Appl. Mater. Interfaces* 1 (11) (2009) 2602–2612.
- [33] A. Ari, M. Karahan, M. Kopar, M. Ahrari, The effect of manufacturing parameters on various composite plates under ballistic impact, *Polym. Polym. Compos.* 30 (2022) 1–15.
- [34] B.A. Cheeseman, T.A. Bogetti, Ballistic impact into fabric and compliant composite laminates, *Compos. Struct.* 61 (2003) 161–173.
- [35] R.A. Prosser, Penetration of nylon ballistic panels by fragment-simulating projectiles1 Part I: a linear approximation to the relationship between the square of the  $V_{50}$  or  $V_c$  striking velocity and the number of layers of cloth in the ballistic panel, *Text Res J.* 58 (1998) 61–85.
- [36] M. Karahan, A. Jabbar, N. Karahan, Ballistic impact behavior of the aramid and ultra high molecular weight polyethylene composites, *J. Reinf. Plast. Compos.* 34(1) (2015) 37–48.
- [37] T.G. Zhang, S.S. Satapathy, L-R. Vargas-Gonzalez, S.M. Walsh, Ballistic impact response of Ultra-HighMolecular-Weight Polyethylene (UHMWPE), *Compos. Struct.* 133 (2015) 191–201.

- [38] Y. Yang, X. Chen, Investigation on energy absorption efficiency of each layer in ballistic armour panel for applications in hybrid design, *Compos. Struct.* 164 (2017) 1–9.
- [39] S.P. Lin, J.L. Han, J.T. Yeh, F.C. Chang, K.H. Hsieh, Composites of UHMWPE fiber reinforced PU/epoxy grafted interpenetrating polymer networks, *Eur. Polym. J.* 43 (2007) 996–1008.
- [40] D.C. Prevorsek, in *oriented polymer materials*, edited by S Fakirov (Huthing & Wept-Verlagzug, Heidelberg, Germany), 1996; 445–446.
- [41] S. Ruan, P. Gao, T.X. Yu, Ultra-strong gel-spun UHMWPE fibers reinforced using multiwalled carbon nanotubes, *Polym.* 47 (2006) 1604–1611.
- [42] A.L.S. Alves, L.F.C. Nascimento, J.C.M. Suarez, Influence of weathering and gamma irradiation on the mechanical and ballistic behavior of UHMWPE composite armor, *Polym. Test.* 24 (2005) 104–113.
- [43] Z. Zhang, Y. Zhao, H. Li, S. Percec, J. Yin, F. Ren, Nanoparticle-infused UHMWPE layer as multifunctional coating for high-performance PPTA single fibers, *Sci. Rep.* 9 (2019) 7183.
- [44] M. Bhattacharya, Polymer Nanocomposites—A Comparison between Carbon Nanotubes, Graphene, and Clay as Nanofillers, *Materials* 9(4) (2016) 262.
- [45] (a) M.M. Harussani, S.M. Sapuan, Gohar Nadeem, Tahrir Rafin, W. Kirubaanand, Recent applications of carbon-based composites in defence industry: A review, *Defence Technol.* 18 (8) (2022) 1281–1300; (b) P.Y. You, S.K. Kamarudin, Recent progress of carbonaceous materials in fuel cell applications: An overview, *Chem. Engin. J.* 309 (2017) 489–502.
- [46] (a) H. Zhang, P.K. Shen, Recent development of polymer electrolyte membranes for fuel cells, *Chem. Rev.* 112 (2012) 2780–2832; (b) O. Suárez-Iglesias, S. Collado, P. Oulego, M. Díaz, Graphene-family nanomaterials in wastewater treatment plants, *Chem. Engin. J.* 313 (2017) 121–135.
- [47] D. Lahiri, R. Dua, C. Zhang, I. Socarras-Novoa, A. Bhat, S. Ramaswamy, A. Agarwal, Graphene nanoplatelet-induced strengthening of ultrahigh molecular weight polyethylene and biocompatibility in vitro, *ACS Appl. Mater. Interfaces.* 4 (4) (2012) 2234–2241.
- [48] K. Shaker, A. Jabbar, M. Karahan, N. Karahan, Y. Nawab, Study of dynamic compressive behaviour of aramid and ultrahigh molecular weight polyethylene composites using Split Hopkinson Pressure Bar, *J. Compos. Mater.* 51(1) (2017) 81–94.
- [49] M. Karahan, N. Karahan, Development of an innovative sandwich composites for the protection of lower limbs against landmine explosions, *J. Reinf. Plast. Compos.* 35(24) (2016) 1776–1791.
- [50] M. Karahan, E.A. Karahan, Development of an innovative sandwich composite material for protection of lower limb against landmine explosion: mechanical leg test results, *Text. Res. J.* 87(1) (2017) 15–30.
- [51] M.I. Khan, M. Umair, R. Hussain, M. Karahan, Y. Nawab, Investigation of impact properties of para-aramid composites made with a thermoplastic-thermoset blend. *J. Thermoplast. Compos. Mater.* 36 (2) (2023) 866–893.
- [52] Chitrangad. Hybrid ballistic fabric, ed. Patent 5187003, USA, 16 February 1993.

- [53] M. Karahana, A. Kus, R. Eren, An investigation into ballistic performance and energy absorption capabilities of woven aramid fabrics, *Int. J. Impact Eng.* 35 (2008) 499–510.
- [54] M. Karahan, Comparison of ballistic performance and energy absorption capabilities of woven and unidirectional aramid fabrics, *Text. Res. J.* 78(8) (2008) 718–730.
- [55] M. Karahan, N. Karahan, N.A. Nasir, Y. Nawab, Effect of structural hybridization on ballistic performance of aramid fabrics, *J. Thermoplast. Compos. Mater.* 32(6) (2019) 795–814.
- [56] J. Jüstia, E.H. Kammer, L. Neckela, N.J. Lóha, W. Trindadeb, A.O. Silvaa, O.R.K. Montedoa, A. De Noni Jr, Ballistic performance of  $\text{Al}_2\text{O}_3$  mosaic armors with gap-filling materials, *Ceram. Inter.* 43 (2017) 2697–2704.
- [57] E.P. Hofmeister, M. Mazurek, J. Ingari, Injuries sustained to the upper extremity due to modern warfare and the evolution of care, *J. Hand Surg.* 32(8) (2007) 1141–1147.
- [58] (a) S. Mallakpour, E. Khadem, Recent development in the synthesis of polymer nanocomposites based on nano-alumina, *Prog. Polym. Sci.* 51 (2015) 74–93; (b) M.S. Selim, H. Yang, F.Q. Wang, N.A. Fatthallah, X. Li, Y. Li, Y. Huang, Superhydrophobic silicone/SiC nanowire composite as a fouling release coating material, *J. Coat. Technol. Res.* 16 (2019) 1165–1180.
- [59] S.A. Tekalur, A. Shukla, K. Shivakumar, Blast resistance of polyurea based layered composite materials, *Compos. Struct.* 84 (3) (2008) 271–281.
- [60] A. Krell, E. Strassburger, Ballistic strength of opaque and transparent armor, *Am. Ceram. Soc.* 86 (2007) 9201–9207.
- [61] M.J. Pawar, A. Patnaik, S.K. Biswas, U. Pandel, I.K. Bhat, S. Chatterjee, A.K. Mukhopadhyay, R. Banerjee, B.P. Babu, Comparison of ballistic performances of  $\text{Al}_2\text{O}_3$  and AlN ceramics, *Int. J. Impact Eng.* 98 (2016) 42–51.
- [62] S.N. Monteiro, L.H.L. Louro, A.V. Gomes, C.F.M. Chagas, A.B. Caldeira, E.P. Lima Jr, How effective is a convex  $\text{Al}_2\text{O}_3$ – $\text{Nb}_2\text{O}_5$  ceramic armor?. *Ceram. Int.* 42 (2016) 7844–7847.
- [63] U. Mawkhlieng, A. Majumdar, A. Laha, A review of fibrous materials for soft body armour applications, *RSC Adv.* 10 (2020) 1066–1086.
- [64] J. Karger-Kocsis, H. Mahmood, A. Pegorett, Recent advances in fiber/matrix interphase engineering for polymer composites, *Prog. Mater. Sci.* 73 (2015) 1–43.
- [65] G. Martínez-Barrera, H. López, V. M. Castaño, R. Rodríguez, Studies on the rubber phase stability in gamma irradiated polystyrene-SBR blends by using FT-IR and Raman spectroscopies, *Rad. Phys. Chem.* 69 (2003) 2, 155–162.
- [66] (a) M.S. Selim, S.A. El-Safty, M.A. Shenashen, S.A. Higazy, A. Elmarakbi, Progress in biomimetic leverages for marine antifouling by nanocomposite coatings, *J. Mater. Chem. B.* 8 (2020) 3701–3732; (b) M.S. Selim, S.A. El-Safty, M.A. Abbas, M.A. Shenashen, Facile design of graphene oxide-ZnO nanorod-based ternary nanocomposite as a superhydrophobic and corrosion-barrier coating, *Colloids Surf. A Physicochem. Eng. Asp.* 611 (2021) 125793.

- [67] B.A. Cheeseman, T.A. Bogetti, Ballistic impact into fabric and compliant composite laminates, *Compos. Struct.* 61 (2003) 161–173.
- [68] X. Li, P. Sun, L. Fan, M. Zhu, K. Wang, M. Zhong, J. Wei, D. Wu, Y. Cheng, H. Zhu, Multifunctional graphene woven fabrics, *Sci. Rep.* 2 (2012) 395.
- [69] (a) E.T. Thostenson, C. Li, T.W. Chou, Review, Nanocomposites in context, *Compos. Sci. Technol.* 65 (2005) 491–516; (b) M.S. Selim, M.A. Shenashen, N.A. Fatthallah, A. Elmarakbi, S.A. El-Safty, In situ fabrication of one-dimensional-based lotus-like silicone/ $\gamma$ - $\text{Al}_2\text{O}_3$  nanocomposites for marine fouling release coatings, *ChemistrySelect* 2 (30) (2017) 9691–9700; (c) M.S. Selim, M.A. Shenashen, A. Elmarakbi, N.A. Fatthallah, S. Hasegawa, S.A. El-Safty, Synthesis of ultrahydrophobic and thermally stable inorganic–organic nanocomposites for self-cleaning foul release coatings, *Chem. Engin. J.* 320 (2017) 653–666.
- [70] M. Rahman, M. Hosur, S. Zainuddin, U. Vaidya, A. Tauhid, A. Kumar, J. Trovillion, S. Jeelani, Effects of amino functionalized MWCNTs on ballistic impact performance of E-glass/epoxy composites using a spherical projectile, *Int. J. Impact Eng.* 57 (2013) 108–118.
- [71] U.A. Shakil, S.B. Abu Hassan, M.Y. Yahya, Mujiyono, D. Nurhadiyanto, A review of properties and fabrication techniques of fiber reinforced polymer nanocomposites subjected to simulated accidental ballistic impact, *Thin-Walled Struct.* 158 (2021) 107150.
- [72] L. Peponi, D. Puglia, L. Torre, L. Valentini, J.M. Kenny, Processing of nanostructured polymers and advanced polymeric based nanocomposites, *Mater. Sci. Eng. R: Rep.* 85 (2014) 1–46.
- [73] E.A. Coppage (Jr), R.W. Coppage, *High Perform Text.* 13(9) (1992) 12.
- [74] (a) R.C. Laible, E. Barron, *History of Armour, Ballistic materials and penetration mechanics*, ed. Roc C. Laible, Elsevier Scientific Publisher Company. New York. 1980; 13–40; (b) D.J. Papetti, *Metallic armour materials, ballistic materials and penetration mechanics*, ed. Roc C. Laible, Elsevier Scientific Publisher Company, New York, 1980; 146.
- [75] P.J. Hazell, *Armour Materials, Theory and Design*. CRC Press Taylor and Francis Group. 2016.
- [76] (a) R.F. Burton, *The book of the sword, barnes and noble*. New York, 1972; (b) H.R. Robinson, *The armor of imperial Rome*, Charles Scribner's Sons, New York, 1970.
- [77] *Encyclopedia Britannica*, *Armor*. 2 (1974) 27.
- [78] N. Saxtorph, *Warriors and weapons of early times*. Macmillan Co., New York. 1965.
- [79] V. Hurley, *Arrows against Steel: The History of the Bow*. Mason/Charter, NY. 1975.
- [80] S.V. Grancsay, *Catalogue of Armor*. Davis Press, Worchester, MA, 1961.
- [81] B. Grohskopf, *The treasure of Sutton Hoo Ship*, Atheneum Press, New York, 1973.
- [82] R. Maddin, J.D. Muhly, T.S. Wheeler, How the Iron Age began. *Sci. Am.* 237(4) (1977) 122–131.
- [83] A. Snodgrass, *Early Greek Armor and Weapons*, Edinburgh University Press, Edinburgh. 1964.
- [84] C.J. Foulkes, *Arms and Armor*. British, Edgware Middlesex, England, 1967.
- [85] F.O. Braga, Curaua non-woven fabric composite for ceramic multilayered armors: a lightweight, natural, and low-cost alternative to kevlar. In: 3rd Pan American materials congress, 2017, 339–346.

- [86] P.V. Cavallaro, Soft body armor: An overview of materials, manufacturing, testing, and ballistic impact dynamics. NUWC-NPT Technical Report, 12 (2011) 057.
- [87] G.R. Villanueva, W.J. Cantwell, The high velocity impact response of composite and FML-reinforced sandwich structures, *Comp. Sci. Technol.*, 64 (1) (2004) 35-54.
- [88] Y.Q. Zhu, T. Sekine, Y.H. Li, M. Fay, W.X. Wang, H. Edwards, P.D. Brown, N. Fleischer, R. Tenne, WS<sub>2</sub> and MoS<sub>2</sub> inorganic fullerenes: Super shock absorber at very high pressures, *Adv. Mater.* 17 (2005) 1500-1503.
- [89] M. Zhang, K.R. Atkinson, R.H. Baughman, Multifunctional carbon nanotube yarns by downsizing an ancient technology, *Science* 306 (2004) 1358–1361.
- [90] P. Tran, T. Ngo, E.C. Yang, P. Mendis, W. Humphries, Effects of architecture on ballistic resistance of textile fabrics: Numerical study, *Inter. J. Damage Mech.* 23(3) (2014) 359–376.
- [91] L.A. Rohen, F.M. Margem, S.N. Monteiro, B.M. Vieira, de Araujo, E.S. Lim, Ballistic efficiency of an individual epoxy composite reinforced with Sisal fibers in multilayered armor, *Mater. Res.* 18 (Suppl 2) (2015) 55-62.
- [92] N.M. Nurazzi, M.R.M. Asyraf, A. Khalina, N. Abdullah, H.A. Aisyah, S.A. Rafiqah, F.A. Sabaruddin, S.H. Kamarudin, M.N.F. Norrrahim, R.A. Ilyas, S.M. Sapuan, A Review on Natural Fiber Reinforced Polymer Composite for Bullet Proof and Ballistic Applications, *Polymers* 13 (2021) 646.
- [93] W. Gray, P.H. Zabal, in *International encyclopaedia of composites*. Vol. 6, edited by S M Lee (VCH Publishers Inc, USA), 1991; 125-140.
- [94] F. Alkhatib, E. Mahdi, A. Dean, Design and evaluation of hybrid composite plates for ballistic protection: Experimental and numerical investigations, *Polymers* 13 (2021) 1450.
- [95] M.S. Risby, S.V. Wong, A.M.S. Hamouda, A.R. Khairul, M. Elsadig, Ballistic Performance of Coconut Shell Powder/Twaron Fabric against Non-armour Piercing Projectiles. *Def. Sci. J.* 58(2) (2008) 248-263.
- [96] X. Yang, X. Jiang, Y. Huang, Z. Guo, L. Shao, Building nanoporous metal–organic frameworks “Armor” on fibers for high-performance composite materials, *ACS Appl. Mater. Interfaces* 9 (6) (2017) 5590–5599.
- [97] (a) S.L. Phoenix, P.K. Porwal, A new membrane model for the ballistic impact response and V50 performance of multi-ply fibrous systems, *Inter. J. Solids Struct.* 40 (24) (2003) 6723-6765; (b) J.P. Attwood, B.P. Russell, H.N.G. Wadley, V.S. Deshpande, Mechanisms of the penetration of ultra-high molecular weight polyethylene composite beams, *Inter. J. Impact Engin.* 93 (2016) 153-165.
- [98] B. Hu, P. Eberhard, Symbolic computation of longitudinal impact waves, *Comp. Meth. Appl. Mechan. Engin.* 190(37) (2001) 4805-4815.
- [99] M. Jacoby, Fibers get a boost in performance. *Chem. Eng. News Archive* 93 (6) (2015) 27–28.
- [100] V. Mahesh, S. Joladarashi, S.M. Kulkarni, A comprehensive review on material selection for polymer matrix composites subjected to impact load, *Defence Technol.* 17(1) (2021) 257-277.

- [101] D. Sun, Ballistic performance evaluation of woven fabrics based on experimental and numerical approaches, In: *Advanced fibrous composite materials for ballistic protection*, (Ed. Chen X) 409-435, Woodhead Publishing, Elsevier Ltd., Cambridge, 2016.
- [102] S. Borman, Green route to stronger fibers, *Chem. Eng. News Archive* 93 (47) (2015) 5.
- [103] F. Maulana, A.R. Prabowo, R. Ridwan, U. Ubaidillah, D. Ariawan, J.M. Sohn, N. Muhayat, D. Tjahjana, W.P. Danardono, Q.T. Do, Antiballistic material, testing, and procedures of curved-layered objects: A systematic review and current milestone, *Curved and Layered Struct.* 10 (1) (2023) 20220200.
- [104] J. deMarre, Perforation of iron and steel sheets with normal Firing (trans.), *Memorial de l'Artillerie de Marine*. 1987, 14.
- [105] Y. Zhou, G. Li, Q. Fan, Y. Wang, H. Zheng, L. Tan, X. Xu, Study on Protection Mechanism of 30CrMnMo-UHMWPE Composite Armor, *Materials* 10(4) (2017) 405.
- [106] G.E. Hauver, P.H. Netherwood, R.F. Benck, W.A. Gooch, W.J. Perciballi, M.S. Burkins, Variation of target resistance during long rod penetration into ceramics, *Proceedings of the 13<sup>th</sup> International Symposium on Ballistics*, Stockholm, Sweden, 1992.
- [107] M-Y. Shen, T-Y. Chang, T-H. Hsieh, Y-L. Li, C-L. Chiang, H. Yang, M.C. Yip, Mechanical properties and tensile fatigue of graphene nanoplatelets reinforced polymer nanocomposites, *J. Nanomaterials* 2013 (2013) 1-9.
- [108] A.K. Bhakta, S. Kumari, S. Hussain, R.J. Mascarenhas, P. Martis, J. Delhalle, Z. Mekhalif, Lanthanum hydroxide nanoparticles/multi-wall carbon nanotubes nanocomposites, in *Advanced Materials for Defense* (Eds: R. Fangueiro, & S. Rana) Vol. 4, 25-34, Springer Proceedings in Materials, 2020.
- [109] T. Kitagawa, K. Yabuki, An analysis of capillary water behaviour in poly-p phenylenebenzobis-oxazole fibers, *J. Appl. Polym. Sci.*, 80 (2001) 1030.
- [110] B.A. Cheeseman, T.A. Bogetti, Ballistic impact into fabric and compliant composite laminates. *Compos. Struct.* 61 (2003) 161–173.
- [111] Y. Duan, M. Keefe, T.A. Bogetti, B. Powers, Finite element modeling of transverse impact on a ballistic fabric, *Int. J. Mech. Sci.* 48 (2006) 33–43.
- [112] Y. Duan, Keefe, T.A. Bogetti, B.A. Cheeseman, B. Powers, A numerical investigation of the influence of friction on energy absorption by a high-strength fabric subjected to ballistic impact, *Int. J. Impact Eng.* 32 (2006) 1299–1312.
- [113] F.D.C.G. Filho, M.S. Oliveira, A.C. Pereira, L.F.C. Nascimento, J.R.G. Matheus, S.N. Monteiro, Ballistic behavior of epoxy matrix composites reinforced with piassava fiber against high energy ammunition, *J. Mater. Res. Technol.* 9 (2) (2020) 1734-1741.
- [114] H. Chouhan, N.A. Bhalla, N. Bhatnagar, High strain rate performance of UHMWPE composites: Effect of moisture ingress and egress, *Mater. Tod. Communicat.* 26 (2021) 101709.



- [115] Y. Wang, Q. Liu, B. Zhang, H. Wang, P. J. Hazell, B. Li, T. Song, L. Li, F. Liu, F. Ye, Improved ballistic performance of a continuous-gradient B<sub>4</sub>C/Al composite inspired by nacre, *Mater. Sci. Engin. A*, 874 (2023) 145071.
- [116] M.B. Karamis, A. Tasdemirci, F. Nair, Failure and tribological behaviour of the AA5083 and AA6063 composites reinforced by SiC particles under ballistic impact, *Compos. A. Appl. S.* 34 (3) (2003) 217–226.
- [117] H. Ji, X. Li, D. Chen, *Cymbiola nobilis* shell: toughening mechanisms in a crossed lamellar structure, *Sci. Rep.* 7 (2017), 40043.
- [118] M. Zhang, D. Jiao, G. Tan, J. Zhang, et al., Strong, fracture-resistant biomimetic silicon carbide composites with laminated interwoven nanoarchitectures inspired by the crustacean exoskeleton, *ACS Appl. Nano Mater.* 2 (2) (2019) 1111–1119.
- [119] Z. Zhou, G. Wu, L. Jiang, R. Li, Z. Xu, Analysis of morphology and microstructure of B<sub>4</sub>C/2024Al composites after 7.62 mm ballistic impact, *Mater. Des.* 63 (2014) 658–663.
- [120] R.G. Crookes, B. Marz, H. Wu, Ductile deformation in alumina ceramics under quasi-static to dynamic contact impact, *Mater. Des.* 187 (2020) 108360.
- [121] K.S. Cheong, E.P. Busso, Discrete dislocation density modelling of single phase FCC polycrystal aggregates, *Acta Mater.* 52 (19) (2004) 5665–5675.
- [122] P.J. Jackson, The formation of microbands by cross-slips, *Scripta Metall.* 17 (2) (1983) 199–202.
- [123] Y.S. Chaves, S.N. Monteiro, L.F.C. Nascimento, T.G. Rio, Mechanical and Ballistic Properties of Epoxy Composites Reinforced with Babassu Fibers (*Attalea speciosa*), *Polymers (Basel)*. 16 (7) (2024) 913.
- [124] X. Li, M. Yuan, C. Huang, S. Wang, Influence of surface polyurea coating on the ballistic performance of kevlar fabric, *Heliyon* 10 (8) (2024) e29113.
- [125] L.S. Gallo, M.O.C.V. Boas, A.C.M. Rodrigues, F.C.L. Melo, E.D. Zanotto, Transparent glass–ceramics for ballistic protection: materials and challenges, *J. Mater. Res. Technol.* 8(3) (2019) 3357–3372.
- [126] G. Cooper, P. Gotts, Ballistic protection. *Ballistic Trauma: A Practical Guide*. 2005; 67–90.
- [127] R.A. Prosser, S.H. Cohen, R.A. Segars, Heat as a factor in the penetration of cloth ballistic panels by 0.22 caliber projectiles, *Text. Res. J.* 70 (2000) 709–722.
- [128] S. Wu, P. Sikdar, G.S. Bhat, Recent progress in developing ballistic and anti-impact materials: Nanotechnology and main approaches, *Defence Technol.* 21 (2023) 33–61.
- [129] S. Bhattacharjee, R.C. Das, S. Mondal, Md. S. Islam, C.R. MacIntyre, Chapter 9 - Potential of graphene modified nanostructures for multifunctional personal protective clothing, Editor(s): R. Khan, M.A. Sadique, *Smart Nanomaterials to Combat the Spread of Viral Infections*, Academic Press, 2023; 195–218.
- [130] V.M. Castaño, R. Rodríguez, Nanotechnology for ballistic materials: from concepts to products, *Mater. Technol.* 47(3) (2013) 267–271.
- [131] P. Kumar, S. Som, M.K. Pandey, S. Das, A. Chanda, J. Singh, Investigations on optical properties of ZnO decorated graphene oxide (ZnO@GO) and reduced graphene oxide (ZnO@r-GO), *J. Alloys Compds.* 744 (2018) 64–74.

- [132] G. Thilagavathi, A.S.M. Raja, T. Kannaian, Nanotechnology and protective clothing for defense personnel, *Defence Sci. J.*, 58 (4) (2008) 451-459.
- [133] N. Naik, P. Sharirao, Composite structures under ballistic impact, *Comp. Struct.* 66 (2004) 579-590.
- [134] J.S. Jayan, S. Appukuttan, R. Wilson, K. Joseph, G. George, K. Oksman, Chapter 1 - An introduction to fiber reinforced composite materials, Editor(s): K. Joseph, K. Oksman, G. George, R. Wilson, S. Appukuttan, In *Woodhead Publishing Series in Composites Science and Engineering, Fiber Reinforced Composites*, Woodhead Publishing, 2021, 1-24.
- [135] United Defense Ground Systems Division, 1107 Coleman Avenue, Box 367, San Jose, CA 95103.
- [136] H. Gower, D. Cronin, A. Plumtree, Ballistic impact response of laminated composite panels, *Inter. J. Impact Engin.* 35 (2008) 1000-1008.
- [137] I.G. Crouch, Body armour – New materials, new systems, *Defence Technol.* 15(3) (2019) 241-253.
- [138] S. Feli, M.R. Asgari, Finite element simulation of ceramic/composite armor under ballistic impact. *Compos, Part B Eng.* 42 (2011) 771–780.
- [139] (a) M.S. Selim, H. Yang, F.Q. Wang, N.A. Fatthallah, Y. Huang, S. Kuga, Silicone/ZnO nanorod composite coating as a marine antifouling surface, *Appl. Surf. Sci.* 466 (2019) 40–50; (b) M.S. Selim, H. Yang, S.A. El-Safty, N.A. Fatthallah, M.A. Shenashen, F.Q. Wang, Y. Huang, Superhydrophobic coating of silicone/ $\beta$ -MnO<sub>2</sub> nanorod composite for marine antifouling, *Coll. Surf. A: Physicochem. Eng. Asp.* 570 (2019) 518–530; (c) M.S. Selim, M.A. Shenashen, S.A. El-Safty, S.A. Higazy, M.M. Selim, H. Isago, A. Elmarakbi, Recent progress in marine foul-release polymeric nanocomposite coatings, *Prog. Mater. Sci.* 87 (2017) 1–32; (d) M.S. Selim, S.A. El-Safty, M.A. El-Sockary, A.I. Hashem, O.M. Abo Elenien, A.M. EL-Saeed, N.A. Fatthallah, Smart photo-induced silicone/TiO<sub>2</sub> nanocomposites with dominant [110] exposed surfaces for self-cleaning foul-release coatings of ship hulls, *Mater. Des.* 101 (2016) 218–225.
- [140] (a) M.F. Ashby, *Materials selection in mechanical design*. 3rd ed. Oxford: Pergamon Press; 2005; (b) M.S. Selim, H. Yang, F.Q. Wang, X. Li, Y. Huang, N.A. Fatthallah, Silicone/Ag@SiO<sub>2</sub> core-shell nanocomposite as a self-cleaning antifouling coating material, *RSC Adv.* 8 (2018) 9910–9921; (c) M.S. Selim, A. Elmarakbi, A.M. Azzam, M.A. Shenashen, A.M. EL-Saeed, S.AA. El-Safty, Eco-friendly design of superhydrophobic nano-magnetite/silicone composites for marine foul-release paints, *Prog. Org. Coat.* 116 (2018) 21–34; (d) M.S. Selim, A.M. Azzam, S.A. Higazy, S.A. El-Safty, M.A. Shenashen, Novel graphene-based ternary nanocomposite coatings as ecofriendly antifouling brush surfaces, *Prog. Org. Coat.* 167 (2022) 106803; (e) M.S. Selim, N.A. Fatthallah, M.A. Shenashen, R.M. Hekmat, M.M. Selim, S.A. El-Safty, Bioinspired graphene oxide-magnetite nanocomposite coatings as protective superhydrophobic antifouling surfaces, *Langmuir* 39(6) (2023) 2333–2346.
- [141] (a) E.P. Giannelis, Polymer layered silicate nanocomposites, *Adv Mater.* 8(1) (1996) 29–35; (b) M.S. Selim, S.A. El-Safty, M.A. El-Sockary, A.I. Hashem, O.M. Abo Elenien, A.M. EL-Saeed, N.A. Fatthallah, Tailored design of Cu<sub>2</sub>O nanocube/silicone composites as efficient foul-release coatings, *RSC Adv.* 5(26) (2015) 19933–43; (c) M.S. Selim, S.A. El-Safty, M.A. El-Sockary, A.I. Hashem, O.M. Abo Elenien, A.M.

- EL-Saeed, N.A. Fatthallah, Modeling of spherical silver nanoparticles in silicone-based nanocomposites for marine antifouling. *RSC Adv.* 5(78) (2015) 63175–85.
- [142] J. Zhu, W. Cao, M. Yue, Y. Hou, J. Han, M. Yang, Strong and stiff aramid nanofiber/ carbon nanotube nanocomposites, *ACS Nano* 9 (3) (2015) 2489–2501.
- [143] A. Srivastava, A. Majumdar, B.S. Butola, Improving the impact resistance of textile structures by using shear thickening fluids: a review, *Crit. Rev. Solid State Mater. Sci.* 37(2) (2012) 115–29.
- [144] A. Majumdar, B.S. Butola, A. Srivastava, An analysis of deformation and energy absorption modes of shear thickening fluid treated Kevlar fabrics as soft body armour materials, *Mater. Des.* 51 (2013) 148–53.
- [145] T.A. Hassan, V.K. Rangari, S. Jeelani, Synthesis, processing and characterization of shear thickening fluid (STF) impregnated fabric composites, *Mater. Sci. Eng. A.* 527(12) (2010) 2892–2899.
- [146] Y.S. Lee, E.D. Wetzel, N.J. Wagner, The ballistic impact characteristics of Kevlar woven fabrics impregnated with a colloidal shear thickening fluid, *J. Mater. Sci.* 38(13) (2003) 2825–33.
- [147] S.Z.H. Shah, S. Karuppanan, P.S.M. Megat-Yusoff, Z. Sajid, Impact resistance and damage tolerance of fiber reinforced composites: A review, *Compos. Struct.* 217 (2019) 100–121.
- [148] H-S. Hwang, M.H. Malakooti, B.A. Patterson, H.A. Sodano, Increased inter yarn friction through ZnO nanowire arrays grown on aramid fabric, *Compos. Sci. Technol.* 107 (2015) 75–81.
- [149] T.H. Sydenstricker, S. Mochnaz, S.C. Amico, Pull-out and other evaluations in Sisal-reinforced polyester biocomposites. *Polym. Test.* 22 (4) (2003) 375–380.
- [150] N. Cristescu, L.E. Malvern, R.L. Sierakowski, Failure mechanisms in composite plates impacted by blunt-ended penetrators, In: *Foreign object impact damage to composites materials*, ASTM STP 568, American Society for Testing and Materials. 1975, 159–172.
- [151] (a) R. Xiong, A.M. Grant, R. Ma, S. Zhang, V.V. Tsukruk, Naturally-derived biopolymer nanocomposites: Interfacial design, properties and emerging applications, *Mater. Sci. Eng. R: Rep.* 125 (2018) 1–41; (b) C.R. Vandenabeele, S. Lucas, Technological challenges and progress in nanomaterials plasma surface modification – A review. *Mater. Sci. Eng. R: Rep.* 139 (2020) 100521.
- [152] (a) B. Liu, K. Zhou, Recent progress on graphene-analogous 2D nanomaterials: Properties, modeling and applications, *Prog. Mater. Sci.* 100 (2019) 99–169; (b) M. Yang, Y. Liu, T. Fan, D. Zhang, Metal-graphene interfaces in epitaxial and bulk systems: A review, *Prog. Mater. Sci.* 110 (2020) 100652; (c) A. Stergiou, R. Cantón-Vitoria, M.N. Psarrou, S.P. Economopoulos, N. Tagmatarchis, Functionalized graphene and targeted applications – Highlighting the road from chemistry to applications, *Prog. Mater. Sci.* 114 (2020) 100683.
- [153] (a) P.L. Kumar, A. Lombardi, G. Byczynski, S.V.S.N. Murty, B.S. Murty, L. Bichler, Recent advances in aluminium matrix composites reinforced with graphene-based nanomaterial: A critical review, *Prog. Mater. Sci.* 128 (2022) 100948; (b) Y. Chen, T. Bai, N. Dong, F. Fan, S. Zhang, X. Zhuang, J. Sun, B. Zhang, X. Zhang, J. Wang, W.J. Blau, Graphene and its derivatives for laser protection, *Prog. Mater. Sci.* 84 (2016) 118–157; (c) V. Morales-Flórez, A. Domínguez-Rodríguez, Mechanical properties of ceramics

- reinforced with allotropic forms of carbon, *Prog. Mater. Sci.* 128 (2022) 100966; (d) C. Wang, D. Astruc, Recent developments of metallic nanoparticle-graphene nanocatalysts, *Prog. Mater. Sci.* 94 (2018) 306-383.
- [154] J. Liu, Y. Zhang, L. Zhang, F. Xie, A. Vasileff, S-Z. Qiao, Graphitic carbon nitride (g-C<sub>3</sub>N<sub>4</sub>)-derived N-rich graphene with tuneable interlayer distance as a high-rate anode for sodium-ion batteries, *Adv. Mater.* 31 (2019) 1901261.
- [155] P. Liu, V.B. Koman, D. Kozawa, M.S. Strano, 20 - Materials design for robotic platforms enabling unique mechanisms of projectile protection, Editor(s): Shawn M. Walsh, Michael S. Strano, In *Woodhead Publishing in Materials, Robotic Systems and Autonomous Platforms*, Woodhead Publishing, 2019; 493-521.
- [156] Automotive Tank Purchase Description ATPD 2352, Transparent Armor, Revision R, (U.S. Army, 26 April 2010).
- [157] L. Sun, R.F. Gibson, F. Gordaninejad, J. Suhr, Energy absorption capability of nanocomposites: A review, *Comp. Sci. Technol.* 69 (2009) 2392–2409.
- [158] J.T. Han, K. Cho, Nanoparticle-induced enhancement in fracture toughness of highly loaded epoxy composites over a wide temperature range, *J. Mater. Sci.* 41(13) (2006) 4239–4245.
- [159] J.C. Viana, Polymeric materials for impact and energy dissipation, *Plast. Rubber Compos.* 35(6–7) (2006) 260–267.
- [160] B.D. Wetzel, F. Hauptert, M. Zhang, Epoxy nanocomposites with high mechanical and tribological performance, *Compos. Sci. Technol.* 63(14) (2003) 2055–2067.
- [161] Z.H. Liu, K.W. Kwok, R.K.Y. Li, C.L. Choy, Effect of coupling agent and morphology on the impact strength of high density polyethylene/CaCO<sub>3</sub> composites, *Polym.* 43(8) (2002) 2501–2506.
- [162] A.K. Subramanian, C.T. Sun, Interlaminar fracture behavior of nanoclay reinforced glass fiber composites, *J. Compos. Mater.* 42(20) (2008) 2111–2122.
- [163] I.L. Dubnikova, S.M. Berezina, A.V. Antonov, Effect of rigid particle size on the toughness of filled polypropylene, *J. Appl. Polym. Sci.* 94(5) (2004) 1917–1926.
- [164] C.A. Cooper, D. Ravich, D. Lips, J. Mayer, H.D. Wagner, Distribution and alignment of carbon nanotubes and nanofibrils in a polymer matrix, *Compos. Sci. Technol.* 62(7–8) (2002) 1105–1112.
- [165] M. Kireitseu, D. Hui, G. Tomlinson, Advanced shock-resistant and vibration damping of nanoparticle-reinforced com-posite material, *Compos. Part B: Eng. B.* 39(1) (2008) 128–138.
- [166] H. Zhang, Z. Zhang, K. Friedrich, C. Eger, Property improvements of in-situ epoxy nanocomposites with reduced in-terparticle distance at high nanosilica content, *Acta Materialia* 54(7) (2006) 1833–1842.
- [167] B. Qi, Q.X. Zhang, M. Bannister, Y.W. Mai, Investigation of the mechanical properties of DGEBA-based epoxy resin with nanoclay additives, *Compos. Struct.* 75(1–4) (2006) 514–519.
- [168] C.B. Ng, L.S. Scbadler, R.W. Siegel, Synthesis and mechanical properties of TiO<sub>2</sub>-epoxy nanocomposites, *Nanostruct. Ma-ter.* 12(1) (1999) 507–510.
- [169] B. Sadeghi, P. Cavaliere, A. Shabani, Design strategies for enhancing strength and toughness in high performance metal matrix composites: A review, *Mater. Tod. Commun.* 37 (2023) 107535.

- [170] F.O. Braga, T.L. Milanezi, S.N. Monteiro, L.H.L. Louro, A.V. Gomes, E.P. Lima, Ballistic comparison between epoxy-ramie and epoxy-aramid composites in Multilayered Armor Systems, *J. Mater. Res. Technol.* 7 (4) (2018) 541-549.
- [171] Y. Zhang, K.E. Tanner, Effect of filler surface morphology on the impact behavior of hydroxyapatite reinforced high density polyethylene composites, *J. Mater. Sci. Mater. Med.* 19(2) (2008) 761-766.
- [172] E. Yousefi, A. Sheidaei, M. Mahdavi, M. Baniassadi, M. Baghani, G. Faraji, Effect of nanofiller geometry on the energy absorption capability of coiled carbon nanotube composite material, *Compos. Sci. Technol.* 153 (2017) 222-231.
- [173] M.Z. Rong, M.Q. Zhang, S.I. Pan, B. Lehmann, K. Friedrich, Analysis of the interfacial interactions in polypropylene/silica nano-composites, *Polym. Int.* 53(2) (2004) 176-183.
- [174] P.C. Ma, J.K. Kim, B.Z. Tang, Effects of silane functionalization on the properties of carbon nanotube/epoxy nanocomposites, *Compos. Sci. Technol.* 67(14) (2007) 2965-2972.
- [175] Y. Geng, M.Y. Liu, J. Li, X.M. Shi, J.K. Kim, Effects of surfactant treatment on mechanical and electrical properties of cnt/epoxy nanocomposites, *Compos. Part A. Appl. Sci. Manuf.* 39(12) (2008) 1876-1883.
- [176] H. Miyagawa, L.T. Drzal, Effect of oxygen plasma on mechanical properties of vapor grown carbon fiber nanocomposites, *Compos. Part A.* 36 (2005) 1440-1448.
- [177] Z. Yang, J. Ren, Z. Zhang, X. Chen, G. Guan, L. Qiu, Y. Zhang, H. Peng, Recent advancement of nanostructured carbon for energy applications, *Chem. Rev.* 115 (11) (2015) 5159-5223.
- [178] A. Eitan, F.T. Fisher, R. Andrews, L.C. Brinson, L.S. Schadler, Reinforcement mechanisms in MWCNT-filled polycarbonate, *Compos. Sci. Technol.* 66(9) (2006) 1162-1173.
- [179] G.A. Shen, S. Namilaee, N. Chandra, Load transfer issues in the tensile and compressive behavior of multiwall carbon nanotubes, *Mater. Sci. Eng. A.* 429(1-2) (2006) 66-73.
- [180] F.H. Gojny, M.H.G. Wichmann, B. Fiedler, K. Schulte, Influence of different carbon nanotubes on the mechanical properties of epoxy matrix composites – A Comparative study, *Compos. Sci. Technol.* 65(15-16) (2005) 2300-2313.
- [181] J.C. Lin, Investigation of impact behavior of various silica-reinforced polymeric matrix nanocomposites, *Compos. Struct.* 84(2) (2008) 125-31.
- [182] J.T. Han, K. Cho, Nanoparticle-induced enhancement in fracture toughness of highly loaded epoxy composites over a wide temperature range, *J. Mater. Sci.* 41(13) (2006) 4239-4245.
- [183] D.P.N. Vlasveld, P.P. Parlevliet, H.E.N. Bersee, S.J. Picken, Fibre-matrix adhesion in glass-fibre reinforced polyamide-6 sili-cate nanocomposites, *Compos Part A Appl Sci Manuf.* 36(1) (2005) 1-11.
- [184] C. Deshmane, Q. Yuan, R.D.K. Misr, On the fracture characteristics of impact tested high density polyethylene-calcium carbonate nanocomposites, *Mater. Sci. Eng. A.* 452-453 (2007) 592-601.
- [185] A.F. Avila, M.L. Soares, A. Silva Neto, A study on nanostructured laminated plates behavior under low-velocity impact loadings, *Int. J. Impact Eng.* 34(1) (2007) 28-41.

- [186] C. Deshmane, Q. Yuan, R.S. Perkins, R.D.K. Misra, On striking variation in impact toughness of polyethylene–clay and polypropylene–clay nanocomposite systems: the effect of clay–polymer interaction. *Mater. Sci. Eng. A.* 458 (1–2) (2007) 150–157.
- [187] S. Zhao, L.S. Schadler, R. Duncan, H. Hillborg, T. Auletta, Mechanisms leading to improved mechanical performance in nanoscale alumina filled epoxy, *Compos. Sci. Technol.* 68(14) (2008) 2965–2975.
- [188] S. Bourbigot, D.L. Vanderhart, J.W. Gilman, W.H. Awad, R.D. Davis, A.B. Morgan, C.A. Wilkie, Investigation of nanodispersion in polystyrene–montmorillonite nanocomposites by solid-state NMR, *J. Polym. Sci. Part B Polym. Phys.* 2003; 41(24): 3188–3213.
- [189] F.H. Gojny, M.H.G. Wichmann, B. Fiedler, K. Schulte, Influence of different carbon nanotubes on the mechanical properties of epoxy matrix composites—A Comparative Study, *Compos. Sci. Technol.* 65(15–16) (2005) 2300–2313.
- [190] G. Caprino, V. Lopresto, D. Santoro, Ballistic impact behavior of stitched graphite/epoxy laminates. *Comp. Sci. Technol.* 67(2) (2007) 325–335.
- [191] G.S. Langdon, S.L. Lemarski, G.N. Nurick, M.C. Simmons, W.J. Cantwell, G.K. Scheleyer, Behavior of fibre-metal laminates subjected to localized blast loading: Part I: Experimental observations, *Inter. J. Impact Engin.* 34(8) (2007) 1202–1222.
- [192] R.K. Luo, E.R. Green, C.J. Morrison, Impact damage analysis of composite plates, *Inter. J. Impact Engin.* 22(5) (1999) 435–447.
- [193] S. Ozden, P.A.S. Autreto, C.S. Tiwary, S. Khatriwada, L. Machado, D.S. Galvao, R. Vajtai, E.V. Barrera, P.M. Ajayan, Unzipping Carbon Nanotubes at High Impact, *Nano Lett.* 14 (7) (2014) 4131–4137.
- [194] R.A.W. Mines, A.M. Roach, N. Jones, High velocity perforation behavior of polymer composite laminates, *Inter. J. Impact Engin.* 22(6) (1999) 561–588.
- [195] W.L. Cheng, S. Langlie, S. Itoh, High velocity impact of thick composites, *Inter. J. Impact Engin.* 29(2) (2003) 167–184.
- [196] B. Gu, Analytical modeling for ballistic perforation of planar plain-woven fabric target by projectile, *Comp. Part B.* 34(3) (2003) 361–371.
- [197] S.V. Potti, C.T. Sun, Prediction of impact induced penetration and delamination in thick composite laminates, *Inter. J. Impact Eng.* 19(1) (1997) 31–48.
- [198] W.H. Yu, S.L. Sing, C.K. Chua, C.N. Kuo, X.L. Tian, Particle-reinforced metal matrix nanocomposites fabricated by selective laser melting: A state of the art review, *Prog. Mater. Sci.* 104 (2019) 330–379.
- [199] (a) M. Wong, W.L.E. Gupta, Effect of Hybrid Length Scales (micro + nano) of SiC reinforcement on the properties of magnesium, *Solid State Phenom.* 111 (2006) 91–94; (b) M.S. Selim, H. Yang, Y. Li, F.Q. Wang, X. Li, Y. Huang, Ceramic hyper-branched alkyd/ $\gamma$ -Al<sub>2</sub>O<sub>3</sub> nanorods composite as a surface coating, *Prog. Org. Coat.* 120 (2018) 217–227.

- [200] (a) M.S. Selim, M.A. Shenashen, N.A. Fatthallah, A. Elmarakbi, S.A. El-Safty, In situ fabrication of one-dimensional-based lotus-like silicone/ $\gamma$ -Al<sub>2</sub>O<sub>3</sub> nanocomposites for marine fouling release coatings, *Chem. Select.* 2 (30) (2017) 9691–9700; (b) N.A. Fatthallah, M.S. Selim, S.A. El Safty, M.M. Selim, M.A. Shenashen, Engineering nanoscale hierarchical morphologies and geometrical shapes for microbial inactivation in aqueous solution, *Mater. Sci. Eng. C* 122 (2021) 111844.
- [201] S.F. Hassan, M. Gupta, Effect of particulate size of Al<sub>2</sub>O<sub>3</sub> reinforcement on microstructure and mechanical behavior of solidification processed elemental Mg, *J. Alloys Compd.* 419 (2006) 84–90.
- [202] Q.B. Nguyen, M. Gupta, T.S. Srivatsan, On the role of nano-alumina particulate reinforcements in enhancing the oxidation resistance of magnesium alloy AZ31B, *Mater. Sci. Engin. A* 500 (2009) 233–237.
- [203] S.F. Wang, J. Zhang, D.W. Luo, F. Gu, D.Y. Tang, Z.L. Dong, G.E.B. Tan, W.X. Que, T.S. Zhang, S. Li, L.B. Kong, Transparent ceramics: Processing, materials and applications, *Prog. Solid State Chem.* 41 (1-2) (2013) 20-54.
- [204] H.T. Zhang, J.C. Ye, S.P. Joshi, J.M. Schoenung, E.S.C. Chin, G.A. Gazonas, K. Ramesh, Super-light weight nanoengineered aluminum for strength under impact, *Adv. Eng. Mater.* 9(5) (2007) 355–9.
- [205] U.A. Shakil, S.B. Abu Hassan, M.Y. Yahya, Mujiyono, D. Nurhadiyanto, A review of properties and fabrication techniques of fiber reinforced polymer nanocomposites subjected to simulated accidental ballistic impact, *Thin-Walled Struct.* 158 (2021) 107150.
- [206] M-W. Ho, C-K. Lam, K-T. Kau, D.H.L. Ng, D. Hui, Mechanical properties of epoxy-based composites using nanoclays, *Compos. Struct.* 75 (3) (2006) 415-421.
- [207] B.K. Money, K. Hariharan, J. Swenson, Glass transition and relaxation processes of nanocomposite polymer electrolytes, *J. Phys. Chem. B.* 116 (26) (2012) 7762–7770.
- [208] M. Kukreja, R. Balasubramaniam, Q.B. Nguyen, M. Gupta, Enhancing corrosion resistance of Mg alloy AZ31B in NaCl solution using alumina reinforcement at nanolength scale, *Corros. Eng. Sci. Technol.* 44 (2009) 381–383.
- [209] S. Goodarzi, T. Da Ros, J. Conde, F. Sefat, M. Mozafari, Fullerene: biomedical engineers get to revisit an old friend, *Mater. Tod.* 20 (8) (2017) 460-480.
- [210] A.R. Oganov, C.J. Pickard, Q. Zhu, R.J. Needs, Structure prediction drives materials discovery, *Nature Rev. Mater.* 4 (2019) 331–348.
- [211] L.M. Cao, C.X. Gao, H.P. Sun, G.T. Zou, Z. Zhang, X.Y. Zhang, M. He, M. Zhang, Y.C. Li, J. Zhang, D.Y. Dai, L.L. Sun, W.K. Wang, Synthesis of diamond from carbon nanotubes under high pressure and high temperature, *Carbon*, 39 (2001) 311-314.
- [212] J.L. Rivera, C. McCabe, P.T. Cummings, Oscillatory behavior of double-walled nanotubes under extension: a simple nanoscale damped spring, *Nano Lett.* 3 (2003) 1001.
- [213] M. Naffakh, A.M. Diez-Pascual, C. Marco, G.J. Ellis, M.A. Gomez-Fatou, Opportunities and challenges in the use of inorganic fullerene-like nanoparticles to produce advanced polymer nanocomposites, *Prog. Polym. Sci.* 38 (8) (2013) 1163-1231.



- [214] R. Tenne, L. Margulis, M. Genut, G. Hodes, Polyhedral and cylindrical structures of WS<sub>2</sub>, *Nature*. 360 (1992) 444–446.
- [215] L. Margulis, G. Salitra, R. Tenne, M. Talianker, Nested fullerene-like structures, *Nature*. 365 (1993) 113–114.
- [216] R. Tenne, Inorganic nanotubes and fullerene-like materials, *Chem.-A Eur. J.* 8 (2002) 5297–304.
- [217] K. Mylvaganam, L.C. Zhang, Energy absorption capacity of carbon nanotubes under ballistic impact. *Appl. Phys. Lett.* 89 (2006) 123-127.
- [218] M.A. Tian, Z. Tao, G. PengGang, Z. JianChun, Synthesis and properties of ultrahigh molecular weight polyethylene/WS<sub>2</sub> nanoparticle fiber for bullet-proof materials, *Chin. Sci. Bull.* 58(8) (2013) 945-948.
- [219] D. Quan, D. Carolan, C. Rouge, N. Murphy, A. Ivankovic, Carbon nanotubes and core-shell rubber nanoparticles modified structural epoxy adhesives, *J. Mater. Sci.* 52 (2017) 4493–4508.
- [220] X. Liu, L. Dai, Carbon-based metal-free catalysts, *Nature Rev. Mater.* 1 (2016) 16064.
- [221] C. Huang, X. Qian, R. Yang, Thermal conductivity of polymers and polymer nanocomposites, *Mater. Sci. Eng. R Rep.* 132 (2018) 1-22.
- [222] K. Mylvaganam, L.C. Zhang, Energy absorption capacity of carbon nanotubes under ballistic impact, *Appl. Phys. Lett.* 89 (2006) 123-127.
- [223] D. Kong, Z. Xiao, Y. Gao, X. Zhang, R. Guo, X. Huang, X. Li, L. Zhi, Sp<sup>2</sup>-carbon dominant carbonaceous materials for energy conversion and storage, *Mater. Sci. Eng. R Rep.* 137 (2019) 1-37.
- [224] K. Koziol, J. Vilatela, A. Moisala, M. Motta, Ph. Cuniff, M. Sennett, A. Windle, High-performance carbon nanotube fiber. *Science*, 318 (2007) 1892–1895.
- [225] Q. Lu, G. Keskar, R. Ciocan, R. Rao, R.B. Mathur, A.M. Rao, L.L. Larcom, Determination of carbon nanotube density by gradient sedimentation, *J. Phys. Chem. B.* 110 (48) (2006) 24371–24376.
- [226] P. Papanikos, D.D. Nikolopoulos, K.I. Tserpes, Equivalent beams for carbon nanotubes, *Comput. Mater. Sci.* 43(2) (2008) 345–352.
- [227] R.J. Mora, J.J. Vilatela, A.H. Windle, Properties of composites of carbon nanotube fibres, *Compos. Sci. Technol.* 69 (2009) 1558–1563.
- [228] N. Behabtu, M.J. Green, M. Pasquali, Carbon nanotube-based neat fibers, *Nano tod.* 3 (5–6) (2008) 24-34.
- [229] M. Meo, M. Rossi, Prediction of young's modulus of single wall carbon nanotubes by molecular-mechanics based fi-nite element modeling, *Compos. Sci. Technol.* 66(11–12) (2006) 1597–605.
- [230] C. Deng, X. Zhang, D. Wang, Q. Lin, A. Li, Preparation and characterization of carbon nanotubes/aluminum matrix com-posites, *Mater Lett.* 61 (2007) 1725-1728.
- [231] V. Georgakilas, J.A. Perman, J. Tucek, R. Zboril, Broad family of carbon nanoallotropes: classification, chemistry, and applications of fullerenes, carbon dots, nanotubes, graphene, nanodiamonds, and combined superstructures, *Chem. Rev.* 115 (11) (2015) 4744–4822.

- [232] A. Morka, B. Jackowska, Ballistic resistance of the carbon nanotube fibres reinforced composites—numerical study, *Comput. Mater. Sci.* 50 (2011) 1244–1249.
- [233] K.R. Atkinson, S.C. Hawkins, C. Huynh, C. Skourtis, J. Dai, M. Zhang, S. Fang, A.A. Zakhidov, S.B. Lee, A.E. Aliev, C.D. Williams, R.H. Baughman, Multifunctional carbon nanotube yarns and transparent sheets: fabrication, properties, and applications, *Physica B* 394 (2007) 339–343.
- [234] S. Sharma, S.R. Dhakate, A. Majumdar, B.P. Singh, Improved static and dynamic mechanical properties of multiscale bucky paper interleaved Kevlar fiber composites, *Carbon* 152 (2019) 631–642.
- [235] G.R. Villanueva, W.J. Cantwell, The high velocity impact response of composite and FML-reinforced sandwich structures, *Compos. Sci. Technol.* 64(1) (2004) 35–54.
- [236] L. Hao, H. Song, L. Zhang, X. Wan, Y. Tang, Y. Lv, SiO<sub>2</sub>/graphene composite for highly selective adsorption of Pb(II) ion, *J. Colloid Interface Sci.* 369(1) (2012) 381–387.
- [237] M. Rashad, F. Pan, A. Tang, Y. Lu, M. Asif, S. Hussain, J. She, J. Gou, J. Mao, Effect of graphene nanoplatelets (gnps) addition on strength and ductility of magnesium–titanium alloys, *J. Magn. Alloy.* 1 (2013) 242–248.
- [238] (a) T. Kuilla, S. Bhadra, D. Yao, N.H. Kim, S. Bose, J.H. Lee, Recent advances in graphene based polymer composites, *Prog. Polym. Sci.* 35 (11) (2010) 1350–1375; (b) H.H. El-Maghrabi, E.A. Nada, F.S. Soliman, Y.M. Moustafa, A.E. Amin, One pot environmental friendly nanocomposite synthesis of novel TiO<sub>2</sub>-nanotubes on graphene sheets as effective photocatalyst, *Egypt. J. Petrol.* 25 (2016) 575–584.
- [239] Z. Chen, Z. Zhang, Y. Wang, D. Xu, Y. Zhao, Butterfly inspired functional materials, *Mater. Sci. Eng. R: Rep.* 144 (2021) 100605.
- [240] (a) S. Park, R.S. Ruoff, Chemical methods for the production of graphenes, *Nat Nano.* 4 (4) (2009) 217–224; (b) E. Morales-Narváez, L.F. Sgobbi, S.A.S. Machado, A. Merkoçi, Graphene-encapsulated materials: Synthesis, applications and trends, *Prog. Mater. Sci.* 86 (2017) 1–24.
- [241] A. Weerasinghe, C-T. Lu, D. Maroudas, A. Ramasubramaniam, Multiscale shear-lag analysis of stiffness enhancement in polymer–graphene nanocomposites, *ACS Appl. Mater. Interfaces* 9 (27) (2017) 23092–23098.
- [242] (a) M. Inagaki, Y.A. Kim, M. Endo, Graphene: preparation and structural perfection. *J. Mater. Chem.* 21 (2011) 3280–3294; (b) Q. Zheng, Z. Li, J. Yang, J-K. Kim, Graphene oxide-based transparent conductive films, *Prog. Mater. Sci.* 64 (2014) 200–247.
- [243] (a) M.A. Rafiee, J. Rafiee, I. Srivastava, Z. Wang, H. Song, Z-Z. Yu, N. Koratkar, Fracture and fatigue in graphene nanocomposites, *Small* 6 (2) (2010) 179–183; (b) D.G. Papageorgiou, I.A. Kinloch, R.J. Young, Mechanical properties of graphene and graphene-based nanocomposites, *Prog. Mater. Sci.* 90 (2017) 75–127.
- [244] L.M. Veca, M.J. Meziani, W. Wang, X. Wang, F. Lu, P. Zhang, Y. Lin, R. Fee, J.W. Connell, Y-P. Sun, Carbon nanosheets for polymeric nanocomposites with high thermal conductivity, *Adv. Mater.* 21 (20) (2009) 2088–2092.

- [245] (a) Z. Xu, C. Gao, In situ polymerization approach to graphene-reinforced nylon-6 composites, *Macromol.* 43 (16) (2010) 6716–6723; (b) W.L. Zhang, B.J. Park, H.J. Cho, Colloidal graphene oxide/polyaniline nanocomposite and its electrorheology, *Chem. Commun.* 46 (2010) 5596–5598.
- [246] X. An, T. Simmons, R. Shah, C. Wolfe, K.M. Lewis, M. Washington, S.K. Nayak, S. Talapatra, S. Kar, Stable aqueous dispersions of noncovalently functionalized graphene from graphite and their multifunctional high-performance applications, *Nano Lett.* 10 (11) (2010) 4295–4301.
- [247] K.P. Loh, Q. Bao, P.K. Ang, J. Yang, The chemistry of graphene, *J. Mater. Chem.* 20 (2010) 2277–2289.
- [248] D. Galpaya, M. Wang, M. Liu, N. Motta, E. Waclawik, C. Yan, Recent advances in fabrication and characterization of graphene-polymer nanocomposites, *Graphene* 1 (2012) 30–49.
- [249] A.T. Sareshkeh, M.S.S. Dorraji, M.H. Rasoulifard, The role of g-C<sub>3</sub>N<sub>4</sub> as nanofiller in improvement of mechanical, thermal, and X-band wave absorption properties of epoxy vinyl ester coating, *Prog. Org. Coat.* 125 (2018) 472–480.
- [250] L. Ghalamchia, S. Abera, V. Vatanpourb, M. Kian, A novel antibacterial mixed matrixed PES membrane fabricated from embedding aminated Ag<sub>3</sub>PO<sub>4</sub>/g-C<sub>3</sub>N<sub>4</sub> nanocomposite for use in the membrane bioreactor, *J. Indust. Engin. Chem.* 70 (2019) 412–426.
- [251] L. Sun, T. Du, C. Hu, J. Chen, J. Lu, Z. Lu, H. Han, Antibacterial activity of graphene oxide/g-C<sub>3</sub>N<sub>4</sub> composite through photocatalytic disinfection under visible Light, *ACS Sustainable Chem. Eng.* 5(10) (2017) 8693–8701.
- [252] L. Gong, R.J. Young, I.A. Kinloch, I. Riaz, R. Jalil, K.S. Novoselov, Optimizing the reinforcement of polymer-based nano-composites by graphene, *ACS Nano* 6 (3) (2012) 2086–2095.
- [253] T. Kuila, S. Bose, M.K. Mishra, P. Khanra, N.H. Kim, J.H. Lee, Chemical functionalization of graphene and its applications, *Prog. Mater. Sci.* 57 (7) (2012) 1061–1105.
- [254] V. Georgakilas, M. Otyepka, A.B. Bourlinos, V. Chandra, N. Kim, K.C. Kemp, P. Hobza, R. Zboril, K.S. Kim, Functionalization of graphene: covalent and non-covalent approaches, derivatives and applications, *Chem. Rev.* 112 (11) (2012) 6156–6214.
- [255] L. Paliotta, G.D. Bellis, A. Tamburrano, F. Marra, A. Rinaldi, S.K. Balijepalli, S. Kaciulis, M.S. Sarto, Highly conductive multilayer-graphene paper as a flexible lightweight electromagnetic shield, *Carbon* 89 (2015) 260–271.
- [256] J. Rafiee, M.A. Rafiee, Z. Wang, H. Song, Z-Z. Yu, N. Koratkar, Enhanced mechanical properties of nanocomposites at low graphene content, *ACS Nano* 3 (2009) 3884–3890.
- [257] Z. Meng, J. Han, X. Qin, Y. Zhang, O. Balogun, S. Keten, Spalling-like failure by cylindrical projectiles deteriorates the ballistic performance of multi-layer graphene plates, *Carbon* 126 (2018) 611–619.
- [258] S.J.V. Frankland, V.M. Harik, G.M. Odegard, D.W. Brenner, T.S. Gates, The stress-strain behavior of polymer nanotube composites from molecular dynamics simulation. *Compos. Sci. Technol.* 63 (11) (2003) 1655–1661.

- [259] Z. Hashin, B.W. Rosen, The elastic moduli of fiber-reinforced materials, *J. Appl. Mechanics*. 31 (2) (1964) 223–232.
- [260] Q. Wang, V.K. Varadan, S.T. Quek, Small scale effect on elastic buckling of carbon nanotubes with nonlocal continuum models, *Phys. Lett. A*. 357 (2) (2006) 130 – 135.
- [261] A.P. Awasthi, D.C. Lagoudas, D.C. Hammerand, Modeling of graphene polymer interfacial mechanical behavior using mo-lecular dynamics, *Model. Simul. Mater. Sci. Eng.* 17 (2009) 015002.
- [262] J. Cho, J.J. Luo, I.M. Daniel, Mechanical characterization of graphite/epoxy nanocomposites by multi-scale analysis, *Compos. Sci. Technol.* 67 (1112) (2007) 2399–2407.
- [263] A. Montazeri, H. Rafii-Tabar, Multiscale modeling of graphene- and nanotube-based reinforced polymer nanocompo-sites. *Phys. Let. A*. 375 (45) (2011) 4034 – 4040.
- [264] A. Parashar, P. Mertiny, Representative volume element to estimate buckling behavior of graphene/polymer nanocom-posite, *Nanoscale Research Lett.* 7 (1) (2012) 515.
- [265] A. Elmarakbi, W. Jianhua, W.L. Azoti, Non-linear elastic moduli of graphene sheet-reinforced polymer composites, *Inter. J. Sol. Struct.* 81 (2015) 383–392.
- [266] A. Elmarakbi, W. Azoti, M. Serry, Multiscale modelling of hybrid glass fibres reinforced graphene platelets polyamide {PA6} matrix composites for crashworthiness applications, *Appl. Mater. Tod.* 6 (2017) 1–8.
- [267] O.M. Istrate, K.R. Paton, U. Khan, O.A. Neill, A. Bell, J.N. Coleman, Reinforcement in melt-processed polymer graphene com-posites at extremely low graphene loading level, *Carbon* 78 (2014) 243–249.
- [268] M. Zhang, Y. Li, Z. Su, C. Wei, Recent advances in the synthesis and applications of graphene-polymer nanocomposites, *Polym. Chem.* 6 (2015) 6107–6124.
- [269] K. Hu, D.D. Kulkarni, I. Choi, V.V. Tsukruk, Graphene-polymer nanocomposites for structural and functional applications, *Prog. Polym. Sci.* 39 (11) (2014) 1934–1972.
- [270] M. Bahiraei, S. Heshmatian, Graphene family nanofluids: A critical review and future research directions, *Energy Convers. Manag.* 196 (2019) 1222-1256.
- [271] J-H. Lee, P.E. Loya, J. Lou, E.L. Thomas, Dynamic mechanical behavior of multilayer graphene via supersonic projectile penetration, *Science* 346 (6213) (2014) 1092-1096.
- [272] S. Wang, E. Gao, Z. Xu, Interfacial failure boosts mechanical energy dissipation in carbon nanotube films under ballistic impact, *Carbon* 146 (2019) 139-146.
- [273] F. Findik, N. Tarim, Ballistic impact efficiency of polymer composites, *Compos. Struct.* 61 (2003) 187–192.
- [274] G.R. Villanueva, W.J. Cantwell, The mechanical properties of fibre-metal laminates based on glass fibre reinforced polypropylene, *Compos. Sci. Technol.* 60(7) (2000) 1085-1094.
- [275] A.K. Bandaru, S. Ahmad, N. Bhatnagar, Ballistic performance of hybrid thermoplastic composite armors reinforced with Kevlar and basalt fabrics, *Compos. Part A Appl. Sci. Manuf.* 97 (2017) 151-165.

- [276] E.E. Haro, A.G. Odeshi, J.A. Szpunar, The energy absorption behavior of hybrid composite laminates containing nano-fillers under ballistic impact, *Inter. J. Impact Engin.* 96 (2016) 11–22.
- [277] M. Übeyli, E. Balci, B. Sarikan, M.K. Öztas, N. Camus, R.O. Yildirim, O. Keles, The ballistic performance of sic–aa7075 functionally graded composite produced by powder metallurgy, *Mater. Des.* 56 (2014) 31–36.
- [278] V. Obradovic, D.B. Stojanovic, B. Jokic, M. Zrilic, V. Radojevic, P.S. Uskokovic, R. Aleksic, Nanomechanical and anti-stabbing properties of kolon fabric composites reinforced with hybrid nanoparticles, *Compos. Part B.* 108 (2017) 143–152.
- [279] X. Wang, Z.Z. Yong, Q.W. Li, P.D. Bradford, W. Liua, D.S. Tucker, W. Caid, H. Wang, F.G. Yuan, Y.T. Zhu, Ultrastrong, stiff and multifunctional carbon nanotube composites, *Mater. Res. Lett.* 1(1) (2013) 19–25.
- [280] (a) J.M. Zhang, Z. Mousavi, N. Soykeabkaew, P. Smith, T. Nishino, T. Peijs, All-aramid composites by partial fiber dissolution, *Appl. Mater. Inter.* 2(3) (2010) 919–926; (b) J. Jiang, Y. Li, C. Gao, N.D. Kim, X. Fan, G. Wang, Z. Peng, R.H. Hauge, J.M. Tour, Growing carbon nanotubes from both sides of graphene. *ACS Appl. Mater. Interfaces*, 8 (11) (2016) 7356–7362.
- [281] D.K. Patel, A.M. Waas, Damage and failure modelling of hybrid three-dimensional textile composites: a mesh objective multi-scale approach, *Phil. Trans. R. Soc. A* 374 (2016) 20160036.
- [282] B. Yu, R.S. Bradley, C. Soutis, P.J. Hogg, P.J. Withers, 2D and 3D imaging of fatigue failure mechanisms of 3D woven composites, *Compos. Part A Appl. Sci. Manuf.* 77 (2015) 37–49.
- [283] M.R. O’Masta, B.G. Compton, E.A. Gamble, F.W. Zok, V.S. Deshpande, H.N.G. Wadley, Ballistic impact response of an UHMWPE fiber reinforced laminate encasing of an aluminum-alumina hybrid panel, *Inter. J. Impact Engin.* 86 (2015) 131–144.
- [284] P. Turner, T. Liu, X. Zeng, Collapse of 3D orthogonal woven carbon fibre composites under in-plane tension/compression and out-of-plane bending, *Compos. Struct.* 142 (2016) 286–297.
- [285] W. Xiong, X. Zhang, M. Tan, C. Liu, X. Wu, The energy release characteristics of shock-induced chemical reaction of Al/Ni composites, *J. Phys. Chem. C.* 120 (2016) 24551–24559.
- [286] J. Lin, S.H. Bang, M.H. Malakooti, H.A. Sodano, Isolation of aramid nanofibers for high strength and toughness polymer nanocomposites, *ACS appl. Mater. Inter.* 9 (12) (2017) 11167–11175.
- [287] A. Yasmin, J.L. Abot, I.M. Daniel, Processing of clay–epoxy nanocomposites by shear mixing, *Script Mater.* 49 (2003) 81–86.
- [288] M.W. Ho, C.K. Lam, K.T. Kau, D.H.L. Ng, D. Hui, Mechanical properties of epoxy based composites using nanoclays, *Compos. Struct.* 75 (2006) 415–421.
- [289] A.F. Avila, M.I. Soares, A. Silva Neto, An experimental investigation on nanocomposites under impact loading. In M. Alves and N. Jones, editors, *Impact loading of lightweight structures*, Florianopolis (Santa Catarina, Brazil), 2005; 89–102 WIT Press.

- [290] K. Krishnan, S. Sockalingam, S. Bansal, S.D. Rajan, Numerical simulation of ceramic composite armor subjected to ballistic impact, *Compos. Part B: Engin.* 41 (8) (2010) 583-593.
- [291] V. Viswanathan, T. Laha, K. Balani, A. Agarwal, S. Seal, Challenges and advances in nanocomposite processing techniques, *Mater. Sci. Eng. R: Rep.* 54 (5-6) (2006) 121-285.
- [292] M. Gupta, W.L.E. Wong, Magnesium-based nanocomposites: Lightweight materials of the future, *Mater. Character.* 105 (2015) 30-46.
- [293] I.G. Crouch, Chapter 12: The future of armor materials, *Sci. Arm. Mater.* 2017, 675-692.
- [294] G.D. Cole, Magnesium. *Chem. Eng. News Archive.* 81 (36) (2003) 52.
- [295] A.O. Silva, K.G.C. Monsoro, S.S.A. Oliveira, R.P. Weber, S.N.J. Monteiro, Ballistic behavior of a hybrid composite reinforced with curaua and aramid fabric subjected to ultraviolet radiation, *J. Mater. Res. Technol.* 7(4) (2018) 584-591.
- [296] H.Z. Ye, X.Y. Liu, Review of recent studies in magnesium matrix composites, *J. Mater. Sci.* 9 (2004) 6153-6171.
- [297] P. Wambua, B. Vangrimde, S. Lomov, I. Verpoest, The response of natural fibre composites to ballistic impact by fragment simulating projectiles, *Compos. Struct.* 77 (2007) 232-240.
- [298] (a) L-L. Sun, D.S. Xiong, C-Y. Xu, Application of shear thickening fluid in ultra-high molecular weight polyethylene fabric, *J. Appl. Polym. Sci.* 129(4) (2013) 1922-1928; (b) R. Żurowski, A. Antosik, M. Głuszek, M. Szafran, Shear thickening ceramic-polymer composite, *Compos. Theory Pract.* 15 (4) (2015) 255-258.
- [299] M.R. O'Masta, V.S. Deshpande, H.N.G. Wadley, Mechanisms of projectile penetration in Dyneema® encapsulated aluminum structures, *Inter. J. Impact Engin.* 74 (2017) 16-35.
- [300] K. Krishnan, S. Sockalingam, S. Bansal, S.D. Rajan, Numerical simulation of ceramic composite armor subjected to ballistic impact, *Compos. Part B: Engin.* 41 (8) (2010) 583-593.
- [301] M. Fejdyś, K. Kośła, A. Kucharska-Jastrzębek, M. Łandwajt, Hybrydowe systemy zbrojeniowe z zaawansowanymi ceramicznymi i ultra-wysokimi włóknami polietylenowymi (UHMWPE), *FIBRES & TEXTILES in Eastern Europe*, 24 (2016) 3(117): 79-89.
- [302] J.P. Attwood, N.A. Fleck, H.N.G. Wadley, V.S. Deshpande, The compressive response of ultra-high molecular weight polyethylene fibers and composites, *Inter. J. Solids Struct.* 71 (2015) 141-155.
- [303] M.L. Ericson, Macroscopic, neat, single-walled carbon nanotube fiber, *Science* 305 (2004) 1447-1450.
- [304] N. Orlovskaya, M. Lugovy, V. Subbotin, V. Rachenko, J. Adams, M. Chheda, J. Shih, J. Sankar, S. Yarmolenko, Design and manufacturing of B<sub>4</sub>C-SiC layered ceramics for armour applications, *Proceedings of the ceramic armour and armour systems symposium*, 105 Annual Meeting of the American Ceramic Society, USA, 2003; 59-70.
- [305] A. Makeev, D. Srivastava, Molecular dynamics simulations of hypersonic velocity impact protection properties of CNT/a-SiC composites, *Compos. Sci. Technol.* 68(12) (2008) 2451-2455.

- [306] A.F. Avila, A.S. Neto, H. Nascimento Jr, Hybrid nanocomposites for mid-range ballistic protection. *Inter. J. Impact Engin.* 38 (2011) 669–675.
- [307] D. Pedrazzoli, A. Pegoretti, K. Kalaitzidou, Synergistic effect of graphite nanoplatelets and glass fibers in polypropylene composites, *J. Appl. Polym. Sci.* 132 (12) (2015) 41682.
- [308] X. Yang, Z. Wang, M. Xu, R. Zhao, X. Liu, Dramatic mechanical and thermal increments of thermoplastic composites by multi-scale synergetic reinforcement: carbon fiber and graphene nanoplatelet, *Mater. Des.* 44 (2013) 74 – 80.
- [309] G. Hernandez-Padron, F. Rojas, V.M. Castano, Ordered SiO<sub>2</sub>-(phenolic-formaldehyde resin) in-situ nanocomposites, *Nanotechnol.* 15 (1) (2003) 98.
- [310] M. Baniasadi, J. Huang, Z. Xu, S. Moreno, X. Yang, J. Chang, M.A. Quevedo-Lopez, A. Naraghi, M. Minary-Jolandan, High-performance coils and yarns of polymeric piezoelectric nanofibers, *ACS Appl. Mater. Interfaces* 79 (2015) 5358–5366.
- [311] S.H. Ji, Y-S. Cho, J.S. Yun, Wearable core-shell piezoelectric nanofiber yarns for body movement energy harvesting, *Nanomaterials* 9(4) (2019) 555.
- [312] H.A. Aisyah, M.T. Paridah, S.M. Sapuan, R.A. Ilyas, A. Khalina, N.M. Nurazzi, S.H. Lee, C.H.A. Lee, Comprehensive review on advanced sustainable woven natural fiber polymer composites, *Polymers* 13 (3) (2021) 471.
- [313] "Nano-Armor: Protecting The Soldiers of Tomorrow". *Isracast.com*. Archived from the original on 6 April 2009. Re-trieved 2009-04-06.
- [314] H. Parmar, T. Khan, F. Tucci, R. Umer, P. Carlone, Advanced robotics and additive manufacturing of composites: towards a new era in Industry 4.0, *Mater. Manuf. Process.* 37 (5) (2022) 483–517.
- [315] N.T. Tuli, S. Khatun, A.B. Rashid, Unlocking the future of precision manufacturing: A comprehensive exploration of 3D printing with fiber-reinforced composites in aerospace, automotive, medical, and consumer industries, *Heliyon* 10 (5) (2024) e27328.
- [316] X. Tian, et al., 3D printing of continuous fiber reinforced polymer composites: development, application, and prospective, *Chinese J. Mech. Eng. Addit. Manuf. Front.* 1 (1) (2022) 100016.
- [317] A. Sayam, et al., A review on carbon fiber-reinforced hierarchical composites: mechanical performance, manufacturing process, structural applications and allied challenges, vol. 32, no. 5, Springer Nature Singapore (2022).
- [318] N. Li, G. Link, J. Ma, J. Jelonnek, LiDAR based multi-robot cooperation for the 3D printing of continuous carbon fiber reinforced composite structures, *Adv. Transdiscipl. Eng.* 15 (2021) 125–132.
- [319] R.L. Ellis, F. Lalande, H.Y. Jia, Ballistic Impact resistance of SMA and spectra hybrid composites, *J. Reinforced Plastic Compos.* 17 (1998) 147–164.



- [320] R.J. Muhi, F. Najim, M.F.S.F. de-Moura, The effect of hybridization on the GFRP behavior under high velocity impact, *Compos. Part B-Engin.* 40 (2009) 798–803.
- [321] P.J. Hazell, G.J. Appleby-Thomas, A study on the energy dissipation of several different CFRP based targets completely penetrated by a high velocity projectile, *Compos Struct.* 91 (2009) 103–110.
- [322] K.S. Pandya, K. Akella, M. Joshi, N.K. Naik, Ballistic impact behaviour of carbon nanotube and nanosilica dispersed resin and composites, *J. Appl. Physics, AIP*, 112 (2012) 1–8.
- [323] F.O. Bragaa, L.T. Bolzana, F.S. da Luz, P.H.L. Machado Lopes, É.P.L. Jr., S.N. Monteiro, High energy ballistic and fracture comparison between multilayered armor systems using non-woven curaua fabric composites and aramid laminates, *J. Mater. Res. Technol.* 6(4) (2017) 417–422.
- [324] A. Ghazlan, T. Ngo, P. Tan, Y.M. Xie, P. Tran, M. Donough, Inspiration from Nature's body armours – A review of biological and bioinspired composites, *Compos. Part B: Engin.* 205 (2021) 108513.
- [325] F.L. McCrackin, H.F. Schiefer, J.C. Smith, W.K. Stone, Stress-strain relationships in yarns subjected to rapid impact loading: 2. Breaking velocities, strain energies, and theory neglecting wave propagation. *Text. Res. J.* 25 (1955) 529.
- [326] J.C. Smith, F.L. McCrackin, H.F. Schiefer, Stress strain relationships in yarns subjected to rapid impact loading: effect of wave propagation, *Text. Res. J.* 25 (1955) 701.
- [327] U. Mawkhlieng, A. Majumdar, Soft body armour, *Textile Prog.* 51 (2) (2019) 139–224.
- [328] Y.Q. Zhu, T. Sekine, Y.H. Li, M.W. Fay, Y.M. Zhao, C.H. Patrick Poa, Shock absorbing and failure mechanisms of WS<sub>2</sub> and MoS<sub>2</sub> nanoparticles with fullerene-like structures under shock wave pressure, *J. Am. Chem. Soc.* 127(46) (2015) 16263–16272.
- [329] L. Joly-Pottuz, J.M. Martin, F. Dassenoy, M. Belin, G. Montagnac, B. Reynard, N. Fleischer, Pressure-induced exfoliation of inorganic fullerene-like WS<sub>2</sub> particles in a hertzian contact, *J. Appl. Phys.* 99(2) (2006) 023524.
- [330] L. Hua, L.C. Brinson, Reinforcing efficiency of nanoparticles: a simple comparison for polymer nanocomposites, *Compos. Sci. Technol.* 68(6) (2008) 1502–1512.
- [331] M.S. Selim, S.A. El-Safty, N.A. Fatthallah, M.A. Shenashen, Silicone/graphene oxide sheet-alumina nanorod ternary compo-site for superhydrophobic antifouling coating, *Prog. Org. Coat.* 121 (2018) 160–172.

## Figures:

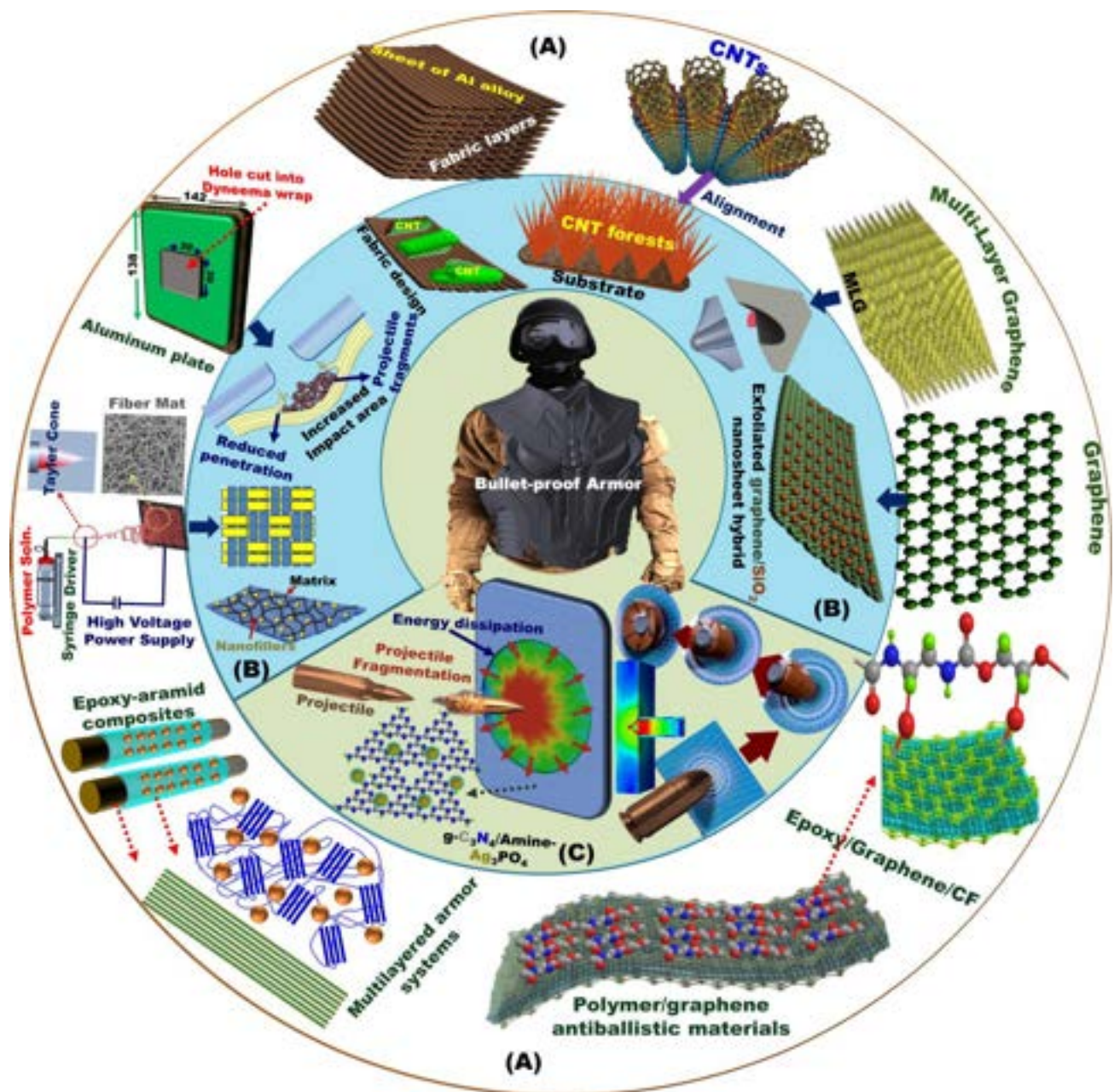


**Fig. 1.** Armors protect personnel from ballistic impacts. (A, B) Schematic design and building blocks of various anisotropic nanocomposite materials as an advanced filler terminology for fabrication of protective clothes for armors protect personnel from ballistic impacts. (C) The failure mechanism of antiballistic armors against bullets is based on absorption and dispersion of the transmitted impact energy result in bullet's deformation and mushrooming. The super lightweight nanocomposite fabrics are ideal bulletproof armors due to their robustness against speedy projectiles.

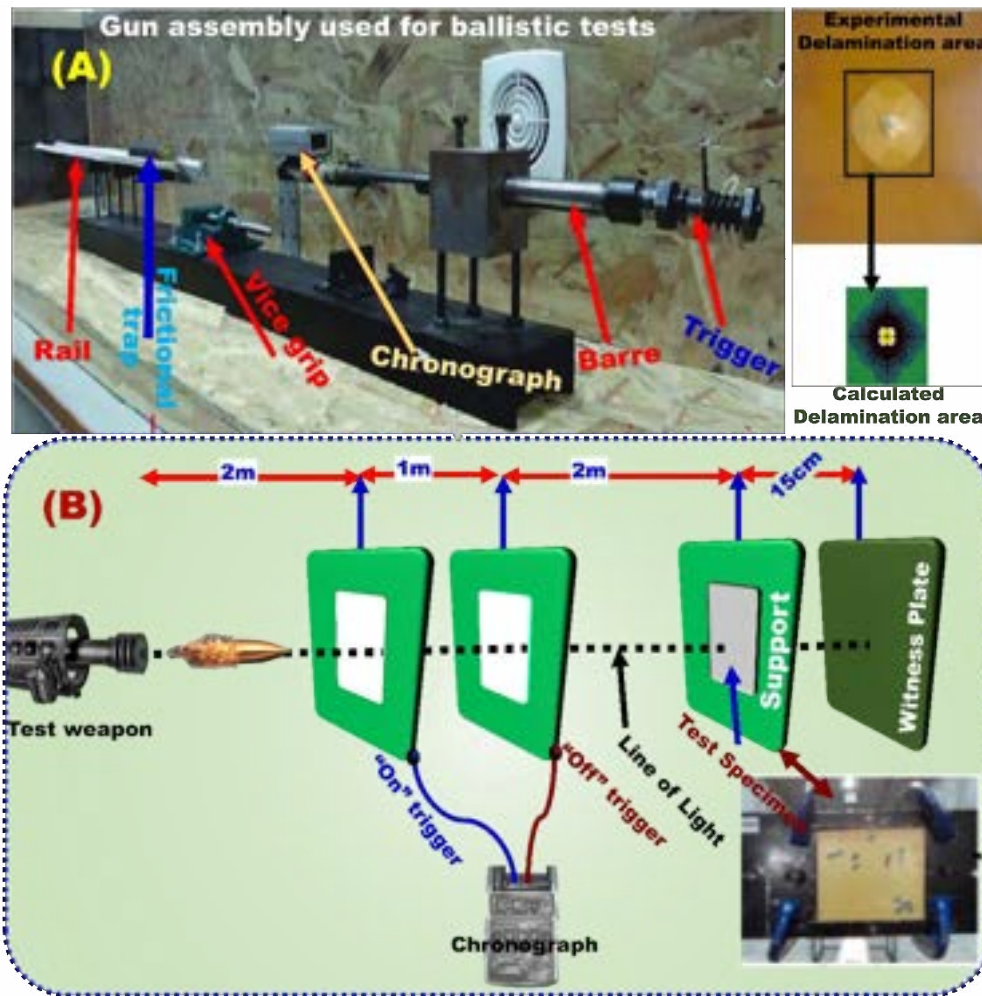


**Fig. 2.** Testing the ballistic-proof materials. (A) Schematic diagram of the gun assembly used in ballistic test, and the delamination area: experimental and calculated. (B) A ballistic testing device according to NIJ standard which also describes the bullet-penetration mechanism in an impact and the transfer from low mass and speed projectile to high mass and speed projectile [19]. Copyright 2014, Reprinted with permission from [19].

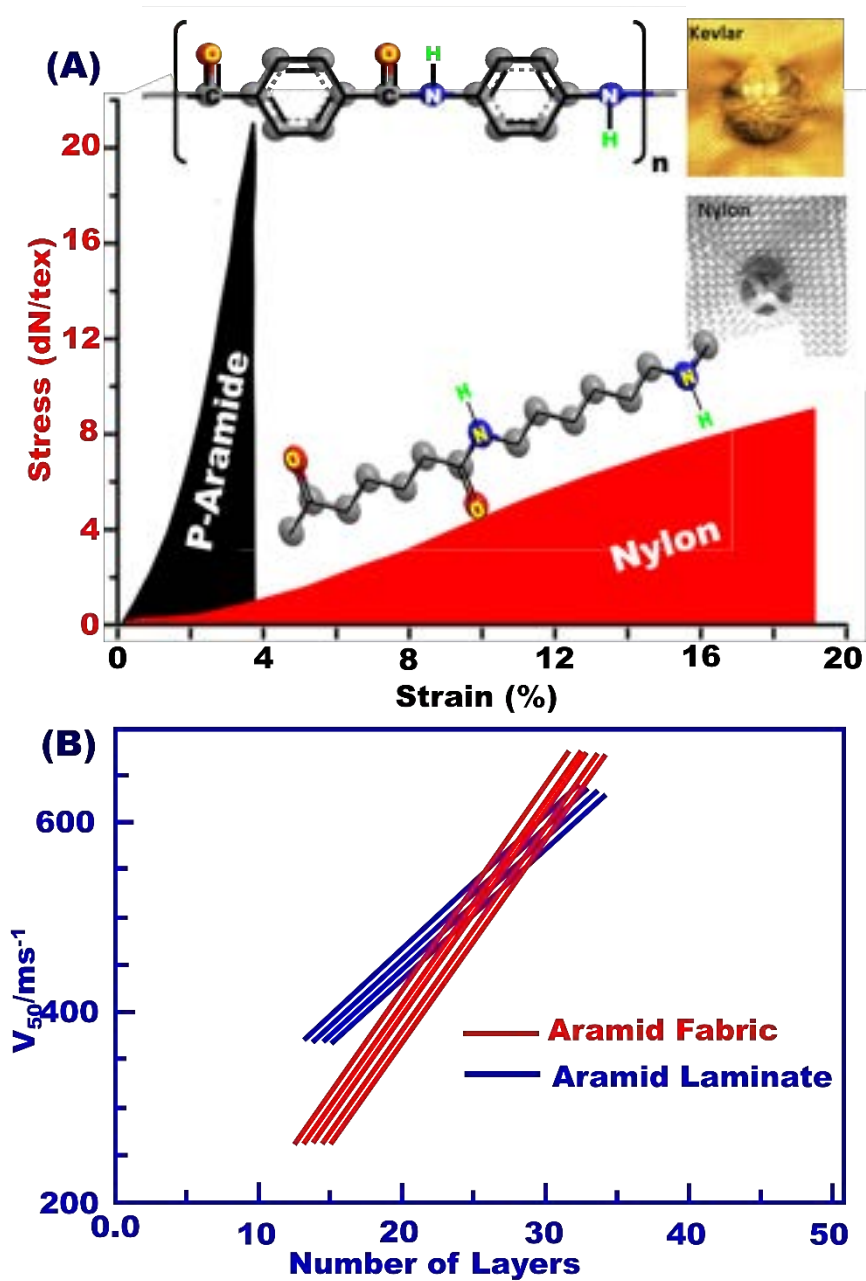


**Fig. 3.** Selecting bulletproof fiber. (a) Nylon and p-Aramid structures and stress-strain relationship of their fibers; while (b) represents the ballistic behavior of soft aramid fabric vs. hard laminate components [8]. Copyright 1993, reproduced with permission from Elsevier Ltd.



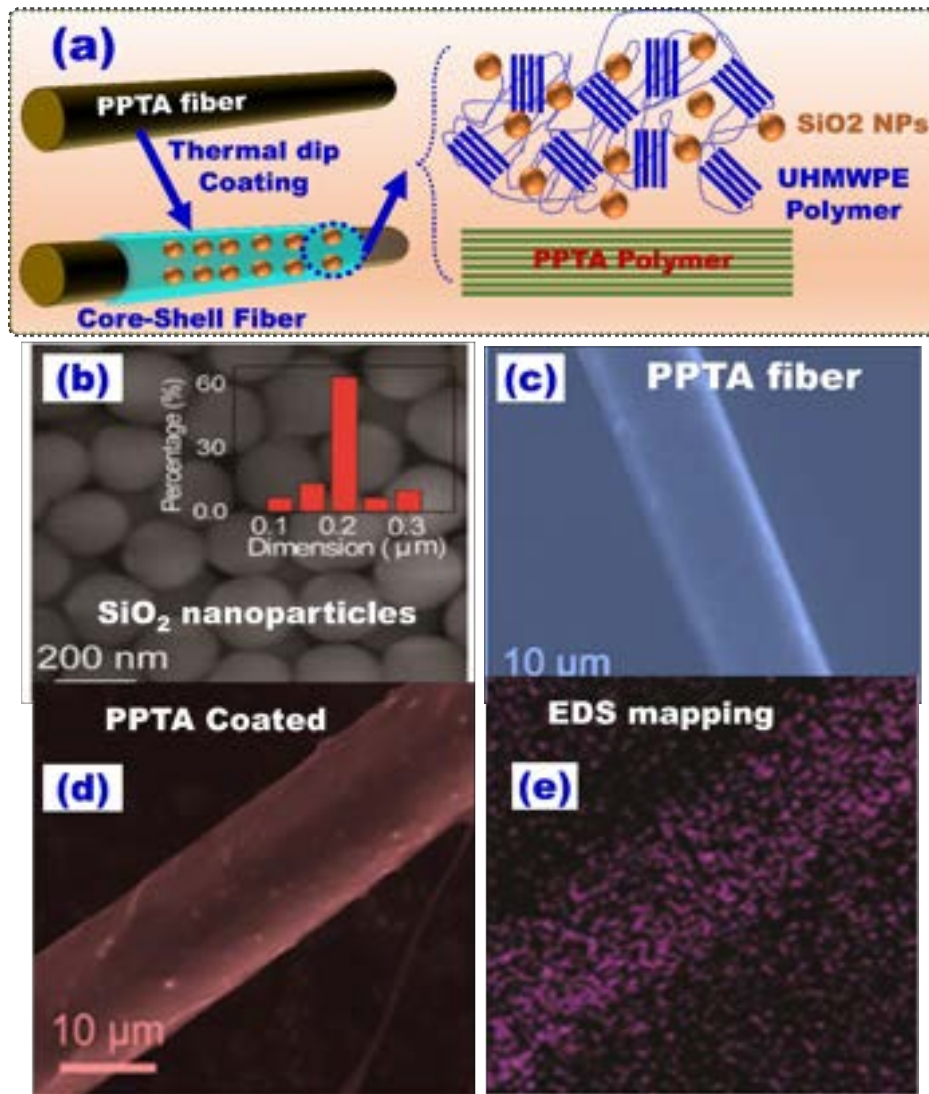


**Fig. 4.** UHMWPE for ballistic-proof armor. (a) Schematic design representing the High-performance fibers fabricated by coating poly-(p-phenylene terephthalamide) (PPTA) with UHMWPE and SiO<sub>2</sub> nanoparticles. (b- d) SEM image of the SiO<sub>2</sub> NPs, PPTA fiber, and PPTA fiber coated with UHMWPE and SiO<sub>2</sub> NPs. (e) EDS mapping of the coated fiber [43].

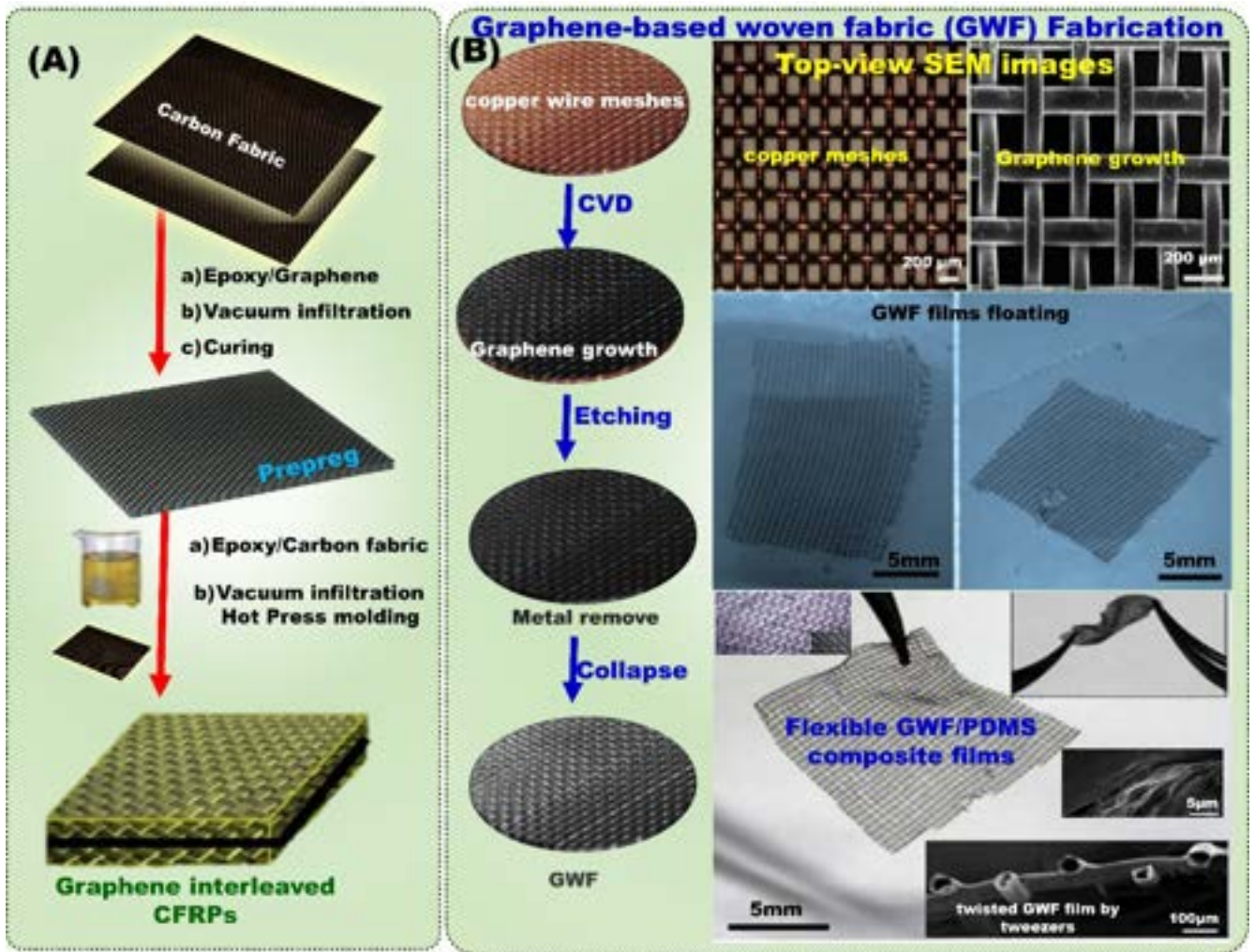


**Fig. 5.** Bulletproof armor composites. (A) Different steps for graphene interleaved epoxy composites synthesis. (B) Schematic of steps for preparation of graphene-based woven fabric (GWF) (left side), and macroscopic optical images of copper meshes, and its top-view SEM image after graphene growth, optical images of GWF films floating on water and deposited on glass, and Optical images of flexible GWF/PDMS composite films [68].

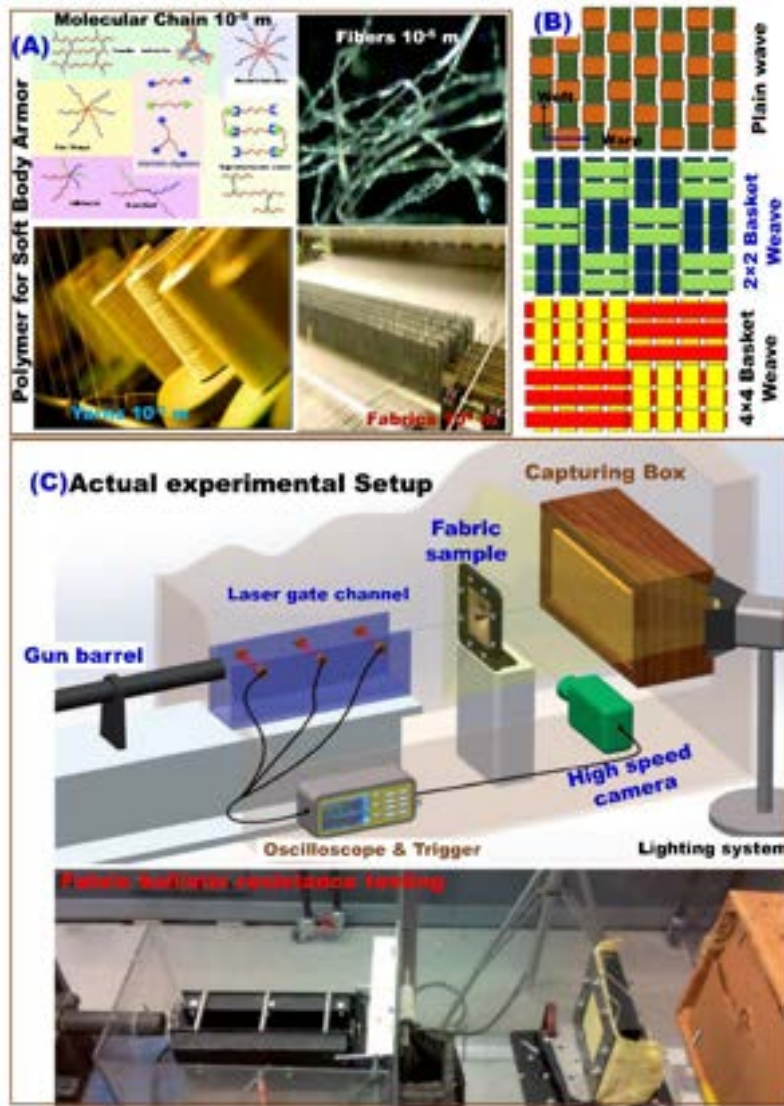


**Fig. 6.** Nanostructured designs for ballistic-proof armors. (A) Representative the polymer materials structure as soft body armor. (B) Schematic of fabric architectures of plain, 2x2 basket weave, and 4x4 basket weave architectures used in the soft body armor designs using aramid fibers [86]. Reproduced with permission from ref [86] (Copyright 2011, Dr. P.V. Cavallaro). (C) Representative the design of ballistic resistance test for actual experimental setup of fabric [90].



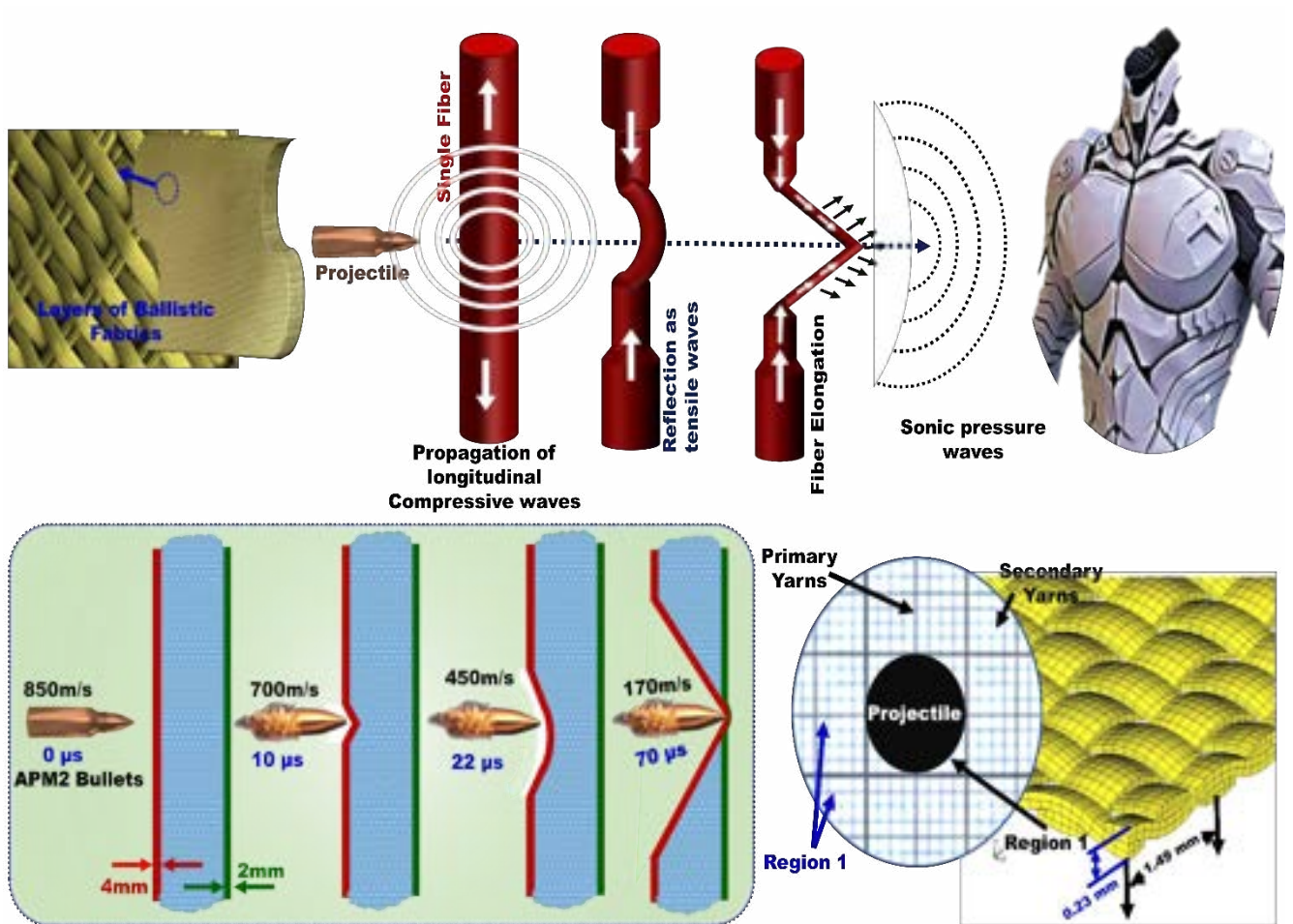


**Fig. 7.** Failure mechanism of fabric fibers. (A) Schematic illustration of the Failure mechanism of single fibre against bullet impact and on the right a photo of bullet-proof armor [6]. Copyright 2016, reproduced with permission from RSC. (B) Schematic of a layered fibrous structure envisioned arrangement of a typical 2D woven fabric composite target side view to stop armour piercing APM2 bullets, and different impact regions and yarns in front view [95].



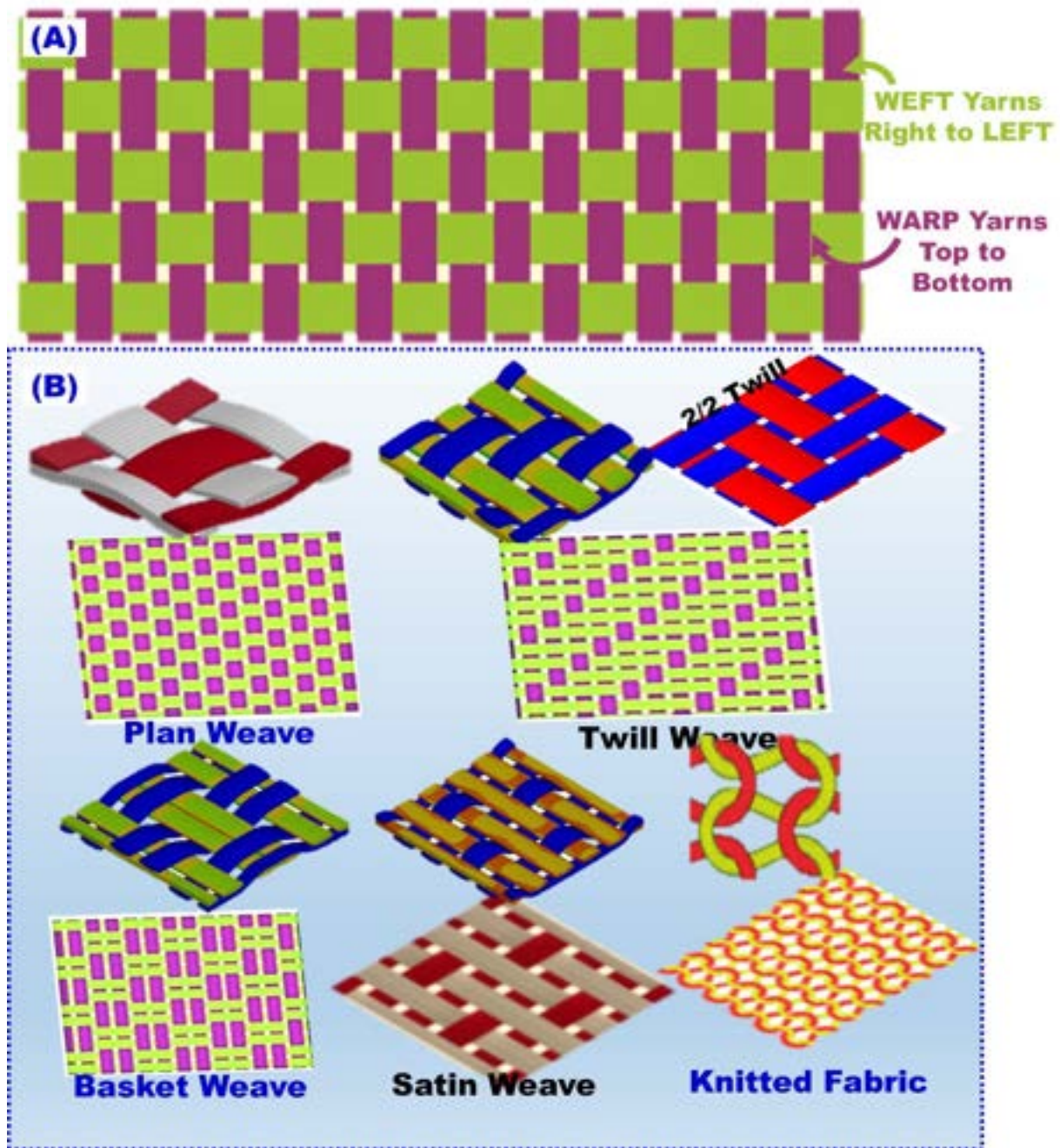


**Fig. 8.** Antiballistic factors of woven fabrics. (A) A layer fabric with binding of warp and weft yarns through the thickness, and (B) different architectures of woven fabrics including plain and basket weaves can be utilized in soft body armors.

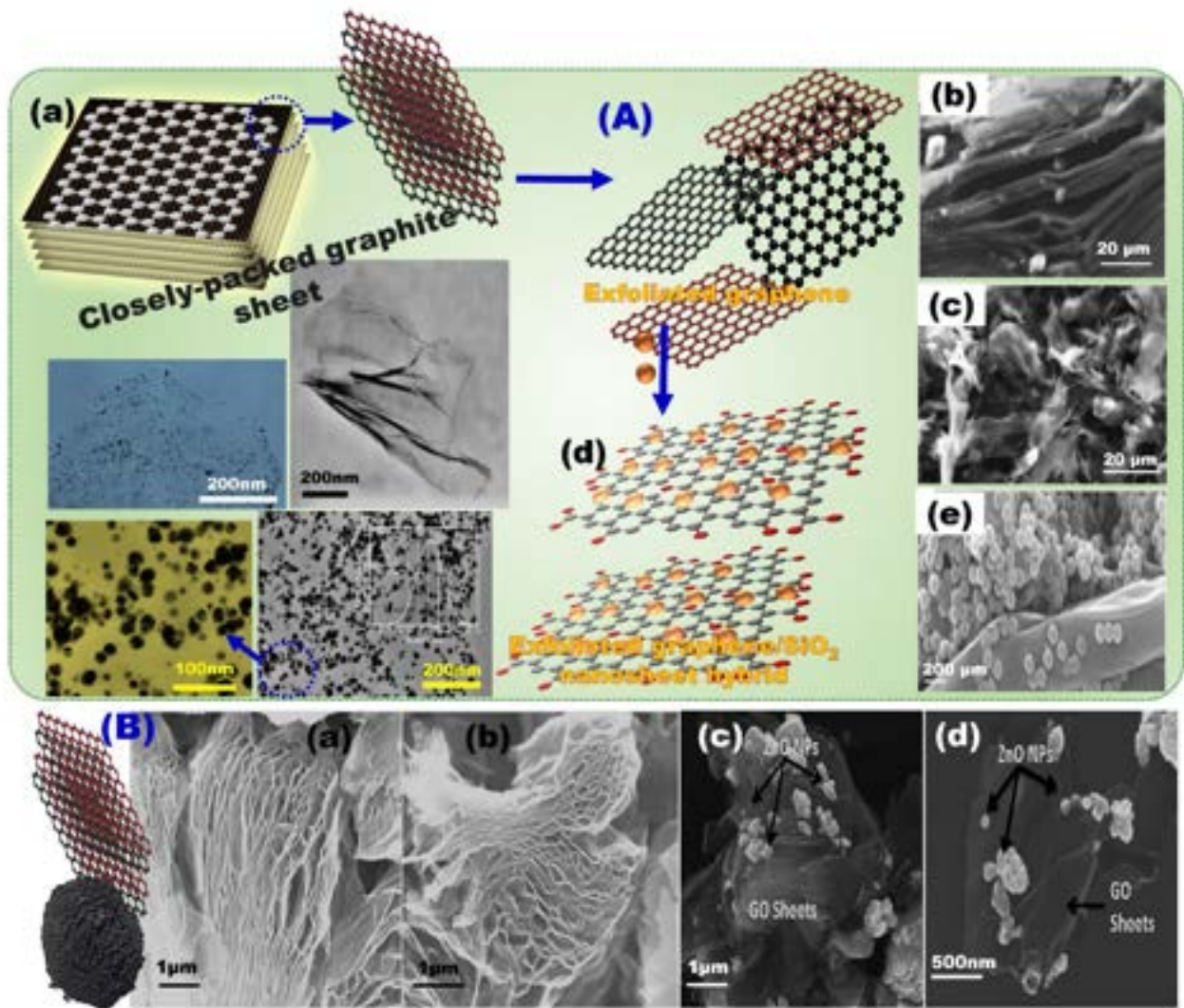


**Fig. 9.** Nanomaterial-building blocks for armors. (A) Schematic design of the NPs doped graphene: (a) Typical closely-packed graphite sheets which suffer from poor distribution properties; (B) Graphite sheets before expansion or exfoliation; (c) SEM micrograph of the closely-packed sheets after thermal shocking; (d) Typical exfoliated graphene sheet through anchoring with SiO<sub>2</sub> NPs; and (e) represents the SEM image of exfoliated graphene/SiO<sub>2</sub> nanosheet hybrid [128]. Fig. (B) show the SEM analysis of the synthesized GO using Hummers' methods (a, b) & doped GO sheets with ZnO NPs by hydrolysis process (c, d). Copyright 2023, reproduced with permission from Elsevier Ltd.



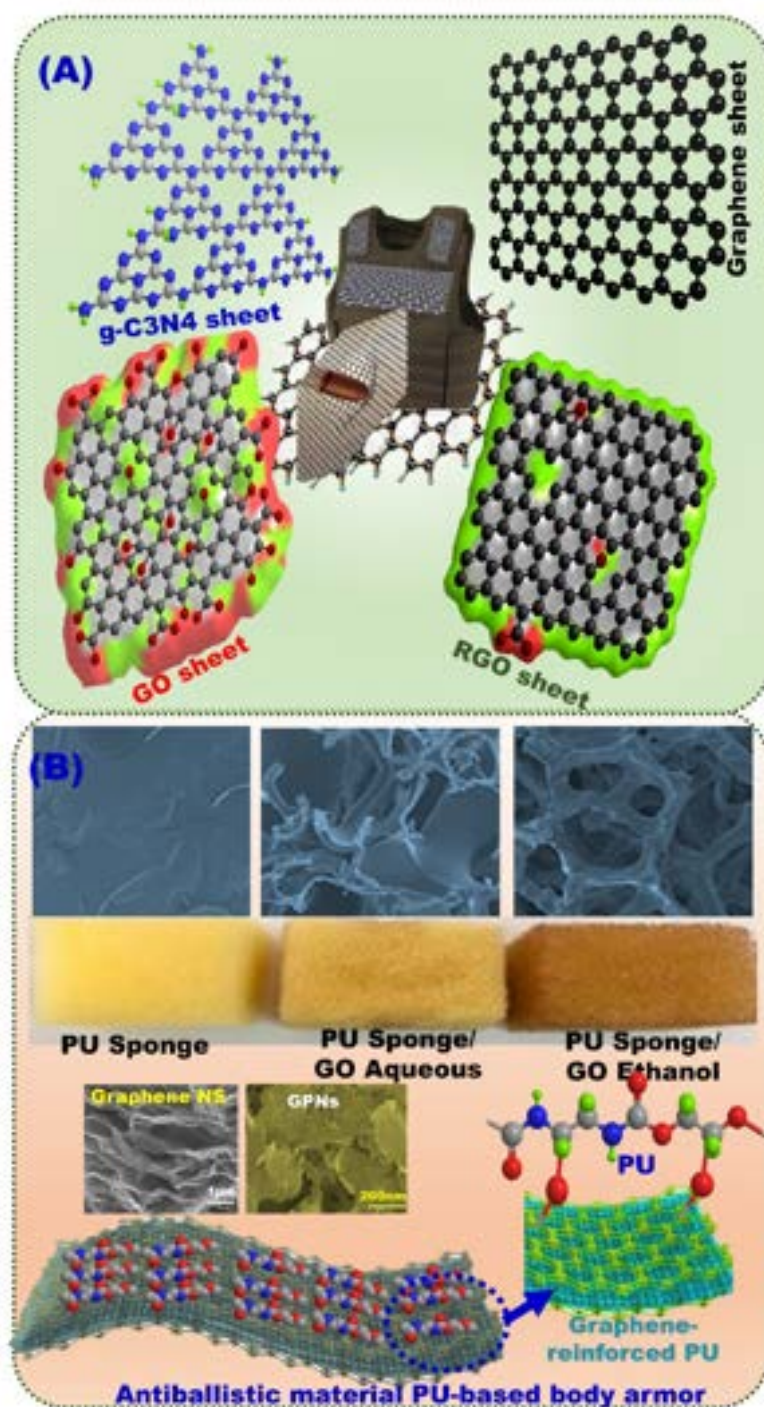


**Fig. 10.** Recent body armor nanocomposite designs. (A) Representative the different forms of graphene and its derivatives that have been used for the construction of armored architectures containing multilayer graphene, GO, RGO, and g-C<sub>3</sub>N<sub>4</sub>. (B) Tailored design of PU reinforced with graphene nanosheets and GNPs as robust nanocomposites for using in bullet-proof armor design applications [148]. Copyright 2015, reproduced with permission from Elsevier.

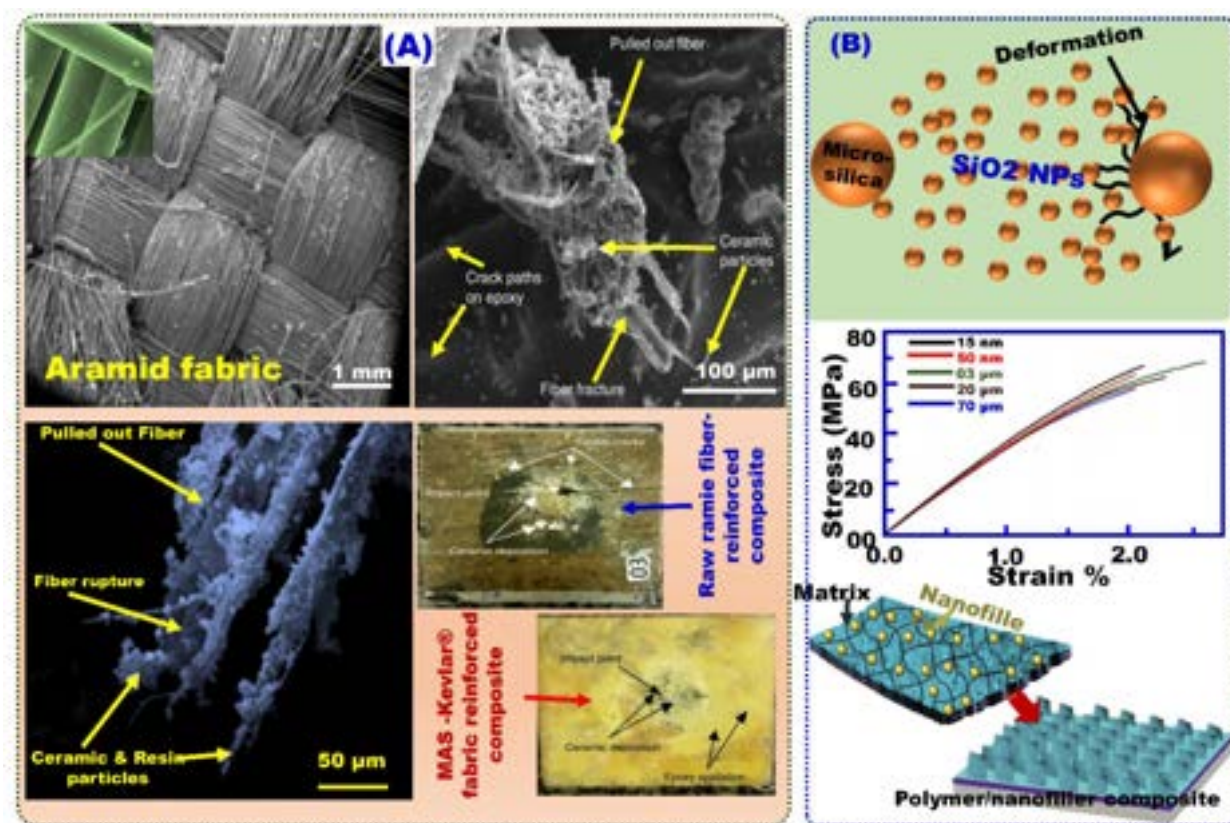


**Fig. 11.** Fabric nanostructures for ballistic-proof applications. (A) Illustration of the fabric plain weave and microscopic detail of the fibers of the aramid fabric, the fracture in the composites near the impact zone of ramie and aramid fiber, and the overall aspect of the tested specimens of multilayered armor systems (MAS) with raw ramie fiber, and Kevlar® fabric reinforced composites [151]. (B) Schematic design that indicates the layer deformation of the epoxy resin filled with micro-silica and incorporated with silica NPs to reduce the effect; influence of different particle size diameter for 3 vol.% alumina particles in vinyl ester resin on stress-strain curves; and reflects the well-distribution of nanofillers in the polymer matrix which significantly affect the surface mechanical features [163]. Copyright 2004, reproduced with permission from Wiley.



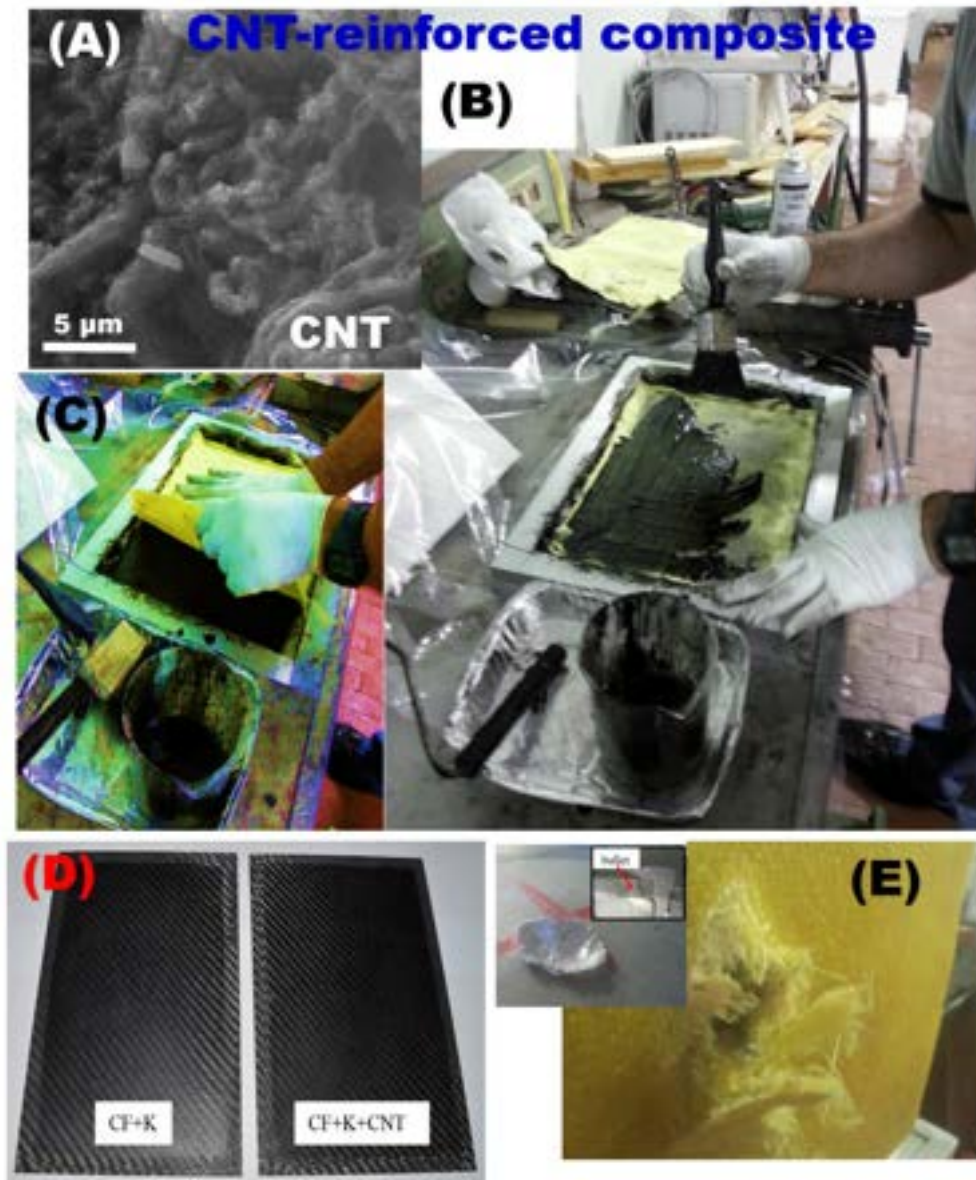


**Fig. 12.** CNTs for antiballistic performance surface. (A-D) Illustration of Ballistic and electromagnetic shielding performance of epoxy/ Kevlar fiber reinforced epoxy composites modified by CNTs, where (A) SEM picture of MWCNT pristine material, (B, C) polymer and Kevlar fabrics for a CNT-reinforced polymeric composite tile manufacture, (D) preform lid and pressure application, and final hybrid composite 3.5 mm thick multilayer tiles manufactured. (E) Visual inspection of a 10 mm thick Kevlar tile after the ballistic test firing at 1000 m/s [16]. Copyright © 2019 Elsevier B.V.

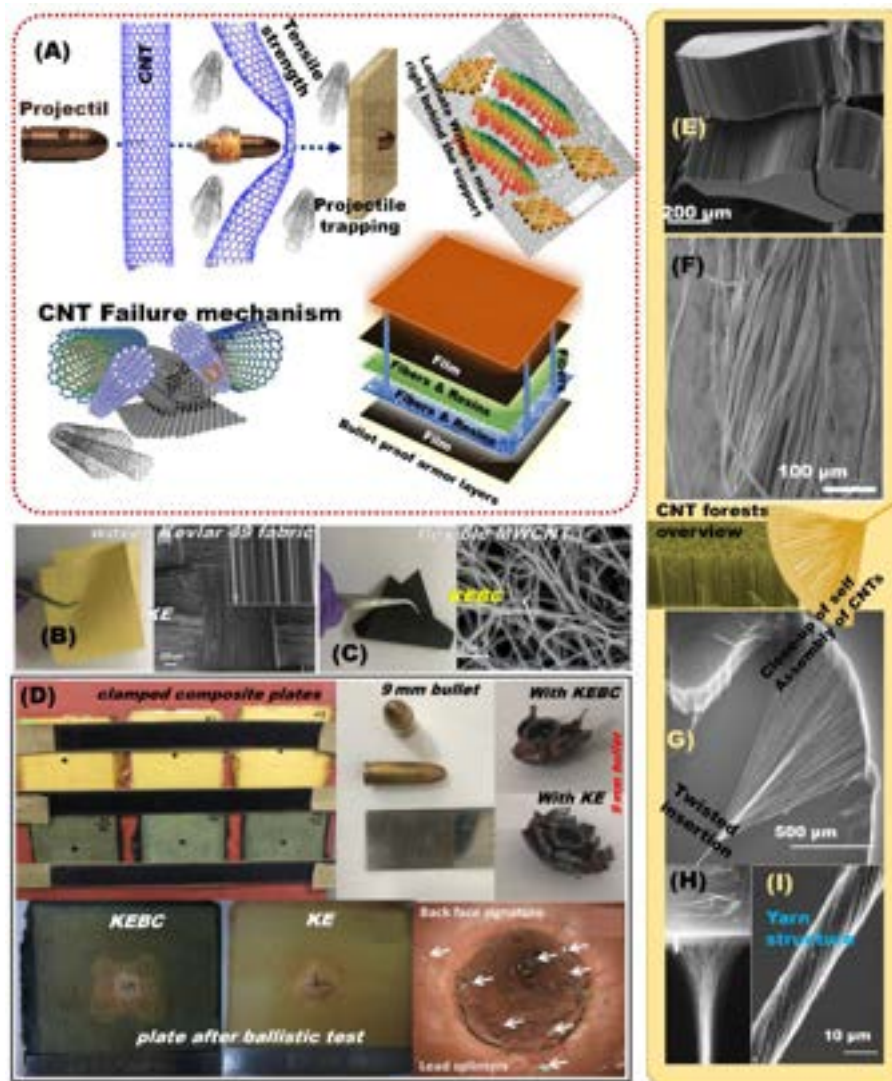


**Fig. 13.** CNTs-based bulletproof armors. (A) The failure mechanism of CNT-based armor model subjected to a ballistic impact; where the model involves impacting the CNT armor by a bullet followed by tensile strength and deformation of CNTs at its maximum energy absorption, the projectile bullet is trapped through absorbing the energy by CNTs. Finally, the bullet is bounced back when the CNT releases its energy is stored. On the right-side examples of laminated based CNT armor fibers [225]. Copyright 2006, Reprinted with permission from the American chemical society. (B) Digital images of plain woven Kevlar 49 fabric and its SEM analysis, (C) flexible MWCNT bucky paper with SEM of randomly oriented bucky paper, and (D) clamped composite plates, 9 mm Full metal jacket (FMJ) bullet for ballistic testing, bullet after striking KEBC and KE plates, KEBC and KE plates after ballistic test, and back face signature over red clay plate with white arrow represents the lead splitters [234]. (E) SEM micrograph of a drawable CNT forest which provides high rate and purity; (F) Conventional cotton-based yarn fibers with ribbon-like structure; (G-I) Structural SEM Images in the draw-twist method of a CNT forest based yarn structure; and (I) represents CNT yarn is much finer with much more fibers than conventional cotton fibers; thus provide high mechanical strength [226]. Copyright 2008, reproduced with permission from Elsevier Ltd.



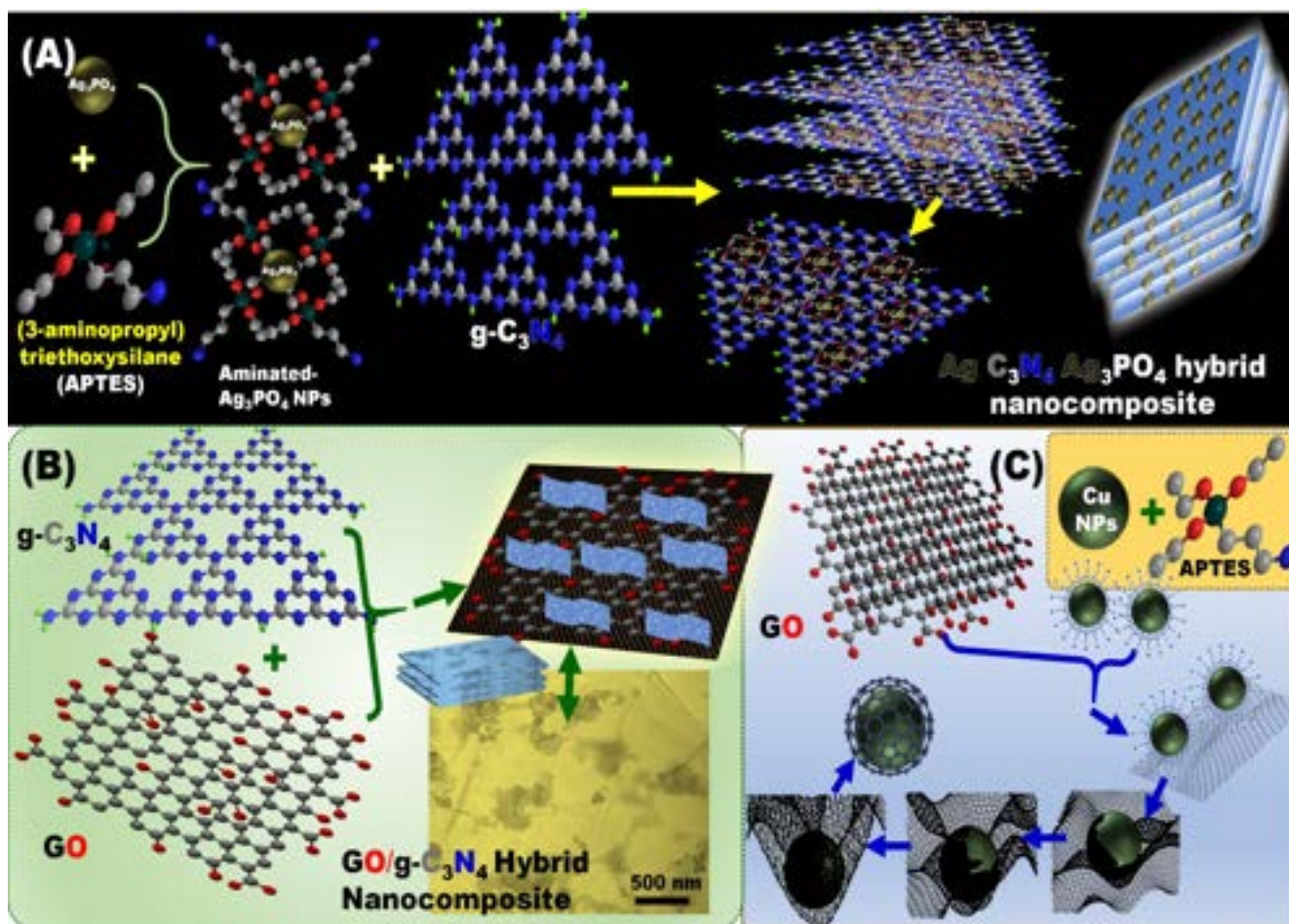


**Fig. 14.** Hybrid polymeric graphene nanocomposites. (A) An illustration shows the steps for the the  $\text{g-C}_3\text{N}_4/\text{Ag}_3\text{PO}_4$  hybrid composite fabrication via the reaction of aminated  $\text{Ag}_3\text{PO}_4$  and  $\text{g-C}_3\text{N}_4$  [242], and (B) Represents the schematic illustration of  $\text{GO}/\text{g-C}_3\text{N}_4$  hybrid nanocomposite [250]. Copyright 2019, reproduced with permission from American Chemical Society.

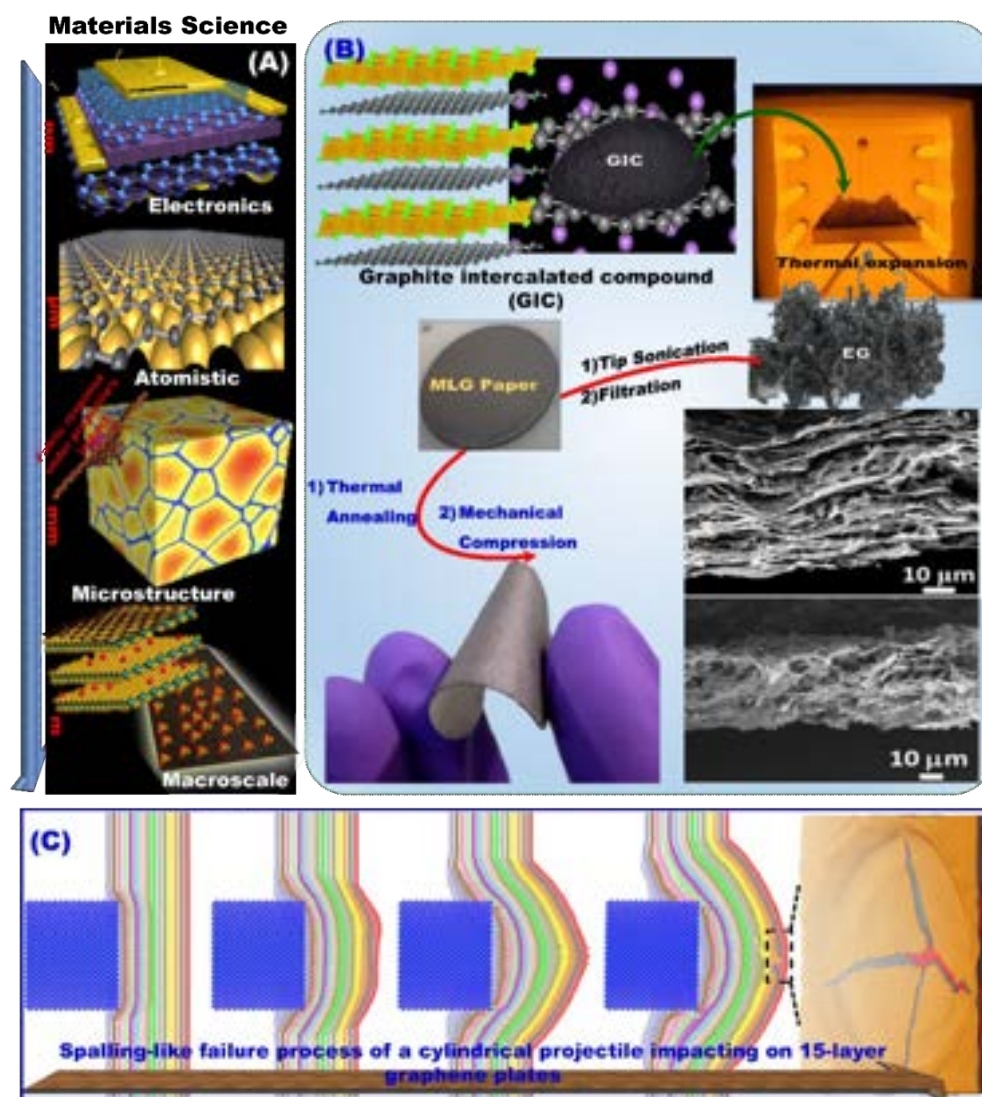


**Fig. 15.** Integrated, super-scalable modeling for graphene functional applications. (A) The multi-scale modeling approach can also be used to model antiballistic fabric materials for various applications. This model can be applied to expect the woven fabric response under the projectile's impact. (B) Displayed different steps that were used for the multilayer graphene (MLG) microsheets flexible paper manufacturing process [255]. Copyright © 2015 Elsevier B.V. Scheme (C) shows the spalling-like failure process of the cylindrical projectile that affects 15 layer graphene plates, this process begins with the compressive wave in the thickness direction, this compressive wave reaches the bottom layer, and this wave is reflected from the bottom layer. Finally, the cracks develop at the bottom of the plates [257].



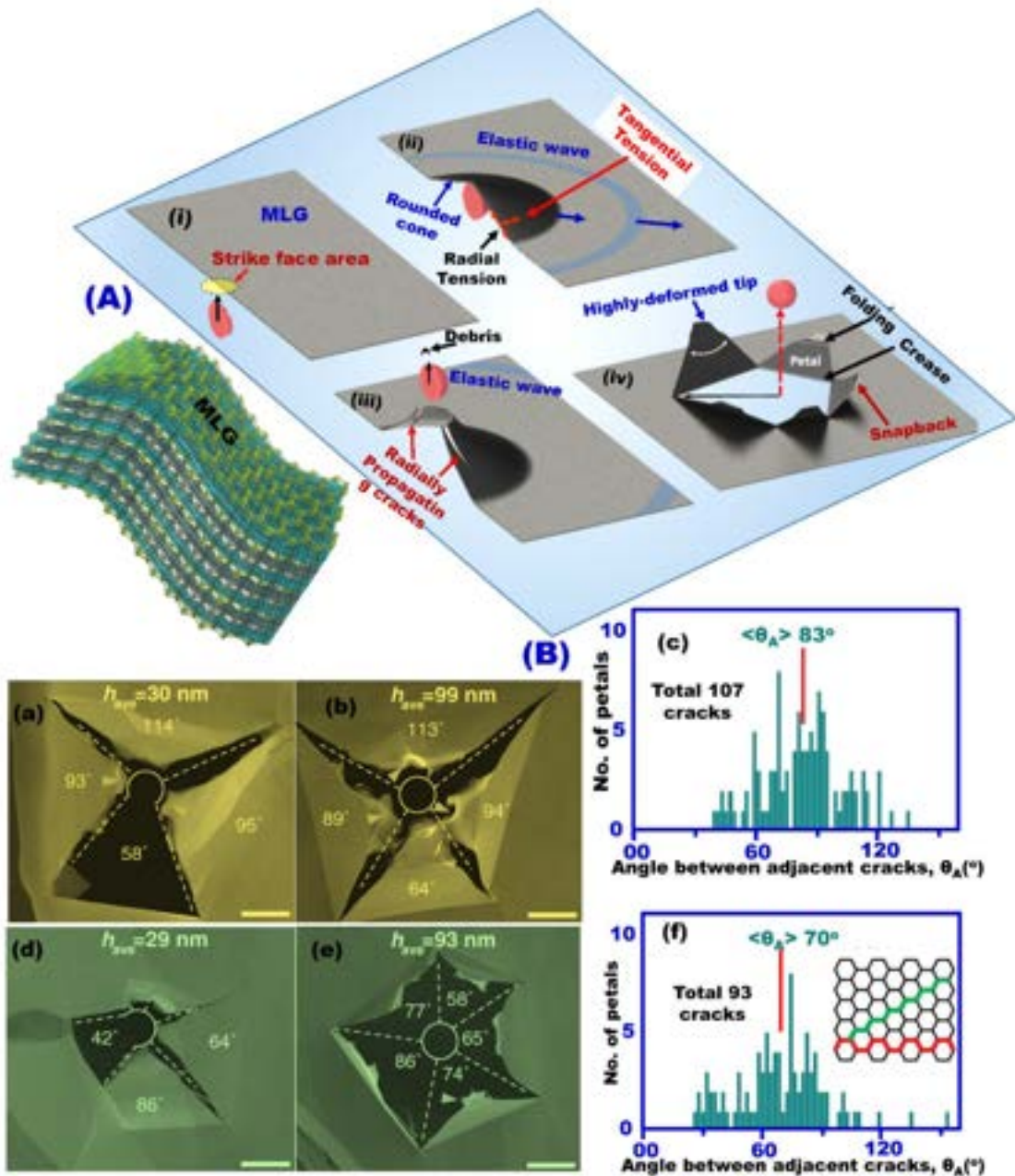


**Fig. 16.** Multilayers graphene-based armor nanocomposite. (A) The schematic design shows the high efficiency of graphene to absorb up to 10 times more energy than steel, where showing how a microbullet traveling at supersonic speed bursts through a sheet of multilayer graphene. (B) Representative penetration features of MLG membranes. SEM extensive damage images of petals, radial cracks, folds, and snap-back damage to the petal tips through complex, fine-scale fractures (a and b), represents the adjacent crack-pair angle distribution for  $v_i = 600$  ms<sup>-1</sup> (c), SEM extensive damage images the adjacent crack-pair angle distribution for  $v_i = 900$  ms<sup>-1</sup> (d and e), and (F) shows the armchair (red) and zigzag (green) directions [271]. Copyright 2014, reproduced with permission from Science Ltd.

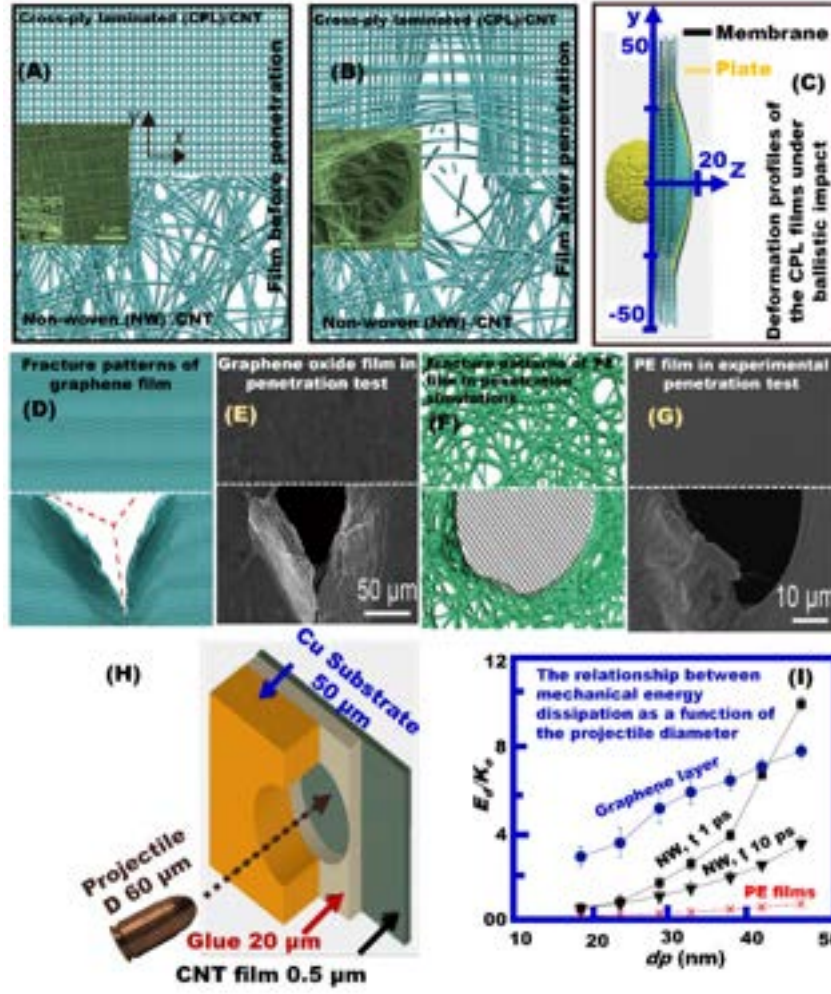


**Fig. 17.** Ballistic-protection of CNT-MLG composites. (A) cross-ply laminated (CPL) and non-woven (NW) CNT films represented in the coarse-grained model with 100 nm in length and 1.62 nm in diameter of double-walled CNTs modeled. (B) Typical fracture pattern of the CNT film after penetration. The insets (A, B) show the SEM images of thin CNT films measured before and after mechanical penetration tests. (C) Deformation profiles of the CPL films under ballistic impact, where the film conforms to the projectile. Representative the fracture patterns in penetration simulations of graphene (D) and PE films (E), and in the experimental penetration tests of graphene oxide (F) and PE films (G). (H) The setup of mechanical penetration experiments. (T) The relationship between mechanical energy dissipation in CNT, graphene and PE films plotted as a function of the projectile diameter [272].

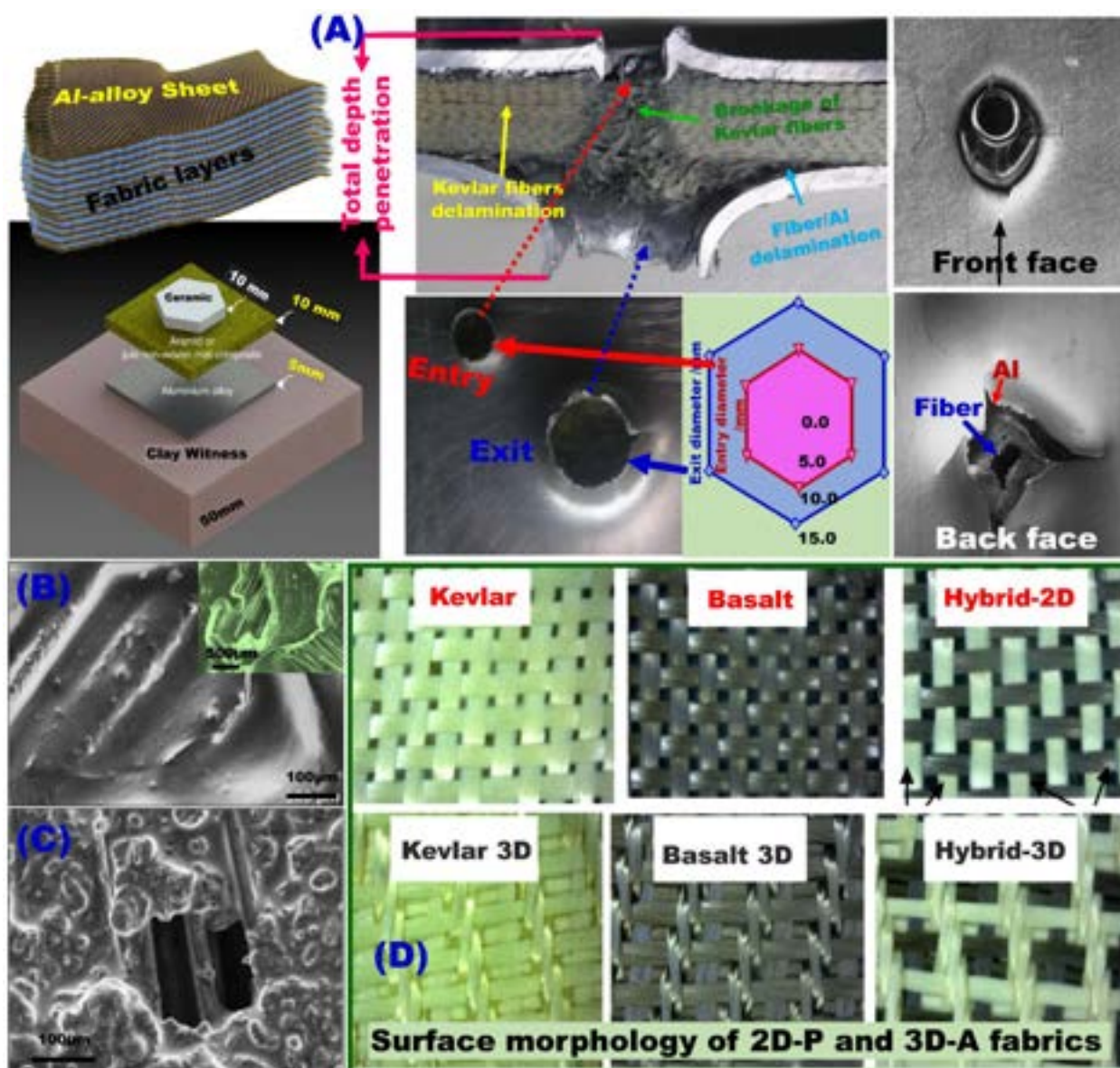


**Fig. 18.** Multifunctional polymer/filler nanocomposites. Represent typical structure of FML composed of epoxy filled with Al nanofillers and reinforced with Kevlar fibers (A); this design shows the Effect of the projectile impact of the two Al sides and Kevlar fibers of FML, entry and exit of the projectile with their size in mm, and the front and back face of the exposed fiber layer surface. Woven Kevlar fiber impregnated with Al and SiC nano-powder to produce reinforced layer (B, C) [259, 275]. Surface structure of ballistic 2D-P & 3D-A hybrid thermoplastic fabrics armors reinforced with Kevlar and basalt fabrics (D) [275]. Copyright 2017267, Reprinted with permission from Elsevier Ltd.



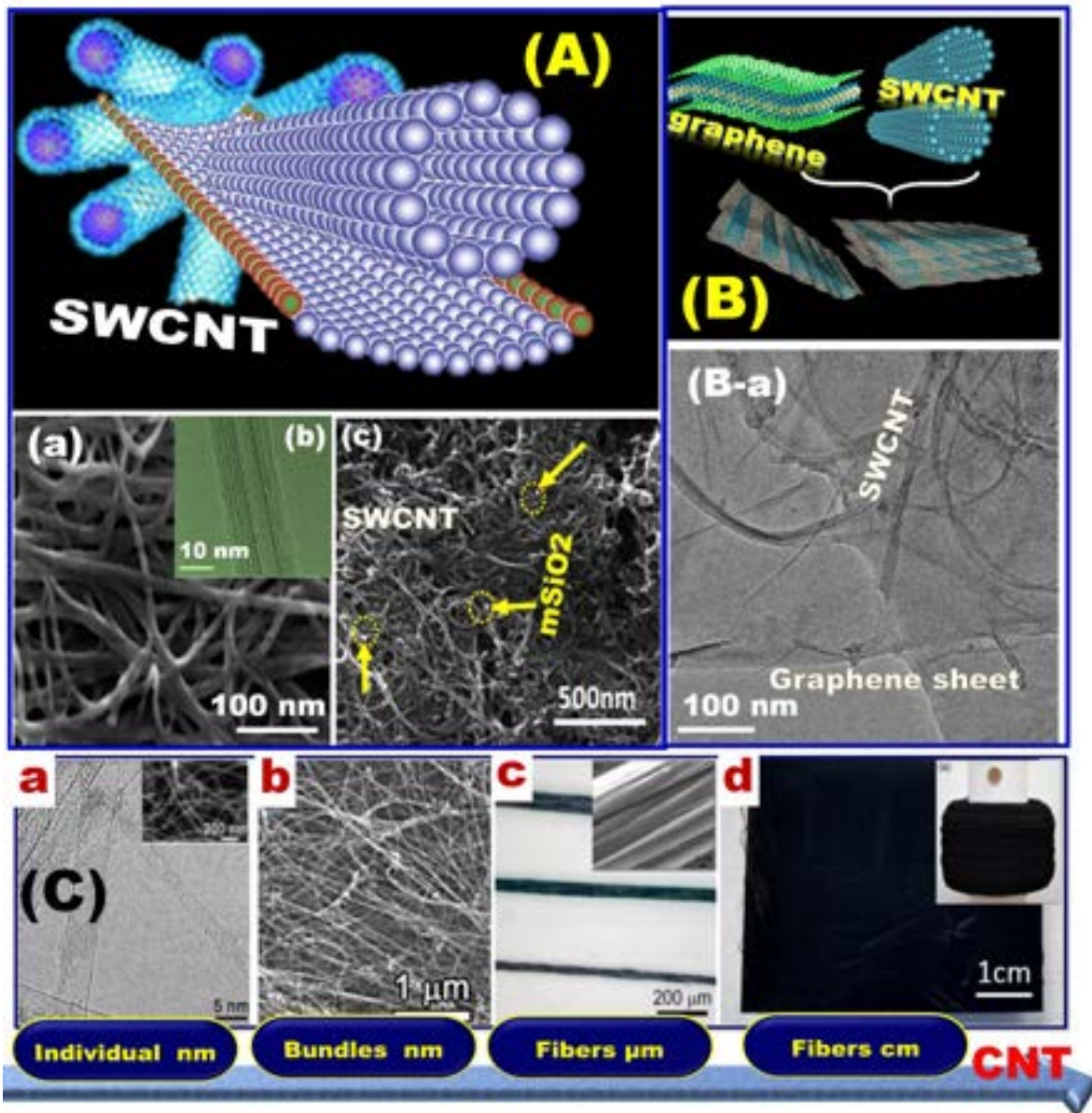


**Fig. 19.** Fabrics nanocomposites reinforced with SWCNT. (A) Illustration of SWCNT shape; (a) and (b) are SEM and TEM images of SWCNTs; (c) hybrid material of o-SWCNT/mSiO<sub>2</sub> NPs which can provide high antiballistic properties; (B) A schematic representation of graphene/SWCNT hybrids developed to provide exfoliation of graphene and reinforced composite material, and (B-a) represent HRTEM image of a graphene nanosheets anchored with SWCNTs hybrid material as a robust structure to be used for armor designs [279]. Copyright 2013, reproduced with permission from Taylor & Francis. (C) Presented the different forms of CNT.

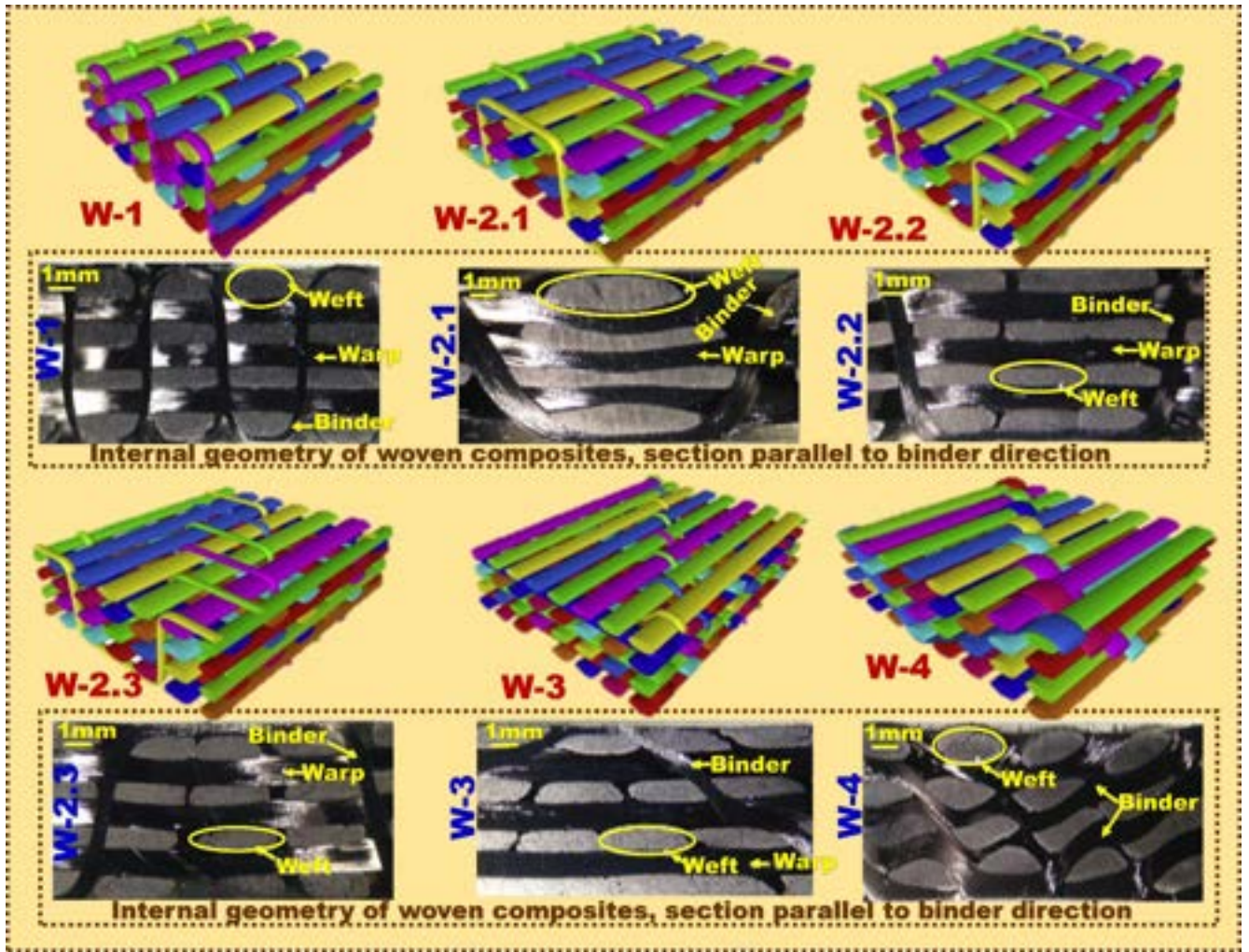


**Fig. 20.** Antiballistic idealized weave architectures. Idealized weave architectures and their internal geometry generated for studying the composite architectures and binder placement. The models introduced six types of 3D woven composites with the same types and different designs (W-1, W2.1, W-2.2, W-2.3, W-3, and W4) were manufactured through the resin transfer modeling conventional and weaving loom with narrow fabrics. The best design performance was shown for W3 angle interlock with the lowest delamination crack between all the weave types [282]. Copyright 2015, reproduced with permission from Elsevier Ltd.



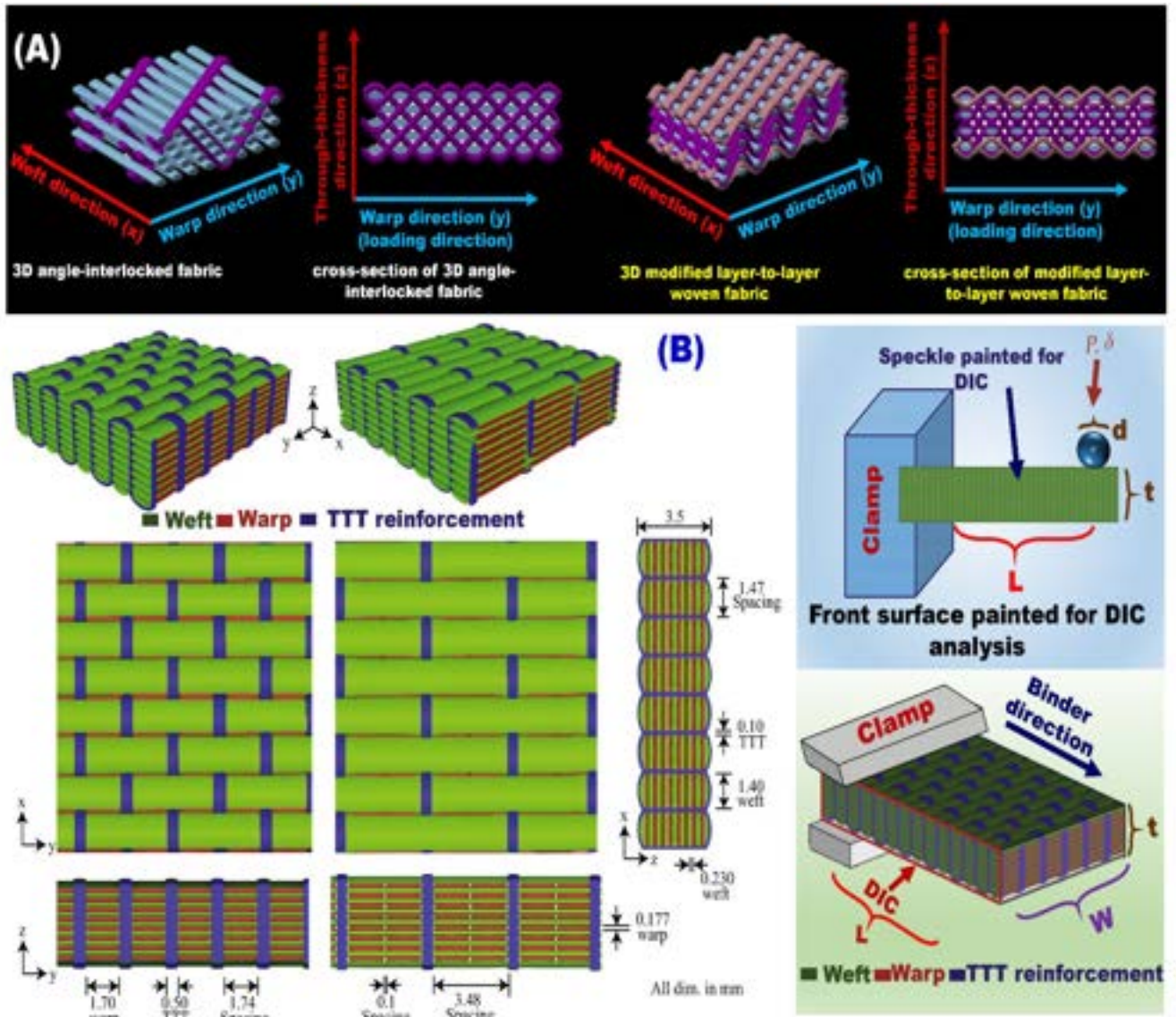


**Fig. 21.** 3D angle-interlocked woven fabrics. (A) Idealized weave architectures and their cross-sections of 3D angle-interlocked fabric and modified layer-to-layer woven fabric [281]. (B) 3D orthogonal woven carbon composites showing Full through-the-thickness (TTT), and design of cantilever beam test and composite beam orientated along the x-direction (warp) [282]. Copyright 2015, reproduced with permission from Elsevier Ltd.

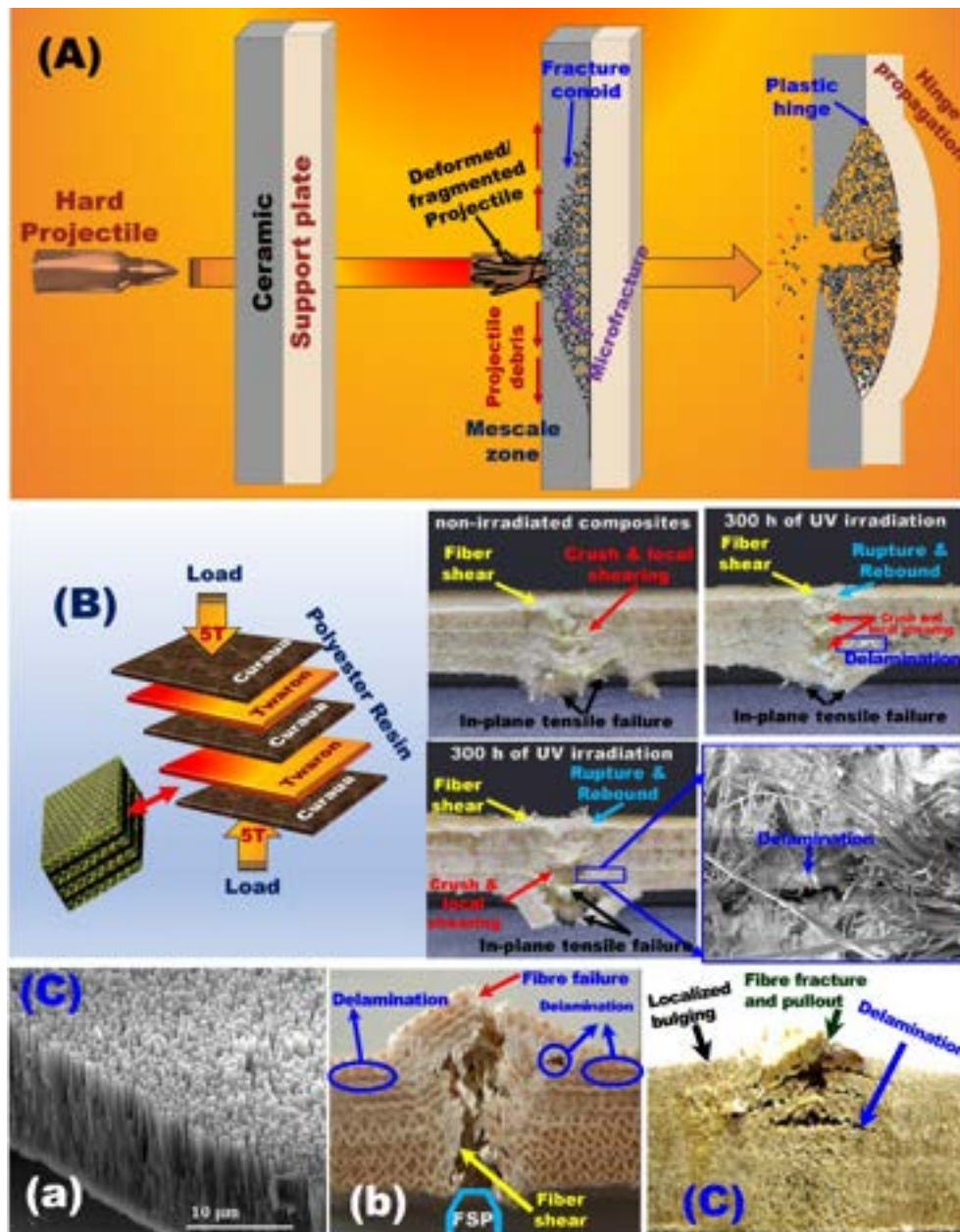


**Fig. 22.** Bullet-penetration in ceramic armor plates (A) The behavior of the penetrator, and the ceramic armor plate in a local zone during a hard projectile impacts a ceramic-faced armor plate. (B) Ballistic performance of a hybrid polyester composite reinforced with curaua mat and aramid fabric, and Cross section of composites after ballistic tests [294]. (C) SEM image of ZnO nanorods and SEM images of composite plates indicating shear, delamination, and fiber (a); represents the fiber's shear, delamination and fracture in the hemp composites under the ballistic impact of a projectile (b); Fracture and delamination (Magnified view of the cross section) of fiber composite upon ballistic impact (c) [297]. Copyright 2007, reproduced with permission from Elsevier Ltd.

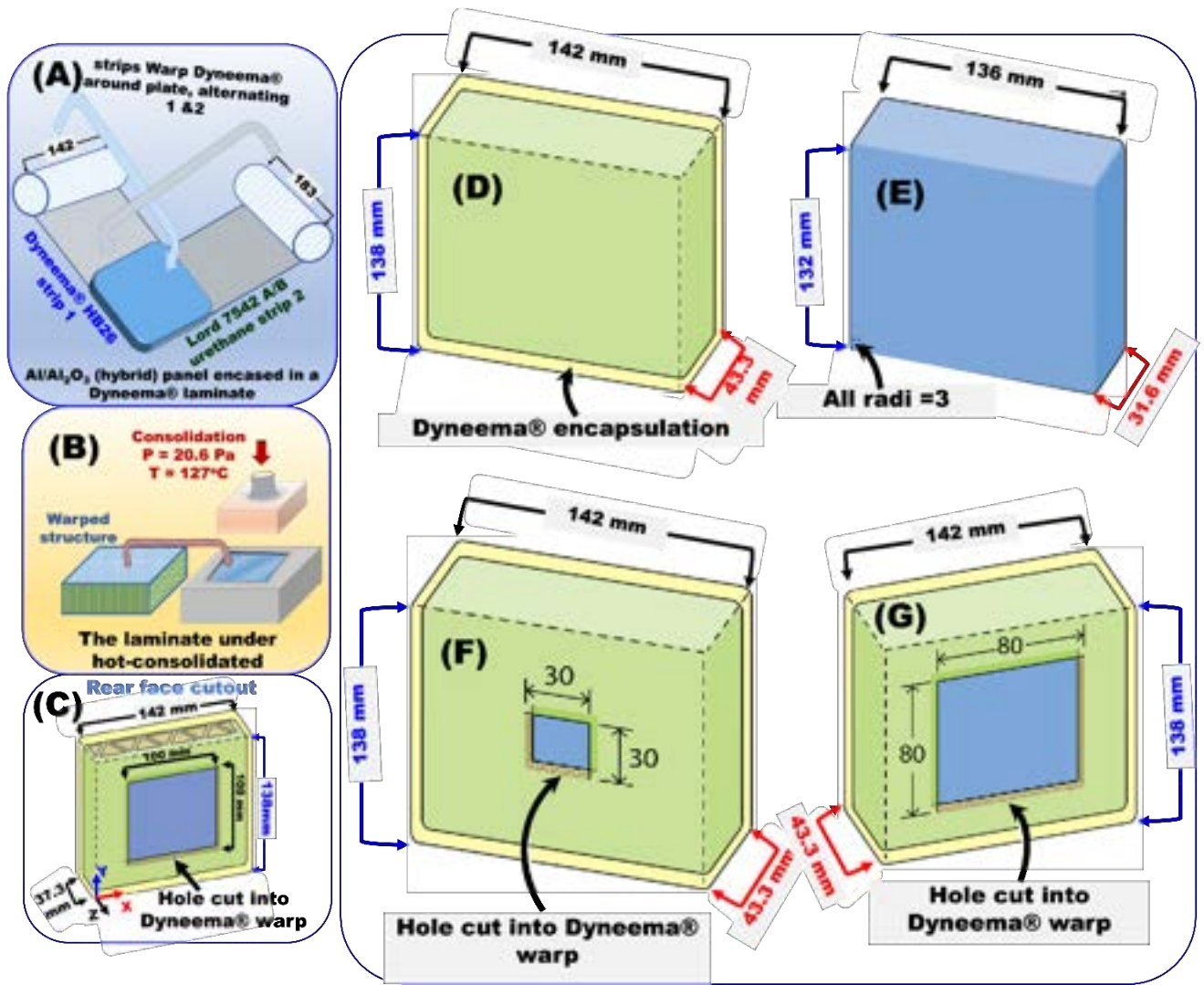


**Fig. 23.** Dyneema® UHWMPE composites targets. (A-C) The schematic design of the Dyneema®-encased aluminium panels fabrication [283]. Copyright 2015, reproduced with permission from Elsevier Ltd. The four model targets employed for studying the structures of penetration resistant; where (D) represents the baseline target with the Al plate fully encased by Dyneema®, (E) the bare Al plate, (F) the front face cutout target, and (G) the rear face cutout target. All the mentioned dimensions are in mm [284]. Copyright 2016, reproduced with permission from Elsevier Ltd.



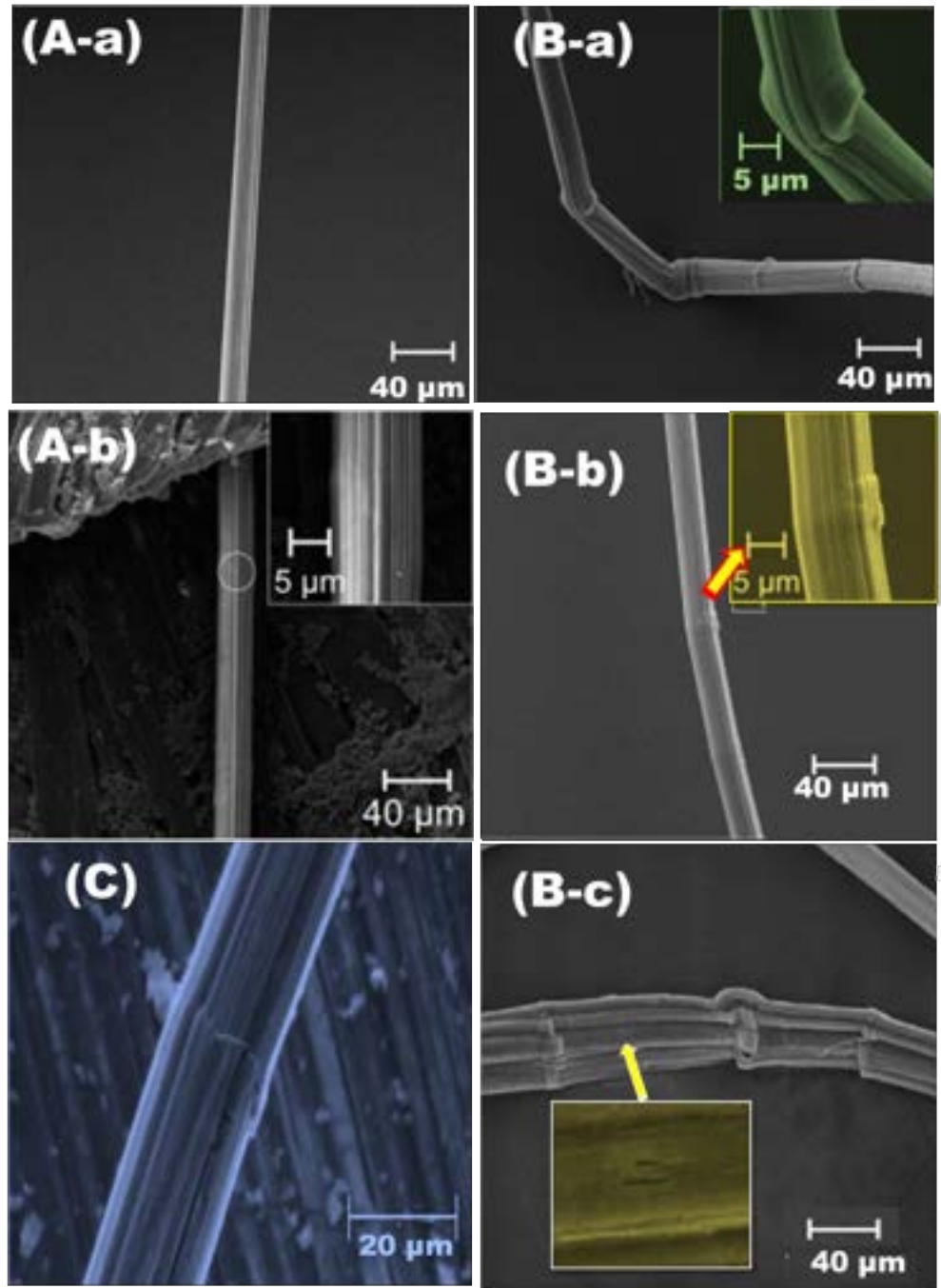


**Fig. 24.** Compression of SK76 fibers. SEM micrographs of the SK76 fibre showing sections near the clamped end, where, (A) shows no kinks were observed in the fiber at 85 mN; (B) shows multiple kinks in the fiber observed after recoil test at 88 mN, and (C) indicating kinks in the fiber observed after knot test at 87 mN [302]. Copyright 2015, reproduced with permission from Elsevier Ltd.

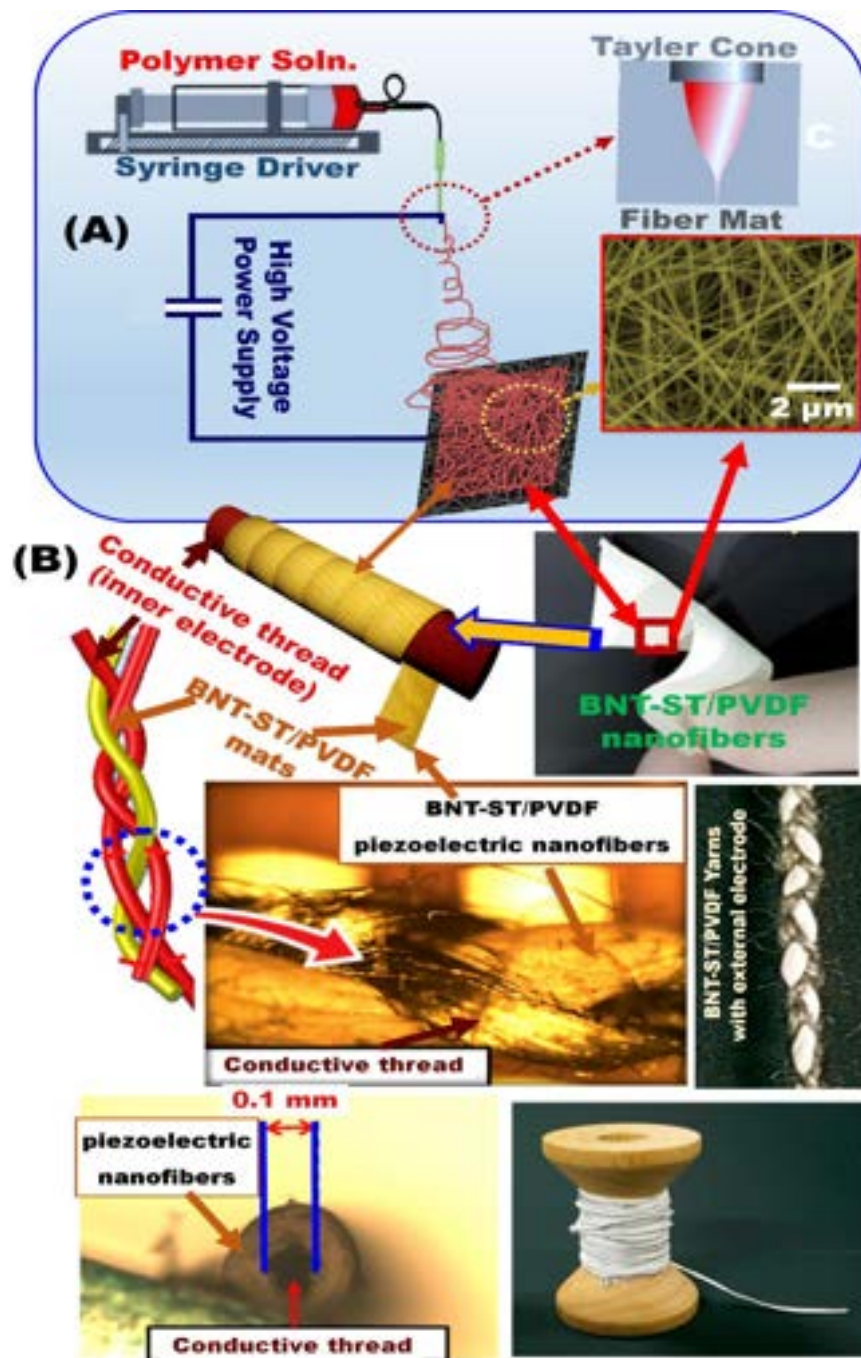


**Fig. 25.** Coils and yarns through electro-spinning. (A) Schematic of the electrospinning process, (B) Electrospun membrane detached from the substrate using tweezers, and (B) represented the core-shell piezoelectric yarns with external electrodes fabrication process [310]. Copyright 2015, reproduced with permission from Elsevier.

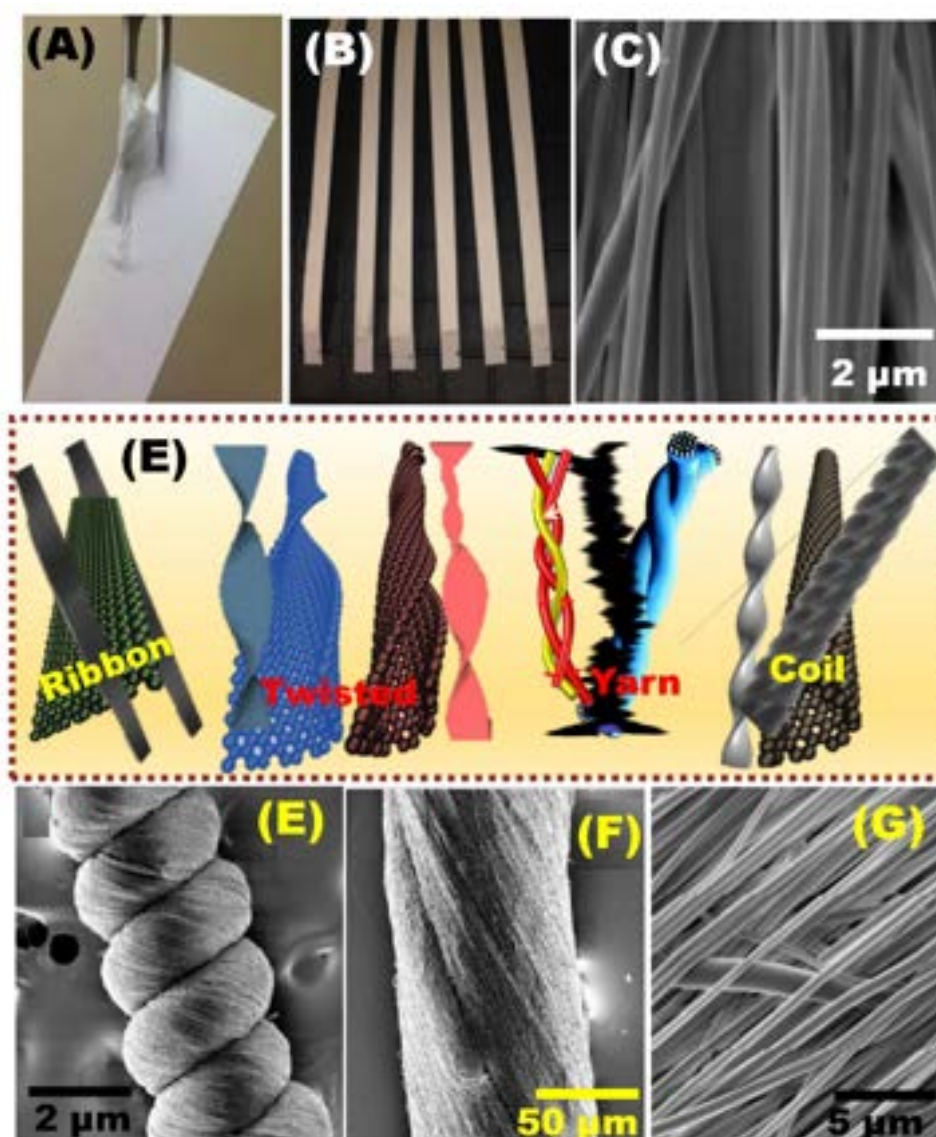


**Fig. 26.** Ribbons Over-twisting to form coils and yarns. Schematic design of the electrospun membrane detached from the substrate using tweezers (A), which has cut into ribbons (B); and SEM micrographs of a ribbon (membrane) with aligned nanofibers (C). Fabrication of yarns and coils from electrospun ribbons by twisting process (D); SEM micrographs of a coil fabricated from aligned nanofibers. The coil has an outer diameter of  $\sim 306 \mu\text{m}$  and a pitch of  $140 \mu\text{m}$  (F); SEM micrographs of a yarn fabricated from aligned nanofibers shown in different magnifications. The yarn has a diameter of  $\sim 175 \mu\text{m}$  (G) [311]. Copyright 2019, reproduced with permission from MDPI.



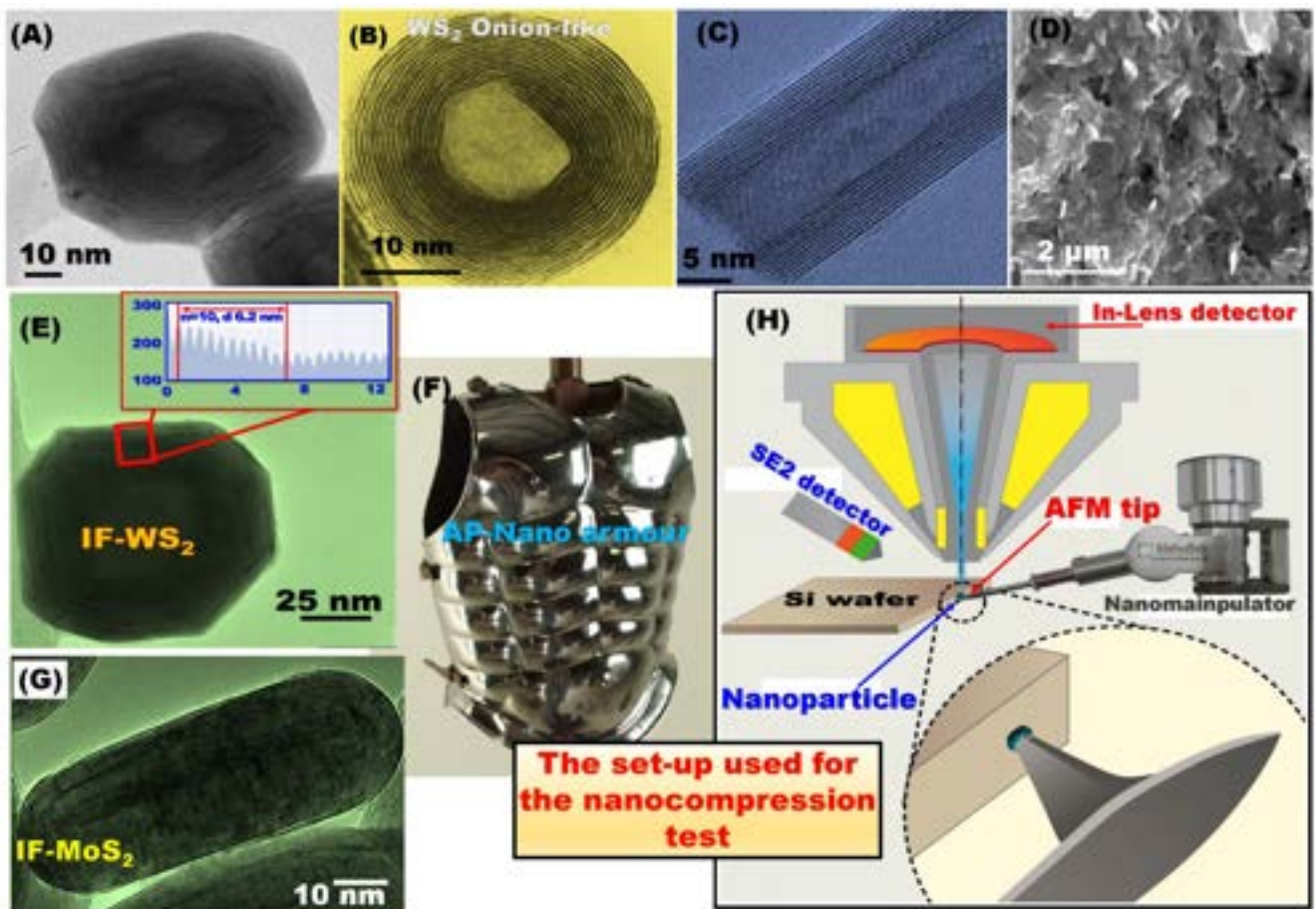


**Fig. 27.** WS<sub>2</sub> onion-like based ApNano armor. (A- C) Typical onion-like structure; TEM image of Onion-Like IF materials at different magnifications; (D) SEM image of the WS<sub>2</sub> nanocomposite of the armor structure; TEM image of multilayered IF-WS<sub>2</sub> nanoparticle (E) and IF-MoS<sub>2</sub> NP (F), and typical AP-Nano Bullet-proof armor (F) Copyright 2009, Reprinted with permission from [313]. (H) Represented the schematic design of the set-up used for the nanocompression test.

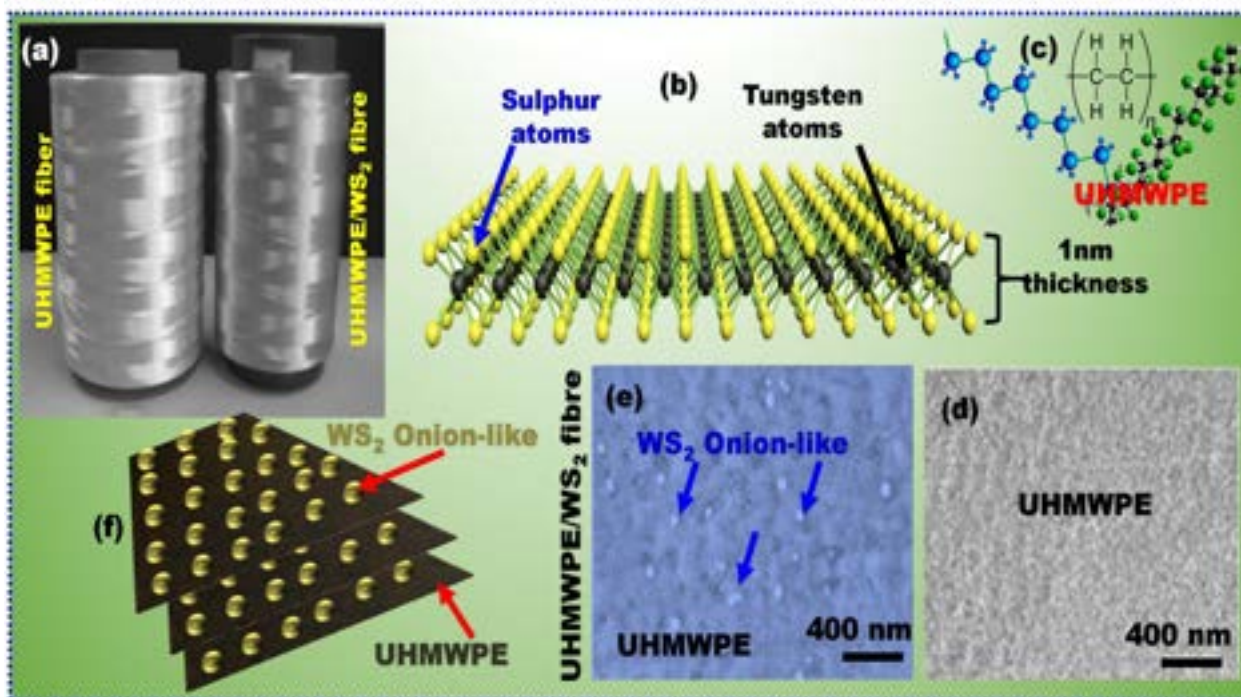


**Fig. 28.** IF-WS<sub>2</sub> and UHMWPE nanocomposite fibers. (A) Typical UHMWPE Fibers and UHMWPE/WS<sub>2</sub> nanocomposite fibers; (B, C) Represents the general structure of WS<sub>2</sub> and UHMWPE, (D) UHMWPE fiber SEM picture; (E) UHMWPE/WS<sub>2</sub> fiber SEM image and (F) Typical UHMWPE/WS<sub>2</sub> nanocomposites [328,329]. Copyright 2015, reproduced with permission from American Chemical Society.

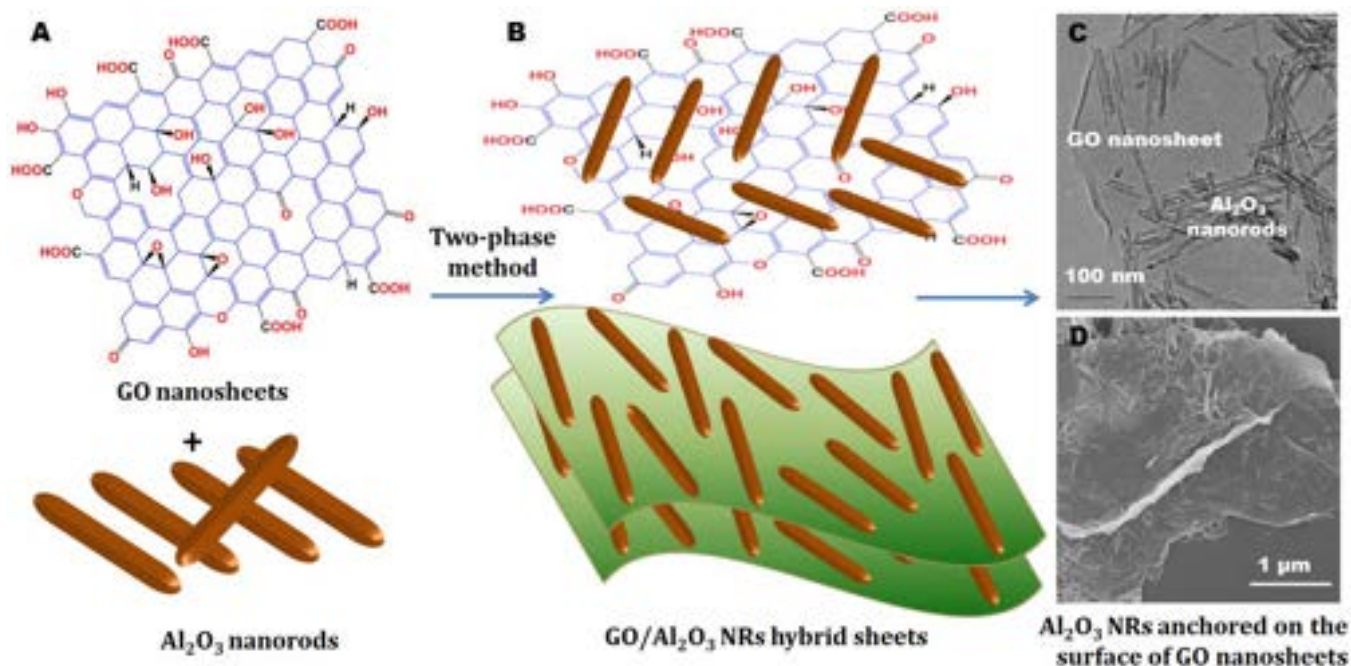


**Fig. 29.** High-strength GO/metal oxide nanocomposite. (A, B) schematic illustration of GO nanosheets- $\gamma$ -Al<sub>2</sub>O<sub>3</sub> nanorods composites as inorganic nanofillers for mechanical with self-cleaning applications; (C, D) represent the HRTEM and FESEM of GO/ $\gamma$ -Al<sub>2</sub>O<sub>3</sub> nanorod hybrid.

### Tables:

**Table 1.** Timeline for the armor development techniques [12].

Technique	Merits	Limitations
layer by layer	Enhanced mechanical strength and high load and stress transfer ability	Poor interfacial adhesion which may result in delamination
<b>Shear thickening fluid (STF)</b>	High fabric deformability for shock absorption because of the Improved impact energy absorption	Critical shock causes fiber rupture and it is necessary to dominate the viscosity
<b>Yarn pull-out</b>	Enhanced friction resistance and impact energy absorption as well as outstanding tensile strength	Increased energy cost
<b>Funcionalizaci3n with NPs</b>	Ultra-strong interfacial adhesion and uniform nanofiller distribution on the fabric layer	Complex preparation route

**Table 2.** Historical development of the fiber-reinforced bullet proof armor [6,70,85-87].

<b>Timeline</b>	<b>Major events</b>
<b>2500 B.C.</b>	Sumerians soldiers used copper helmets and leather body armor
<b>1500 B.C.</b>	A bronze armor was primarily introduced
<b>1100 B.C.</b>	Bronze, linen, and steel were used by Egyptians and Acadians
<b>600 B.C.</b>	An armor system developed of iron, bronze, wood, and wool was introduced
<b>500 B.C.</b>	Persians used Leather, iron and bronze Bronze plates by Greeks and flexible cuirasses made from iron plates by Romans
<b>400-300 B.C.</b>	Chainmail body armor invented by Celtic people
<b>Charlemagne age and later</b>	Jazerant armor, steel armors, and Saxons
<b>14th century</b>	Protective cloths for different parts of the body
<b>1600 AD</b>	Channeled Mg-based armor was used
<b>1700 AD</b>	Use thick armor to resist fire
<b>1642-1648</b>	Using metallic helmet during the English civil war
<b>1905</b>	Silk vests as armor are used in the Japanese–Russian war
<b>1914-1918</b>	Metal helmet, heavy metal breastplate, and armored waistcoat are used in the first world war
<b>1939-1945 and 1950-1953</b>	In the second World War and Korean War, steel laminates contain fiberglass and polyamine materials were used
<b>1960s</b>	Al <sub>2</sub> O <sub>3</sub> based ceramic armor was used for the first time
<b>Mid of 1970s</b>	Kevlar was widely produced for antiballistic clothes
<b>1999</b>	Developments on spider silk bulletproof body armor were introduced
<b>2003</b>	In the Iraq war, the US army used Interceptor Body Armor system which is made from layered Kevlar for the body organs and Kevlar helmet to protect the head
<b>Recently</b>	Bulletproof nanostructured armor research and development was enhanced.
<b>1. Ceramic armors</b>	Aluminum materials and other ceramic composites were developed as efficient antiballistic armor materials. In 2004, Fiber metal laminate (FML) was developed and applied as antiballistic skin material.
<b>2. IF nanocomposites</b>	Extensive production of bullet-proof armors based on IF-materials such as IF-WS <sub>2</sub> and IF-MoS <sub>2</sub> was achieved in 2005.
<b>3. CNT-fiber composite</b>	CNT-fiber reinforced armors with high energy absorption capability and carbon nanotube fibers reinforced composites (CFRCs) were developed recently for antiballistic protection with high efficiency.
<b>4. Nano graphite composites</b>	Graphite sheets and Nanoribbons incorporated in fiberglass/epoxy laminates were used as antiballistic materials
<b>5. Multifunctional armor composite</b>	Hybrid nanomaterials such as Graphene anchored with NPs can provide ultra-high robustness, ultimate strength, and ballistic protection

**Table 3.** Different utilized ballistic test standards.

<b>Specifications (Country of the origin)</b>	<b>Details</b>	<b>Applications</b>
<b>MIL-STD-662F (USA)</b>	Used for standard V-50 determination uses Al witness plate to judge failure.	General use for any armor materials
<b>STANAG 2920 (NATO)</b>	General purpose use for ballistic testing methods	
<b>HOSDB (UK)</b>	General purpose use for UK Police only	
<b>ISO/FDIS 14876 (Switzerland)</b>	Acceptance of the sample will depend upon indentation of depth and no bullet penetration should occur for any acceptable shots	General use for only those materials that provide torso protection
<b>NIJ 0101.06 level II, IIA, IIA (USA)</b>	Widely used ballistic standard for body armor in the case of flexible vests	Applicable only for soft body armors
<b>NIJ 0101.06, level III, IV (USA)</b>	Ballistic standard for body armor, with smaller edge distances and vastly increased sample size compared to NIJ 0101.04	Hard armor plates for more stringent conditions

**Table 4.** CNT fiber properties.

<b>Designation</b>	<b>Unit</b>	<b>CNT fibers</b>
Specific tensile strength (STS)	N/tex	1-10
Linear mass density (LMD)	tex	0.03-0.135
Length (L)	mm	0.3-200
Diameter (D)	μm	4-20
Cross sectional area (CSA)	μm	12.56-314
Bulk density (g/cm <sup>3</sup> )	BD	0.4-1.1
Strain at Fair (SF)	%	1.8-8